

INVESTIGATING THE FUNCTIONAL RELEVANCE OF AFFERENT
INHIBITION

by CLAUDIA VICTORIA TURCO, B.Sc.

A Thesis Submitted to the School of Graduate Studies in Partial Fulfillment of the
Requirements for the Degree Doctor of Philosophy

McMaster University, April 2021

Descriptive Note

DOCTOR OF PHILOSOPHY (2019)
(Kinesiology)
McMaster University, Hamilton, Ontario

TITLE: Investigating the Functional Relevance of Afferent Inhibition

AUTHOR: Claudia Victoria Turco, B.Sc.

SUPERVISOR: Dr. A. J. Nelson

NUMBER OF PAGES: xi, **230**

Lay Abstract

The brain plays an important role in collecting sensory information from the environment and using that information to guide the movement of our limbs in space. The key structures within the brain that are important for this process to occur correctly include the primary motor cortex and primary somatosensory cortex. The primary motor cortex is responsible for executing movements, while the primary somatosensory cortex is responsible for processing tactile information. The connectivity between these two areas is thought to be important for integrating incoming sensory information with plans for movement execution. This thesis explores how we can accurately assess the activity of these sensorimotor connections and why these connections are important for normal human function. Therefore, the findings of this dissertation will contribute to our understanding of motor control.

Abstract

Afferent inhibition is a phenomenon observed when an afferent volley evoked by peripheral nerve stimulation inhibits descending corticospinal output. Notably, this phenomenon is not observed in special populations exhibiting impairments in cognitive and/or sensorimotor function, suggesting that it plays an important role in normal human function. The overall goal of this thesis was to contribute new knowledge to the understanding of afferent inhibition. This was achieved by investigating the functional relevance of afferent inhibition and exploring methods for improving data acquisition. In study 1, I examined the relationship between long-latency afferent inhibition (LAI) and sensory afference, and determined the optimal stimulation parameters that would evoke maximal LAI. In study 2, I sought to determine the underlying neurotransmitter basis of afferent inhibition. The results showed that both LAI and short-latency afferent inhibition (SAI) are modulated by GABA_A receptor activity but not GABA_B receptor activity. Study 3 showed that these measures of afferent inhibition have poor-to-moderate reliability with moderately high levels of within-subject variability. In study 4, I investigated the relationship between afferent inhibition and glucose function. I found that ingestion of a glucose bolus does not modulate the magnitude or variability of afferent inhibition. In study 5, I explored the role of afferent inhibition in motor cortex organization. The results suggest that afferent inhibition may not be a mediator of motor cortex reorganization that occurs following sensory enrichment. Finally, I proposed a model of the neural pathways underlying SAI and LAI that would lead to inhibition of corticospinal output. The findings from this thesis

contribute new knowledge to the afferent inhibition literature that will be useful for improving future study methodologies and understanding the linkage to human function.

Acknowledgements

I started graduate school as a Master's student with no intention of ever pursuing a PhD. However, I did not anticipate the opportunities and excitement that research could bring and the unknowing passion that I had for research. Looking back on this journey, fast-tracking into the PhD program and the incredible challenge that these past 5 years have been, I'm extremely grateful to have gone down this path.

To my supervisor, Dr. Aimee Nelson – if it was not for your confidence in my potential as a researcher, I would not have written this dissertation and I certainly would not be the person that I am today. You not only took a chance on me as a student, but you gave me an invaluable opportunity to grow as a scientist and as a person. I know that I will keep with me always the lessons that I learned from you over the past 6 years as I continue to pursue my future endeavors. To my committee members, Dr. Audrey Hicks and Dr. Daniel Goldreich – I want to thank you for your invaluable support throughout the years. I am incredibly grateful to have had the guidance and mentorship from two exceptional scientists.

My lab mates, both past and present, thank you for your role in getting me here: Hunter Fassett, Jenin El-Sayes, Mitchell Savoie, Mitchell Locke, Diana Harasym, Dr. Chiara Nicolini, Stephen Toepp, Patrick Dans and Stevie Foglia. Your contributions were essential for the success of my experiments and for this dissertation as a whole. Your insight

challenged me to be a better scientist and your friendships over the years is what made my time in the lab more enjoyable than I would have thought possible.

To my family – you are the backbone to my success. I cannot imagine how I would have ever made it to this point without your support through every failure and achievement along the way. To my dear Nonno – I lost you 9 months too early before I achieved my goal and I wish that I could have shared this milestone with you. Your words, “study hard”, will always remain in my mind and follow along with me as I step forward toward my future endeavors. To my father – you are the best teacher that I have ever had. To my mother - you were right, as always, by telling me that I should give research a try when I was dead set against it. To the rest of my family, don't you dare joke that I'm not a real doctor.

Declaration of Academic Achievement

Claudia Turco wrote the entirety of this thesis, conceived of and performed all experiments, and analyzed all datasets.

Chapter 1, Section 1.3 – a version of this section is published in Brain Stimulation

Turco CV, El-Sayes J, Savoie MJ, Fassett HJ, Locke MB, & Nelson AJ (2017). Short- and long-latency afferent inhibition; uses, mechanisms, and influencing factors. *Brain Stimulation, 11: 59-74.*

Claudia V. Turco was responsible for conceptualization of the paper and writing of the manuscript; Dr. Aimee J. Nelson assisted with conceptualization and editing of the manuscript; Jenin El-Sayes, Mitchell J. Savoie, Hunter J. Fassett, and Mitchell B. Locke assisted with editing of the manuscript.

Chapter 3 – published in the Journal of Neurophysiology

Turco CV, El-Sayes J, Fassett HJ, Chen R, & Nelson AJ (2017). Modulation of long-latency afferent inhibition by the amplitude of the sensory afferent volley. *Journal of Neurophysiology, 118(1): 610-618.*

Claudia V. Turco was responsible for conceptualization of the experiment, data collection, data analysis, data interpretation, and writing of the manuscript; Dr. Aimee J. Nelson assisted with conceptualization, data interpretation, and editing of the manuscript; Jenin El-Sayes and Dr. Robert Chen assisted with conceptualization, data interpretation, and editing of the manuscript; Hunter J. Fassett contributed to data interpretation and editing of the manuscript.

Chapter 4 – published in the Journal of Physiology

Turco CV, El-Sayes J, Locke MB, Chen R, Baker S, & Nelson AJ (2018). Effects of lorazepam and baclofen on short- and long-latency afferent inhibition. *J Physiol, 596(21): 5267-5280.*

Claudia V. Turco was responsible for conceptualization of the experiment, data collection, data analysis, data interpretation, and writing of the manuscript; Dr. Aimee J. Nelson and Dr. Robert Chen assisted with conceptualization, data interpretation, and editing of the

manuscript; Jenin El-Sayes, Mitchell B. Locke assisted with data collection and editing of the manuscript; Dr. Steven Baker assisted with the experimental design and editing of the manuscript.

Chapter 5 – published in Brain Research

Turco CV, Turco, Pesevski A, McNicholas PD, Beaulieu LD, & Nelson AJ (2019). Reliability of transcranial magnetic stimulation measures of afferent inhibition. *Brain Research*, 1723: 146394.

Claudia V. Turco was responsible for conceptualization of the experiment, data collection, data analysis, data interpretation, and writing of the manuscript; Dr. Aimee J. Nelson assisted with conceptualization and editing of the manuscript; Angela Pesevski, Dr. Paul D. McNicholas, Dr. Louis-David Beaulieu assisted with statistical analyses and editing of the manuscript.

Chapter 6 – a version of this study is published in Brain Sciences

Toepp SL, Turco CV, Locke MB, Nicolini C, Ravi R, & Nelson AJ (2019). The impact of glucose on corticospinal and intracortical excitability. *Brain Sciences*, 9: 339.

Claudia V. Turco contributed to conceptualization of the experiment, data collection, data analysis, data interpretation, and writing of the manuscript; Stephen L. Toepp contributed to conceptualization, data collection, and editing of the manuscript; Dr. Aimee J. Nelson contributed to conceptualization and editing of the manuscript; Mitchell B. Locke and Dr. Chiara Nicolini contributed to editing of the manuscript; Roshni Ravi assisted with data collection.

Table of Contents

Chapter 1: Literature Review	1
1.1 <i>Sensorimotor Integration</i>	1
1.1.1 What is sensorimotor integration?	1
1.1.2 Overview of the literature review	1
1.2 <i>Organization of the Sensorimotor System</i>	2
1.2.1 Overview of the Cerebral Cortex	2
1.2.2 The Somatosensory System	3
1.2.3 The Motor System.....	6
1.2.4 Integration of the two anatomical systems (M1-S1 connectivity).....	10
1.3 <i>Afferent Inhibition</i>	14
1.3.1 Methodological parameters of afferent inhibition	14
1.3.2 Pharmacology of afferent inhibition	15
1.3.3 Is afferent inhibition useful in practice?	18
1.3.4 Relationship between afferent inhibition and sensorimotor function	21
Chapter 2: Thesis Overview	25
2.1 <i>Goals and impact of the thesis</i>	25
2.2 <i>Summary of studies</i>	26
Chapter 3: Study 1	28
3.1 <i>Introduction</i>	28
3.2 <i>Methods</i>	31
3.3 <i>Results</i>	37
3.4 <i>Discussion</i>	47
3.5 <i>Rationale for Study 2</i>	55
Chapter 4: Study 2	56
4.1 <i>Introduction</i>	56
4.2 <i>Methods</i>	58
4.3 <i>Results</i>	64
4.4 <i>Discussion</i>	77
4.5 <i>Rational for Study 3</i>	84
Chapter 5: Study 3	85
5.1 <i>Introduction</i>	85
5.2 <i>Methods</i>	88
5.3 <i>Results</i>	94
5.4 <i>Discussion</i>	102
5.5 <i>Rationale for Study 4</i>	110
Chapter 6: Study 4	111
6.1 <i>Introduction</i>	111
6.2 <i>Methods</i>	113
6.3 <i>Results</i>	120
6.4 <i>Discussion</i>	125
6.5 <i>Rationale for Study 5</i>	130
Chapter 7: Study 5	131

<i>7.1 Introduction</i>	131
<i>7.2 Methods</i>	135
<i>7.3 Results</i>	142
<i>7.4 Discussion</i>	155
Chapter 8: General Discussion	162
<i>8.1 Optimization of methodology</i>	163
<i>8.1 Functional relevance</i>	167
<i>8.3 Neural pathways underlying afferent inhibition</i>	172
8.3.1 Pathway underlying SAI.....	174
8.3.2 Pathway underlying LAI.....	175
<i>8.5 Limitations</i>	176
<i>8.6 Conclusions</i>	178
Chapter 9: References	180
Chapter 10: APPENDIX A	224

Figures

Figure 1.1: TMS schematic.....	10
Figure 1.2: Schematic of afferent inhibition	13
Figure 3.1: Contralateral Sensory Nerve Action Potential	39
Figure 3.2: Contralateral LAI.....	42
Figure 3.3: Contralateral Polynomial Trends (TMS intensity 0.5 mV).....	45
Figure 3.4: Ipsilateral stimulation (FDI only).....	47
Figure 4.1: Experimental design.....	61
Figure 4.2: Experiment 1, LAI.....	68
Figure 4.3: Experiment 1, individual LAI.....	69
Figure 4.4: Experiment 1, SAI.....	72
Figure 4.5: Experiment 1, SAI individual.....	74
Figure 4.6: Experiment 2, LAI and SAI.....	77
Figure 5.1: Group-averaged MN-evoked SAI data.....	96
Figure 5.2: Group-averaged DN-evoked SAI data.	97
Figure 5.3: Group-averaged LAI data.....	100
Figure 6.1: Experimental design.....	117
Figure 6.2: Glucose and blood pressure levels	122
Figure 6.3: Afferent inhibition.....	124
Figure 7.1: Experimental timeline.	136
Figure 7.2: Maps obtained within the rest condition.	143
Figure 7.3: Maps obtained within the DN stimulation condition.	146
Figure 7.4: Maps obtained within the UN stimulation condition.	149
Figure 7.5: Pre-baseline SAI and LAI.....	152
Figure 7.6: SAI and LAI acquired at T0 and T1.....	154
Figure 8.1: Schematic of studies that address goals of the thesis.....	161
Figure 8.2: Proposed model of afferent inhibition.....	172

Tables

Table 3.1: Data sets included within each condition.	38
Table 3.2: Conover’s ANOVA statistics.....	41
Table 4.1: Experiment 1 group-averaged measures (with standard deviations).....	65
Table 4.2: Experiment 1 two-way ANOVA statistics.....	67
Table 4.3: Experiment 2 group-averaged measures (with standard deviations).....	75
Table 4.4: Experiment 2 ANOVA statistics.....	76
Table 5.1: Group-averaged data.....	95
Table 5.2: Reliability statistics.....	98
Table 6.1: Statistical Analyses.....	123
Table 7.1: Predictions with planned statistical approach and estimated sample sizes.....	157

List of Abbreviations

ACh: acetylcholine	MRI: magnetic resonance imaging
AD: Alzheimer's disease	MSO: maximum stimulator output
ANOVA: analysis of variance	MT: motor threshold
APB: abductor pollicis brevis	MTAT: motor threshold assessment tool
ATP: adenosine triphosphate	MSE: mean square error
BBB: blood brain barrier	MUMC: McMaster University Medical Centre
CoG_{AP}: center of gravity in the anterior-posterior plane	MI: primary motor cortex
CoG_{ML}: center of gravity in the medial-lateral plane	NMDA: N-methyl-D-aspartate
CSF: cerebrospinal fluid	NRS: numeric rating scale
cTBS: continuous theta burst stimulation	NS: nerve stimulation
CV: coefficient of variation	PAS: paired associative stimulation
DBP: diastolic blood pressure	PD: Parkinson's disease
DN: digital nerve	PPC: posterior parietal cortex
D-wave: direct wave	RMT: resting motor threshold
ECR: extensor carpi radialis	rTMS: repetitive transcranial magnetic stimulation
EEG: electroencephalography	SAI: short-latency afferent inhibition
EMG: electromyography	SAI_{24,MN}: SAI acquired with an ISI of 24ms, evoked by median nerve stimulation
EPSP: excitatory post-synaptic potential	SAI_{N20+4,MN}: SAI acquired with an ISI of N20+4ms, evoked by median nerve stimulation
FCR: flexor carpi radialis	SAI_{24,DN}: SAI acquired with an ISI of 24ms, evoked by digital nerve stimulation
FDI: first dorsal interosseous	SAI_{N20+4,DN}: SAI acquired with an ISI of N20+4ms, evoked by digital nerve stimulation
GABA: gamma-aminobutyric acid	SBP: systolic blood pressure
HiREB: Hamilton Integrated Research Ethics Board	SD: standard deviation
ICC: intraclass correlation coefficient	SDC_{individual}: smallest detectable change at the individual level
ICF: intracortical facilitation	SDC_{group}: smallest detectable change at the group level
IPAQ: International Physical Activity Questionnaire	SEMeas: standard error of measurement
IPSP: inhibitory post-synaptic potential	SEMeas%: relative SEMeas
IQ: intelligence quotient	SEP: somatosensory-evoked potential
ISI: interstimulus interval	SES: somatosensory electrical stimulation
I-wave: indirect wave	SICI: short-interval intracortical inhibition
LAI: long-latency afferent inhibition	SNAP: sensory nerve action potential
LAI_{MN}: LAI evoked by median nerve stimulation	SNAP_{max}: maximum SNAP amplitude
LAI_{DN}: LAI evoked by digital nerve stimulation	ST: sensory threshold
LICI: long-interval intracortical inhibition	S1: primary somatosensory cortex
LTP: long-term potentiation	S2: secondary somatosensory cortex
MAP: mean arterial pressure	TCA: tricarboxylic acid cycle
MEP: motor-evoked potential	TMS: transcranial magnetic stimulation
MEP_{conditioned}: MEP evoked by nerve stimulation paired with TMS	UN: ulnar nerve
MEP_{unconditioned}: MEP evoked by TMS alone	VAS: visual analogue scale
MET: metabolic equivalents	VPN: ventral posterior nucleus
ML-PEST: maximum-likelihood parameter estimation by sequential testing	WRST: Wilcoxon-signed rank test
MN: median nerve	

Chapter 1: Literature Review

1.1 Sensorimotor Integration

1.1.1 What is sensorimotor integration?

Activities of daily living are highly dependent upon the ability to extract relevant sensory information from the environment to shape motor output. This process of sensorimotor integration takes place across different sensory modalities and neuroanatomical structures at cortical, subcortical, and spinal levels (Flanders 2011). Notably, the integration of tactile input with corticospinal output is important for generating and executing skilled movements (Rabin and Gordon 2004). Blockade of tactile feedback at the fingers with anesthesia impairs a range of movements including reach to grasp (Gentilucci et al. 1997), typing (Rabin and Gordon 2004), and precision grip (Fisher et al. 2002).

Abnormalities in tactile-motor integration are described in various neurological conditions including Parkinson's disease (PD) (Abbruzzese and Berardelli 2003), Alzheimer's disease (AD) (Terranova et al. 2013), dystonia (Abbruzzese and Berardelli 2003), and stroke (Veldman et al. 2015). Therefore, understanding the neurophysiological mechanisms underlying sensorimotor interactions is required to learn how its disturbance leads to motor impairments. As such, this thesis will be primarily focused on the integration of somatosensory input with output from the primary motor cortex (M1).

1.1.2 Overview of the literature review

This chapter will begin by reviewing the neuroanatomical pathways that convey afferent input to S1 and efferent output from M1, and the non-invasive methods that can be used to probe the integrity of these pathways. Next, the non-invasive protocol and indirect assessment of sensorimotor integration known as afferent inhibition will be introduced. Finally, I will examine the current knowledge surrounding the acquisition of afferent inhibition, the underlying neural mechanisms, usefulness in practice and its relevance to function.

1.2 Organization of the Sensorimotor System

1.2.1 Overview of the Cerebral Cortex

The cerebral cortex is divided into six horizontal layers (Kandel et al. 2007) and is functionally regulated by a balance of excitation and inhibition. Excitatory glutamatergic pyramidal neurons are located within layers III, V, and VI. Non-pyramidal neurons diverge through horizontal projections within the cortex (Molnár and Cheung 2006), and can be further subdivided into spiny and smooth stellate cells. Spiny stellate cells, found in layer IV, are excitatory glutamatergic neurons (DeFelipe 1997; Jones 1993). Smooth stellate cells are inhibitory interneurons that release gamma-aminobutyric acid (GABA) and are found within all layers of the cortex but are most abundant in layer II/III (DeFelipe 1997; Jones 1993). These GABAergic interneurons play a major role in controlling the timing of pyramidal neuron firing (Rudy et al. 2011).

There are two major types of inhibitory GABA receptors. GABA_A receptors are ionotropic, meaning they directly open chloride ion channels in response to the binding of GABA (McCormick 1989). GABA_B receptors are metabotropic, meaning they indirectly open potassium channels through a second messenger system (McCormick 1989). Therefore, GABA_A receptors cause fast-acting inhibitory post-synaptic potentials (IPSPs; ~30 ms) while GABA_B receptors evoke slower IPSPs (~140 ms) (McCormick 1989).

Acetylcholine (ACh) is also a modulator of GABA and glutamate synaptic transmission within the cortex (Metherate and Ashe 1995). ACh binds to muscarinic and nicotinic receptors, which are found in neurons that synapse onto pyramidal neurons and interneurons (Xiang et al. 1998). It is important to understand the different neurotransmitters that interact within the motor and somatosensory cortices because it provides insight into how neuronal circuits within the cortex function and eventually regulate movement.

1.2.2 The Somatosensory System

There are four primary mechanoreceptors within the skin, each relaying distinct tactile information through mechanically gated ion channels. Slowly adapting mechanoreceptors, including Ruffini endings and Merkel cells, convey perception of texture and skin stretch (Johnson 2001). Rapidly adapting mechanoreceptors, including Meissner and Pacinian corpuscles, respond to skin indentation and vibration (Johnson 2001).

These mechanoreceptors are innervated by $A\beta$ afferent fiber types, while $A\alpha$ fibers carry proprioceptive information. Transmission of electrical potentials along afferent fibers can be quantified through the sensory nerve action potential (SNAP). The SNAP is acquired by electrically stimulating a peripheral nerve and recording potentials at a point further along the nerve. The amplitude of the SNAP increases with the application of stronger currents, reflecting the recruitment of more afferent fibers. Weak stimuli that are barely perceptible activate $A\alpha$ fibers, with progressively increasing stimulation intensities activating $A\beta$ fibers (Kandel et al. 2007). With stronger painful electrical stimulation, $A\delta$ and eventually unmyelinated C fibers are recruited, which innervate thermoreceptors and nociceptors (Kandel et al. 2007).

Afferent fibers from the upper body relay information to the central nervous system through the dorsal root ganglion and toward the brain through the cuneate nucleus of the spinal dorsal column. Neurons within the dorsal column form the medial lemniscus that decussates in the medulla, which then ascends to the ventral posterior nucleus (VPN) of the thalamus. Cutaneous input enters the medial and lateral portions of the VPN, painful sensory input is processed in the inferior portion, and proprioceptive input enters the superior portion. Neurons within the VPN project onto layer IV cells within the primary somatosensory cortex (S1), ascending through the internal capsule (Kandel et al. 2007).

S1 contains four cytoarchitectonic areas: Brodmann areas 1, 2, 3a and 3b. Areas 3a and 3b receive projections from the lateral and medial zones of the VPN and send projections to

areas 2 and 1. Area 3a receives proprioceptive information from muscle spindle afferents and area 2 from joint receptors, while 3b and 1 receive afferent input from mechanoreceptors (Kaas 1984).

The somatosensory cortex is arranged in a vertical array of cells, or columns, as first described by Mountcastle et al. (1957). These columns process discrete thalamic input, responding to a specific area of the body. These columns are therefore somatotopically organized roughly according to the body's dermatomes, making up the somatosensory homunculus (Mountcastle 1997). Cortical magnification is a defining feature of the somatosensory homunculus, as areas of the body with higher tactile acuity (i.e. smaller peripheral receptive fields) occupy more space within the homunculus. Intra- and inter-columnar projections underlie somatosensory processing. Thalamic input is relayed to pyramidal and stellate cells of layer IV in S1, which project dorsally to layers II/III. Cells within layers II/III have horizontal connections with neighboring columns and send intra-columnar projections to layer V. Axons within layer V then project out to subcortical areas including the basal ganglia, the brainstem and the spinal cord (Kandel et al. 2007).

S1 activity can be non-invasively quantified with electroencephalography (EEG). Specifically, the somatosensory evoked potential (SEP) is the electrical activity within S1 that results from peripheral stimulation. The N20 component of the SEP signals the arrival of an afferent volley within S1, and the amplitude of the N20-P25 potential increases with greater peripheral nerve stimulation intensities. SEPs evoked by cutaneous nerve

stimulation increase until all cutaneous fibers are recruited (Gandevia and Burke 1984). However, with progressively stronger mixed nerve stimulation, the N20-P25 potential increases and plateaus when 50% of fibers within a mixed nerve bundle are recruited. That is, all sensory afferent fibers recruited at this point, corresponding to 50% of the maximum SNAP (SNAP_{max}) amplitude (Gandevia and Burke 1984).

1.2.3 The Motor System

Early research had suggested that M1, similar to S1, is organized in a columnar fashion that results in topographically organized representations of the contralateral side of the body. Muscles used for finer motor control occupy greater areas within M1, leading to the formation of the motor homunculus (Penfield and Boldrey 1937). However, in more recent years, intracortical microstimulation has made it clear that the organization of M1 is more complex than previously thought. Representations of adjacent body parts within M1 show extensive overlap (Rathelot and Strick 2006). Rather than a map of individual muscles, M1 is more likely to be a map of synergistic muscle movements (Rathelot and Strick 2006).

Another defining feature of M1 is its agranular structure, wherein layer IV is essentially non-existent. Unlike other cortical sensory areas, M1 is majorly responsible for output rather than processing of sensory input from the thalamus. The lack of a granular layer IV in M1 reflects the absence of a major ascending pathway from the periphery (Shipp 2005). However, recent evidence does suggest that M1 receives excitatory input from direct

thalamocortical inputs onto pyramidal neurons in the border of layer V and layer III, reminiscent of layer IV in other sensory cortical areas (Yamawaki et al. 2014).

M1 receives afferent input from intercortical connections through layers II/III and layer VA (described in more detail below) (Mao et al. 2011). In the rat motor cortex, intracortical microstimulation experiments have revealed that cells within layers II/III show excitatory, reciprocal connections to layer V pyramidal cells (Otsuka and Kawaguchi 2008). Further, layer V pyramidal cells show reciprocal intralaminar connections to fast-spiking inhibitory interneurons, thought to shape the output from M1 (Otsuka and Kawaguchi 2009).

Pyramidal tract neurons in layer V, or upper motor neurons, form the beginning of the descending corticospinal tract. These upper motor neurons descend ipsilaterally through the internal capsule, the cerebral peduncles of the midbrain, the pons, and medulla. At the pyramidal decussation of the caudal medulla, most fibers cross the midline to form the lateral corticospinal tract, while the rest remain uncrossed to form the anterior corticospinal tract. The lateral corticospinal tract is responsible for motor control of the extremities while the anterior corticospinal tract controls axial muscles. Upper motor neurons of the lateral corticospinal tract synapse on lower motor neurons within the ventral horn of the spinal cord. These lower motor neurons exit the spinal cord ventrally through the spinal root, sending impulses peripherally to the neuromuscular junction which are transmitted to muscle fibers, resulting in muscle contraction (Kandel et al. 2007).

The seminal work by Barker et al. (1985) introduced the technique of Transcranial magnetic stimulation (TMS) to non-invasively probe the corticospinal tract. When performing TMS, an electric current is passed through a conducting coil that is placed over the scalp which in turn, induces a magnetic field perpendicular to the coil. A secondary electric field is then induced perpendicularly to this magnetic field, which causes the depolarization of cortical neurons (Hallett 2007).

Evidence of the neural populations activated by TMS comes from epidural recordings. Following a pulse of TMS to M1, two types of action potential volleys descending through the corticospinal tract can be measured in the epidural space: direct waves (D-waves) and indirect waves (I-waves). At low-moderate stimulation intensities, TMS is only able to depolarize superficial cortical layers, which results in the occurrence of I-waves. I-waves reflect the indirect, trans-synaptic activation of pyramidal neurons through superficial intracortical interneurons (Di Lazzaro et al. 2012b). As the TMS intensity increases, more I-waves are observed (I1-I4), indicating the activation of more intracortical interneurons before activation of the corticospinal tract (Di Lazzaro et al. 2012b). At very high TMS intensities, the magnetic field can penetrate deeper into the cortex and directly activate the pyramidal output neurons in M1, reflected by a D-wave in the epidural space (Di Lazzaro et al. 2012b).

Overall, TMS can be used to assess the excitability of the corticospinal tract. Following a single pulse of TMS to M1, the upper and lower motor neurons in the corticospinal tract

will be depolarized, leading to a twitch in the muscle of interest. This muscle response is known as a motor-evoked potential (MEP), and the amplitude of this response can be recorded using electromyography (EMG). The lowest TMS intensity that can evoke a MEP of $\geq 50 \mu\text{V}$ in 5 out of 10 trials is known as the resting motor threshold (RMT). RMT is an indicator of the excitability of the lowest threshold neurons within M1. The amplitude of the MEP is an indicator of corticospinal excitability. At a set TMS intensity, greater MEP amplitudes reflects greater corticospinal excitability. Increasing TMS intensity will lead to an increase in MEP amplitudes in a sigmoidal fashion (Devanne et al. 1997), and the sigmoidal relationship reflects the recruitment profile of motor neurons within the corticospinal tract. TMS has been used extensively over the past three decades to study the neuronal circuitry within the cortex, to induce neuroplasticity, and to understand the pathophysiology of neurological injury and disease.

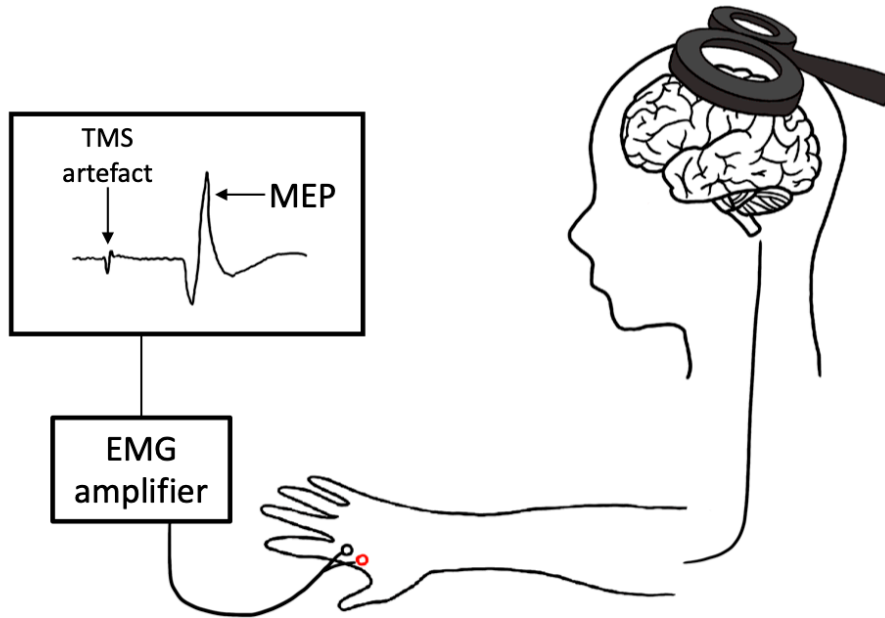


Figure 1.1: TMS schematic

A transcranial magnetic stimulation (TMS) coil is held over the left primary motor cortex (M1), eliciting a motor-evoked potential (MEP) that is recorded from the right first dorsal interosseus (FDI) muscle with surface electromyography (EMG).

1.2.4 Integration of the two anatomical systems (M1-S1 connectivity)

Multiple lines of evidence have shown that M1 and S1 are extensively interconnected. Optogenetic studies in rodents show that reciprocal connections exist between M1 and S1. S1 primarily projects to M1 through layers II/III and layer VA (Mao et al. 2011) while M1 projects to S1 through layer 1 and layers V/VI (Veinante and Deschênes 2003). These connections are organized in a somatotopic fashion, such that the same body part representations are connected between M1 and S1 (Izraeli and Porter 1995; Kaneko et al. 1994).

Electrical stimulation of infragranular S1 evokes excitatory post-synaptic potentials (EPSPs) in M1 measured through whole-cell recordings (Rocco-Donovan et al. 2011). These projections innervate both pyramidal neurons and inhibitory neurons in M1 (Caria et al. 1997; Rocco-Donovan et al. 2011; Rosén and Asanuma 1972). S1 may also have an inhibitory influence over M1, as lesions of S1 have subsequently led to increased excitability within M1 (Domenech et al. 2013; Harrison et al. 2013).

Modulation of S1 activity also induces neuroplasticity within M1. For example, lesions of monkey S1 in the forelimb or hindlimb areas induces degeneration of the corresponding representation in M1 (Jones and Powell 1969). Alternatively, upregulation of activity through tetanic stimulation of S1 induces long-term potentiation (LTP) within layers II/III of M1 (Keller et al. 1990).

The neural connections between M1 and S1 are important for motor control and learning. In animal models, induced lesions to S1 impair motor learning (Pavrides et al. 1993), gross (Gerlai et al. 2000; Kleim et al. 2007) and fine motor function (Brinkman et al. 1985; Hikosaka et al. 1985). In humans, excitatory repetitive TMS (rTMS) applied to S1 improves motor learning in individuals with chronic stroke (Brodie et al. 2014) and inhibitory rTMS over S1 impairs motor learning in healthy individuals (Vidoni et al. 2010). Further, prolonged electrical stimulation of peripheral nerves within the hand enhances motor skill acquisition in healthy individuals (Veldman et al. 2015, 2016) and in individuals with stroke (Celnik et al. 2007; Conforto et al. 2007; Wu et al. 2006).

Sensorimotor interactions can be observed through the process of afferent inhibition. Afferent inhibition is a phenomenon whereby a sensory afferent volley inhibits the motor output to a given muscle. This is observed when peripheral nerve stimulation is delivered prior to a pulse of TMS delivered to M1, resulting in inhibition of the MEP. This inhibitory phenomenon is observed at short interstimulus intervals (ISIs) of ~20-25 ms (Tokimura et al. 2000) and long ISIs of 200-1000 ms (Chen et al. 1999) between peripheral nerve stimulation and TMS. These time-dependent phases are known as short-latency afferent inhibition (SAI) and long-latency afferent inhibition (LAI), respectively. SAI is the result of afferent input suppressing late I2- and I3-waves (Tokimura et al. 2000), whereas the I-wave modulation underlying LAI has yet to be investigated.

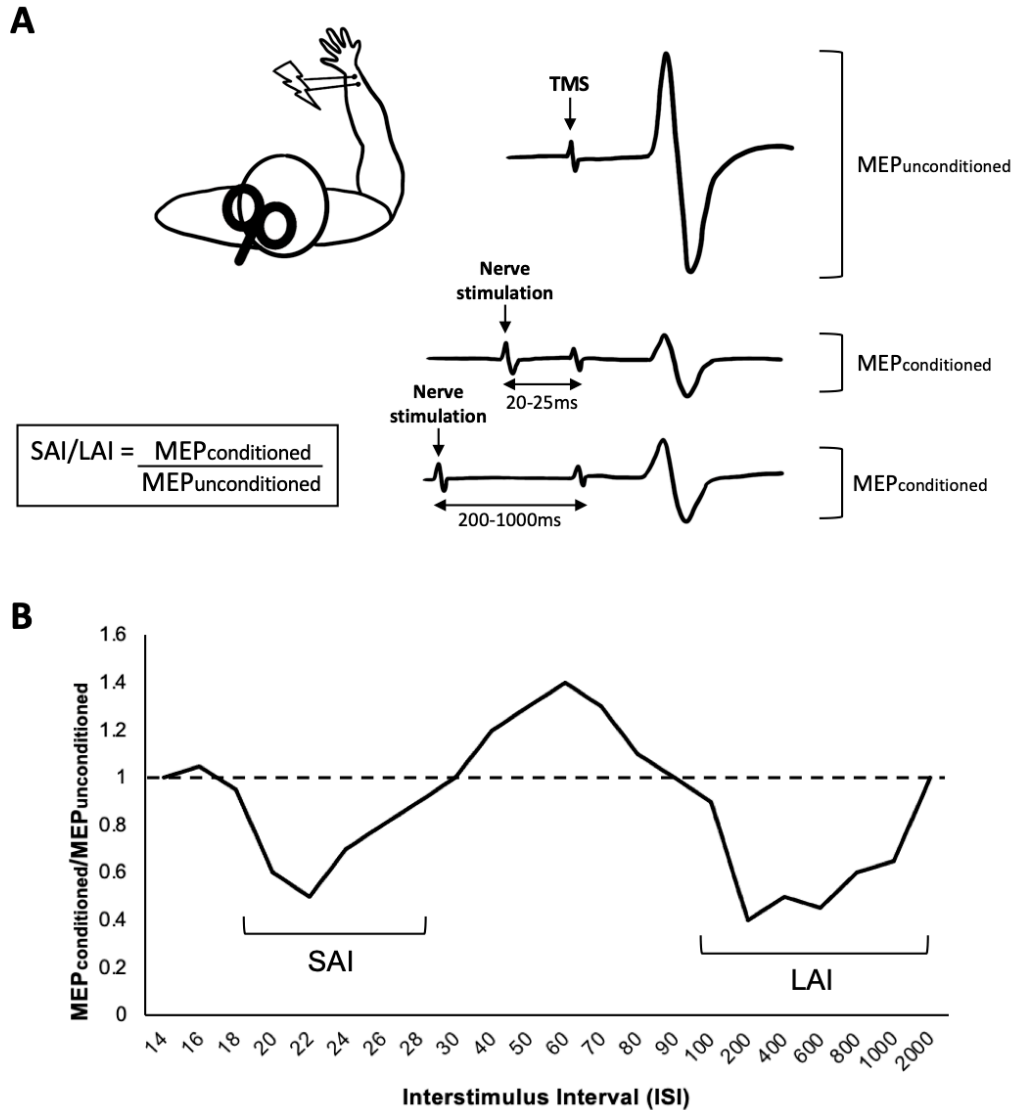


Figure 1.2: Schematic of afferent inhibition

A) Short-latency afferent inhibition (SAI) and long-latency afferent inhibition (LAI) are evoked by delivering peripheral nerve stimulation prior to transcranial magnetic stimulation (TMS) of the primary motor cortex (M1). The magnitude of inhibition is calculated as the ratio between the amplitude of the conditioned motor-evoked potential (MEP_{conditioned}; evoked by paired nerve stimulation and TMS) and the amplitude of the unconditioned MEP (MEP_{unconditioned}; evoked by TMS alone). **B)** Graph shows the afferent inhibition ratio as a function of interstimulus interval (ISI). SAI is observed at ISIs of ~20-25 ms and LAI is observed at ISIs of ~200-1000ms. Inhibition corresponds to data below the dotted line. This graph is based off of data from Tokimura et al. (2000), Devanne et al. (2009), and Chen et al. (1999).

There are a number of notable gaps in the literature that limits the usefulness of SAI and LAI in a practical setting. In the following sections of this literature review, I will discuss the past two decades of research surrounding SAI and LAI, and highlight the gaps that should be addressed in future research.

1.3 Afferent Inhibition

1.3.1 Methodological parameters of afferent inhibition

The magnitude of both SAI (Ni et al. 2011; Udupa et al. 2009) and LAI (Kukaswadia et al. 2005) decrease as a function of increasing TMS intensity. As TMS intensity is increased, a larger volume of cortical pyramidal neurons is activated, as shown by an increase in the MEP amplitude (Devanne et al. 1997). Therefore, the afferent volley evoked by nerve stimulation would be less capable of exerting an inhibitory influence over a larger population of corticospinal neurons targeted by increasing TMS intensity.

Mixed nerve bundles contain both afferent and efferent fibers, including afferents originating from muscle spindles, joint receptors, and cutaneous mechanoreceptors. However, cutaneous nerves originate solely from cutaneous mechanoreceptors. Stimulation of mixed versus cutaneous nerves activates different cytoarchitectonic areas. Despite these differences, stimulation of mixed or cutaneous nerves yields similar magnitudes of SAI (Bailey et al. 2016; Tamburin et al. 2005) and LAI (Abbruzzese et al. 2001; Chen et al. 1999).

The magnitude of SAI increases as nerve stimulation intensity is increased. However, the relationship between SAI and afferent fiber recruitment is dependent upon the type of nerve stimulated. Specifically, as nerve stimulation intensity is increased, SAI increases concomitantly with the SNAP amplitude recorded from the median nerve at the elbow and plateaus when presumably all sensory afferents have been recruited. For the cutaneous digital nerve, SAI acquired from the first dorsal interosseous (FDI) muscle increases until the 50% SNAP_{max} (i.e. when 50% of the cutaneous nerve bundle is recruited) (Bailey et al. 2016). The SNAP evoked by mixed median nerve stimulation reflects activation of both afferents and efferent fibers. Growth in the SNAP amplitude beyond 50% SNAP_{max} (i.e. when 50% of the median nerve bundle is recruited) reflects antidromic activation of motor efferents (Bailey et al. 2016). As such, SAI evoked by mixed nerve stimulation increases as the SNAP amplitude increases, but plateaus once 50% SNAP_{max} is reached (Bailey et al. 2016). Therefore, for both mixed and cutaneous nerve types, maximal SAI is achieved at nerve stimulation intensities corresponding to 50% SNAP_{max}. ***Notably, the relationship between LAI and afferent fiber recruitment has yet to be investigated.***

1.3.2 Pharmacology of afferent inhibition

The use of pharmacology in TMS literature has provided considerable knowledge of the neural mechanisms that underlie various TMS measures. In these studies, known as pharmaco-TMS studies, a TMS measure is assessed before and after the administration of a drug with a known mode of action within the central nervous system. Changes in the TMS

measure following drug administration would indicate that the neural circuit being probed is mediated by the neurotransmitter or neurotransmitter receptor targeted by the drug.

Pharmacology-TMS studies have led to the discovery that MEPs are regulated by glutamate and GABA as ketamine, an N-methyl-D-aspartate (NMDA) antagonist, increases MEP amplitudes (Di Lazzaro et al. 2003) and benzodiazepines, positive allosteric modulators of the GABA_A receptor, decrease MEP amplitudes (Borojerdj et al. 2001). Furthermore, noradrenaline and serotonin agonists both increase MEP amplitudes, suggesting that these neurotransmitters are also involved in the modulation of corticospinal output (Borojerdj et al. 2001; Ilić et al. 2003).

It is well known that ACh plays an important role in the generation of SAI. In their seminal paper, Di Lazzaro et al. (2000b) found that intravenous injection of scopolamine, a muscarinic antagonist, reduces SAI. A subsequent investigation found that acetylcholinesterase inhibitors increase SAI (Di Lazzaro et al. 2005c). Nicotine, a neuromodulator of cholinergic activity, has also been found to modulate SAI. In non-smoking individuals, administration of nicotine increases SAI (Grundey et al. 2013). Further, SAI is greater in smoking compared to non-smoking individuals (Lang et al. 2008).

Di Lazzaro et al. (2007a) investigated the role of the GABA_A receptor in SAI through the administration of various benzodiazepines. Benzodiazepines upregulate GABA_A receptor activity through the benzodiazepine binding site (Sieghart 1995). Diazepam had no effect

on SAI, while lorazepam and zolpidem reduced SAI (Di Lazzaro et al. 2007a). Diazepam binds non-selectively to GABA_A receptors containing $\alpha 1$, $\alpha 2$, $\alpha 3$, or $\alpha 5$ subunits (Möhler 2002; Möhler et al. 2004). Alternatively, zolpidem has high affinity for the $\alpha 1$ subunit, while the affinity profile of lorazepam is unknown (Möhler 2002; Möhler et al. 2004). Therefore, the results by Di Lazzaro et al. (2007a) suggest that SAI is mediated by GABA_A receptors containing the $\alpha 1$ subunit.

Finally, recent research has shown that SAI is reduced following acute or chronic administration of reboxetine, a noradrenaline reuptake inhibitor (Kuo et al. 2017). In human cortical slices, noradrenaline has been shown to inhibit the release of ACh (Vizi and Pasztor 1981). This may suggest that the reduction in SAI following reboxetine administration is the result of noradrenergic-induced suppression of cholinergic activity.

Importantly, *the neurotransmitter or neurotransmitter receptors that underlie LAI are unknown*. Only one study to date has investigated the neurotransmitter basis of LAI. This study found that administration of lorazepam had no effect on LAI (Teo et al. 2009). However, this study acquired LAI at the ISI of 100 ms rather than 200 ms, when LAI is maximal (Chen et al. 1999) and consistently present (Sailer et al. 2002). Therefore, an additional investigation is warranted to determine if LAI is modulated by GABA_A receptor activity.

Other TMS research suggests that LAI is modulated by GABA_B receptor activity. Specifically, LAI inhibits long-interval intracortical inhibition (LICI) (Sailer et al. 2002, 2003). LICI is a TMS measure that is acquired when two suprathreshold pulses of TMS are delivered to M1 with a temporal separation of 50-200 ms (Valls-Solé et al. 1992). Administration of baclofen, a GABA_B receptor agonist, increases LICI (McDonnell et al. 2006). This suggests that LICI is mediated by GABA_B receptor activity. This is likely since GABA_B receptors result in slower IPSPs, corresponding to the longer ISIs used for LICI (Douglas and Martin 1991). Therefore, a future study should investigate whether LAI is reflective of GABA_B receptor activity.

1.3.3 Is afferent inhibition useful in practice?

SAI and LAI are abnormally reduced in various clinical populations. SAI is typically reduced in cognitively impaired populations such as AD (Di Lazzaro et al. 2004, 2006, 2007b, 2008; Marra et al. 2012; Martorana et al. 2009; Nardone et al. 2006), vascular dementia (Nardone et al. 2008b, 2011), dementia with Lewy bodies (Marra et al. 2012), and mild cognitive impairment (Nardone et al. 2012a; Tsutsumi et al. 2012a). Further, SAI is reduced in movement disorders such as PD (Lim et al. 2017; Pelosin et al. 2016; Rochester et al. 2012) and dystonia (Avanzino et al. 2008) and following neurological injury including stroke (Oliviero et al. 2005) and spinal cord injury (Bailey et al. 2015). LAI is also impaired in movement disorders such as PD (Sailer et al. 2003) and dystonia (Richardson et al. 2009), although it is unknown if LAI is also reduced in cognitively impaired populations. For a comprehensive list of studies investigating SAI and LAI in

clinical populations, see Table 2 in Turco et al. (2018b). Overall, these findings suggest that measures of afferent inhibition may prove to be useful biomarkers of function. Indeed, recent studies have shown the potential of SAI as a tool for differential diagnosis of various forms of dementia (Benussi et al. 2017) and mild cognitive impairment (Padovani et al. 2018) subtypes.

In order to achieve greater utility of SAI/LAI in both basic and clinical neuroscience settings, further information regarding the reliability and confounding factors that contribute to the variability in these measures is required. Importantly, rigorous reliability testing within the field is sparse. This is concerning, considering that the validity of a testing technique is dependent on the outcome measure being characterized by low systematic and random error. Only one study has assessed the test-retest reliability of median nerve-evoked SAI and reported a moderate reliability with an Intraclass Correlation Coefficient of 0.67 (Brown et al. 2017). However, as discussed earlier, mixed versus cutaneous nerve stimulation leads to activation of different Brodmann areas within S1. ***It is unknown if the test-retest reliability of SAI is dependent upon the type of nerve stimulated.*** Further, ***the reliability of LAI has yet to be investigated.***

In order to improve the reliability of these measurement techniques, confounding factors should be controlled to minimize measurement error. One factor that may contribute to quality of TMS research is diet. Despite comprising only 2% of body mass, the brain consumes 20% of the body's glucose-derived energy (Mergenthaler et al. 2013). Glucose

is required for many aspects of neurotransmission including generation of action potentials, maintenance of ionic gradients, and neurotransmitter synthesis (Mergenthaler et al. 2013). However, despite the importance of glucose in neural function, its role in sensorimotor integration is unclear.

Several studies have investigated the influence of glucose and carbohydrates on TMS measurements. Specterman et al. (2005) assessed MEPs before and after ingestion of Lucozade, an energy drink containing 68 g of glucose and 46 mg of caffeine. Participants were also administered control solutions in three additional sessions, which includes a caffeine only drink, a glucose only drink, and water. MEP area increased following ingestion of Lucozade, caffeine and glucose ingestion. However, only the glucose condition induced an increase in MEP area that persisted for as long as two hours, and this increase was correlated with the rise in blood glucose levels (Specterman et al. 2005).

In healthy controls, Badawy et al. (2013) assessed changes in cortical and corticospinal excitability following ingestion of a meal, which induced a significant rise in blood glucose levels. Meal ingestion reduced LICI, with no change in the resting motor threshold (Badawy et al. 2013). These results suggest that feeding induces an reduction in intracortical inhibition. Finally, Gant et al. (2010) assessed active MEPs (i.e. MEPs acquired during voluntary contraction) before and after ingestion of a carbohydrate solution in a placebo-controlled, double-blinded protocol. Active MEP amplitudes increased by

~30% following ingestion of the carbohydrate solution compared to the placebo (Gant et al. 2010).

It is unknown whether glucose levels modulate afferent inhibition. Research in the rat cortex has shown that glucose upregulates the activity of the GABA_A receptor (Anju et al. 2010). Given that upregulated GABA_A receptor activity reduces SAI (Di Lazzaro et al. 2005b, 2005a, 2007a), this may suggest that elevated glucose levels have an inhibitory effect on SAI. Further, populations that exhibit impaired afferent inhibition also demonstrate abnormal glucose metabolism. For example, those with AD display reduced cerebral glucose metabolism, and those with PD show cortical hypometabolism with subcortical hypermetabolism of glucose (Mergenthaler et al. 2013). It is important to explore the influence of confounding factors such as diet and glucose levels on afferent inhibition so as to minimize both inter- and intra-individual variability in these measures. This will ultimately optimize the acquisition of these measures and aid in their clinical utility as diagnostic tools and biomarkers of function.

1.3.4 Relationship between afferent inhibition and sensorimotor function

The relationship between afferent inhibition and motor function remains unclear. Afferent inhibition is reflective of the inhibitory control that the somatosensory system has on the corticospinal tract and as such, it can be used as a proxy for understanding the role of sensory input on modulating motor output (Turco et al. 2018b). However, the nature of this

modulation is unclear. Afferent circuits are hypothesized to exert their inhibitory effects on motor output via GABAergic mechanisms (Di Lazzaro et al. 2007a; Turco et al. 2018a).

Evidence suggests that afferent inhibition modulates motor output at the cortical level in a centre-surround fashion. For example, afferent inhibition in the hand is stronger following homotopic stimulation (stimulation near target muscle) versus heterotopic stimulation (stimulation distant from target muscle) (Classen et al. 2000; Tamburin et al. 2001; Voller et al. 2005, 2006). One recent investigation showed that electrical stimulation shapes corticospinal output by inducing centre-inhibition and surround-facilitation, such that the location where TMS evoked the strongest SAI corresponded to the representation of the hand muscle that was homotopic to the nerve that was electrically stimulated (Dubbioso et al. 2017). Indeed, neuroimaging studies in humans have shown that long-range projections from S1 innervate M1 in a somatotopic manner (Izraeli and Porter 1995; Kaneko et al. 1994).

It is unknown if afferent inhibition modulates motor cortex organization. Previous work suggests that cortical representations are under GABAergic control (Jacobs and Donoghue 1991). Temporary deafferentation of the forearm with ischemic nerve blocks induce an enlargement of M1 representations for muscles proximal to the nerve block (Brasil-Neto et al. 1992, 1993; Ridding and Rothwell 1995; Werhahn et al. 2002). This is accompanied by a decrease in the amplitude of the N20 (Hayashi et al. 2019) and P25 (Mercier et al. 2018) SEP potentials and a rapid increase in sensorimotor cortical GABA levels (Levy et al.

2002). Given that SAI is directly related to the amplitude of the N20-P25 potential (Bailey et al. 2016) and is reduced by GABA_A receptor agonists (Di Lazzaro et al. 2007a), this may indicate that the resulting enlargement of muscle representations following ischemic nerve block is mediated by a *release of afferent inhibition* (Vallence et al. 2012b).

Evidence that afferent inhibition plays a role in M1 organization may also be speculated from studies in PD. Individuals with PD display impaired SAI and LAI (Dubbioso et al. 2019; Sailer et al. 2003) and, interestingly, shifted and enlarged representations of hand muscles compared to healthy controls (Filippi et al. 2001; Thickbroom et al. 2006). It is possible that the neurodegenerative changes that accompany this disease may impair inhibitory sensorimotor circuitry, leading to dynamic reorganisation in M1 and overactivity of motor cortical circuitry (Thobois et al. 2000; Valls-Solé et al. 1994).

Finally, the relationship between afferent inhibition and cutaneous function remains unclear. Cutaneous sensory enrichment is achievable using somatosensory electrical stimulation (SES) applied to the digits. SES refers to the prolonged stimulation of a peripheral nerve via electrical or mechanical stimulation (Lesemann et al. 2015). SES enhances temporal (Erro et al. 2016; Rocchi et al. 2017) and spatial tactile acuity of the digit (Lesemann et al. 2015) and increases the size of the digit representation in S1 (Hodzic et al. 2004; Pleger et al. 2003). Further, SES increases paired-pulse inhibition of SEPs and short-interval intracortical inhibition (SICI), suggesting an increase in inhibition within S1 and M1 (Rocchi et al. 2017). Kojima et al. (2018, 2019) found that 20 minutes repetitive

mechanical stimulation of the entire index fingertip temporarily decreases MEPs within the FDI muscle of the same hand. Therefore, mechanical stimulation of the digit tip can induce an inhibitory influence over the corticospinal tract. Overall, this research demonstrates that manipulation of sensory afferents through cutaneous sensory enrichment is capable of inducing neuroplastic changes in the somatosensory and motor pathways. However, no study has investigated the impact of cutaneous sensory enrichment on M1 organization. Further, *it is unknown if cutaneous sensory enrichment modulates afferent inhibition.*

Chapter 2: Thesis Overview

2.1 Goals and impact of the thesis

Afferent inhibition is a phenomenon that can be observed when pairing peripheral nerve stimulation with Transcranial magnetic stimulation (TMS). Depending on the latency between these two stimuli, short-latency afferent inhibition (SAI) or long-latency afferent inhibition (LAI) can be observed.

Multiple studies over the past two decades have shown that the magnitude of inhibition is significantly reduced in various populations with cognitive and sensorimotor impairments, most notably in Alzheimer's disease (AD) and Parkinson's disease (PD) (Turco et al. 2018b). Therefore, afferent inhibition may have potential clinical utility such that it can be used as a biomarker for sensorimotor and/or cognitive function, to further understand the pathophysiology of these conditions, and to develop new therapeutic strategies. However, before this clinical utility can be achieved, there are several unanswered questions at the basic neuroscience level that must be addressed.

The overall goal of the thesis is to further our knowledge of afferent inhibition by addressing two main questions: (1) What is the functional relevance of afferent inhibition, and (2) How can the acquisition of afferent inhibition be optimized? I address these questions through a series of experiments that explore the neurophysiological, neurometabolic, and neuroplastic mechanisms that interact with afferent inhibition. The

studies within the thesis have additional implications in providing insight into the neural pathways that underly afferent inhibition.

2.2 Summary of studies

Chapter 3 (Study 1) will investigate the relationship between LAI and the sensory nerve action potential. As discussed in the previous chapter, SAI scales with the volume of sensory afference recruited by peripheral nerve stimulation (Bailey et al. 2016). However, it is unknown if the magnitude of LAI is also dependent on the volume of sensory afference.

Chapter 4 (Study 2) will address the pharmacology of afferent inhibition. As discussed in the previous chapter, SAI is modulated by GABA_A receptor activity (Di Lazzaro et al. 2005b, 2005a, 2007a). However, it is unknown if (1) LAI is also modulated by GABA_A receptor activity, or (2) if SAI/LAI are modulated by GABA_B receptor activity.

Chapter 5 (Study 3) will quantify the test-retest reliability of afferent inhibition. One previous study found that SAI has moderate relative reliability (Brown et al. 2017). However, the test-retest reliability of LAI in a healthy population remains unknown. Further, it is unknown if the reliability of SAI and LAI differs when evoked by stimulating different nerve types.

Chapter 6 (Study 4) will investigate the role of glucose in afferent inhibition. Given the significant amount of inter- and intra-individual variability in afferent inhibition, it is

unknown if factors such as diet or glucose levels contribute to this variability. Therefore, this study will determine whether or not afferent inhibition is modulated by glucose, and if glucose levels should be accounted for prior to experimental sessions.

Chapter 7 (Study 5) will address the role of afferent inhibition in sensorimotor neuroplasticity. Somatosensory electrical stimulation (SES) is a neuroplasticity-inducing protocol that has been shown to temporarily enlarge muscle representations within M1. This study will investigate the change in afferent inhibition following SES and assess the relationship between afferent inhibition and M1 reorganization. This study will also provide valuable information regarding the somatosensory system's role in governing M1 organization and the cortical mechanisms underlying sensorimotor integration.

Chapter 3: Study 1

Modulation of Long-Latency Afferent Inhibition by the Amplitude of the Sensory Afferent Volley

Turco, C.V., El-Sayes, J., Fassett, H.J, Chen, R., & Nelson, A.J. (2017). Modulation of long-latency afferent inhibition by the amplitude of sensory afferent volley. *Journal of Neurophysiology*, 118, 610-618.

3.1 Introduction

Sensorimotor integration may be investigated by quantifying the influence of peripheral somatosensory inputs on corticospinal excitability using transcranial magnetic stimulation (TMS) paired with preceding nerve stimulation. A single pulse of TMS delivered to the primary motor cortex (M1) results in a motor evoked potential (MEP) in the muscle of interest, which reflects the integrity of the corticospinal tract (Bestmann and Krakauer 2015). Peripheral nerve stimulation applied at specific interstimulus intervals (ISIs) prior to the TMS pulse results in MEP inhibition or facilitation. Short-latency afferent inhibition (SAI), a circuit mediated by GABA_A and acetylcholine receptors (Di Lazzaro et al. 2000b, 2007a), occurs when the TMS pulse follows median or digital nerve stimulation by ~19-21 ms (Tokimura et al. 2000). Median nerve afferent facilitation is observed at ISIs ranging from 45-70 ms (Devanne et al. 2009). However, at longer ISIs ranging from ~200-1000 ms, both median and digital nerve stimulation inhibit MEPs, a circuit called long-latency afferent inhibition (LAI) (Chen et al. 1999).

LAI occurs through the conditioning of corticospinal output by stimulation of the cutaneous digital nerve (DN) or the mixed median nerve (MN) (Chen et al. 1999; Sailer et al. 2003).

Peripheral nerve stimulation activates the primary somatosensory (S1), bilateral secondary somatosensory (S2), and contralateral posterior parietal (PPC) cortices (Boakye et al. 2000; Korvenoja et al. 1999). Therefore, the sensory afferent volley is thought to indirectly inhibit M1 through mechanisms involving the widespread activation of sensory areas (Chen 2004; Sailer et al. 2002, 2003). LAI is altered in clinical populations with sensory deficiencies including Parkinson's disease (Sailer et al. 2003, 2007) and focal hand dystonia (Abbruzzese et al. 2001; Richardson et al. 2009) further implicating the involvement of sensory areas in the genesis of LAI. LAI is also reduced following the resolution of pain (Burns et al. 2016) and in those with complex regional pain syndrome (Morgante et al. 2017). In healthy individuals, LAI has been shown to enhance surround inhibition, a process that may contribute to movement accuracy through the suppression of non-moving muscles (Voller et al. 2005). Further research is required to explore the functional significance of the LAI circuit. It is speculated that LAI is of cortical origin since spinal F-waves are unchanged during the acquisition of median nerve LAI (Chen et al. 1999). However, the precise neural mechanism and pharmacological basis of the LAI circuit remains unknown.

Little is known about the relationship between the magnitude of the sensory afferent volley and the depth of LAI. For DN, LAI is greatest at a stimulation intensity of three times the sensory threshold (ST) for detection of the electrical stimulus and plateaus at higher nerve stimulation intensities (Chen et al. 1999). However, it remains unclear how the depth of LAI relates to the sensory afferent volley, a measure that is achievable by recording the

peripheral sensory nerve action potential (SNAP) that follows nerve stimulation. To date, no studies have examined the relationship between the SNAP amplitude and the magnitude of LAI for either the DN or MN. In contrast, the SAI circuit evoked by DN and MN is reported to increase until full recruitment of sensory afferent fibers (Bailey et al. 2016).

The magnitude of LAI may also be influenced by the intensity of TMS delivered to M1. LAI decreases when the TMS intensity is increased from 1 mV to 4 mV (Kukaswadia et al. 2005; Sailer et al. 2002). However, the magnitude of LAI does not change with TMS intensities ranging from 0.2 mV to 1 mV (Kukaswadia et al. 2005; Sailer et al. 2002). Two TMS intensities were used in this study, 0.5 mV and 1 mV. Therefore, while the magnitude of LAI should not differ between these two TMS intensities, the influence of the sensory afferent volley on MEP amplitude may be dependent on the TMS intensity and therefore impact the relationship between SNAP and LAI magnitude.

The present study explores the relationship between the sensory afferent volley and LAI for the cutaneous DN and the mixed MN at two TMS intensities. One study has demonstrated ipsilateral MN evoked LAI (Chen et al. 1999), yet it remains unclear whether ipsilateral DN evoked LAI exists, and whether the magnitude of LAI reflects the sensory afferent volley. Therefore, we also investigated the relationship between DN and MN LAI and SNAPs when nerve stimulation was delivered to the ipsilateral limb (i.e. ipsilateral to the delivery of the TMS pulse). Our results indicate that the magnitude of contralateral MN LAI increases until all sensory fibers are presumably recruited as assessed with the SNAP

(i.e. $\sim 50\%$ SNAP_{max}) (Bailey et al. 2016) and follows a U-shaped function, a relationship that is contingent on the TMS intensity. In contrast, contralateral DN LAI first appears, is maximum and plateaus by $\sim 50\%$ SNAP_{max}, and this relationship is unaltered by the TMS intensities tested. LAI was evoked following ipsilateral MN but not DN stimulation. This study provides insight about the neural mechanisms mediating LAI and offers practical implications for studies assessing sensorimotor integration using this circuit.

3.2 Methods

Participants

Young, right-handed individuals participated in one (Experiment 1: n = 20; 15 females; 23.4 ± 5.2 years) or two (Experiment 2: n = 18; 14 females; 23.2 ± 5.5 years) experiments. All individuals were screened for contraindications to TMS, completed a modified handedness questionnaire (Oldfield 1971), and provided written consent prior to participation. The research was approved by the McMaster Research Ethics Board and conformed to the declaration of Helsinki.

Electromyography

In experiment 1, surface electrodes (9 mm Ag-AgCl electrodes) were used to record EMG from the right limb including the first dorsal interosseous (FDI) and abductor pollicis brevis (APB) muscles, and SNAP from the MN at the elbow proximal to the medial epicondyle. In experiment 2, EMG was recorded from the right FDI muscle and SNAP from the MN on the left arm. A wet ground was secured around the forearm, distal to the elbow. EMG

recordings were amplified 1000x (Intronix Technologies Corporation Model 2024F, Bolton, Canada) and band-pass filtered between 20 Hz and 2.5 kHz. Using an analog-to-digital interface (Power1401, Cambridge Electronics Design, Cambridge, UK), data were digitized at 5 kHz and analyzed using commercial software (Signal v6.02, Cambridge Electronics Design, Cambridge, UK).

TMS Parameters

TMS was performed using a customized figure-of-eight “branding iron” coil (50 mm diameter), connected to a Magstim 200² stimulator (Magstim, UK) and delivered to the left hemisphere. Specifically, the coil was positioned over the motor hotspot of the right FDI muscle. The motor hotspot was identified as the location that elicited the largest MEP in the relaxed FDI with the coil orientated at a 45-degree angle from the sagittal plane to induce a posterior-anterior current. The location of the motor hotspot was registered digitally using the Brainsight Neuronavigation system (Rogue Research, Canada). The ISI between the nerve stimulus (NS) and TMS pulse was set to 200 ms (Chen et al. 1999).

Sensory Nerve Action Potentials (SNAPs)

SNAPs were recorded from the MN at the elbow (described above) from the right (Experiment 1) or left (Experiment 2) limb. For MN stimulation, SNAPs were elicited using a bar electrode placed over the MN at the wrist with cathode proximal using a constant current stimulator (Digitimer DS7AH; square wave pulses 0.5 ms, 2 Hz). To determine SNAP_{max}, the starting nerve stimulation intensity was set to the motor threshold (MT) for

the APB muscle. MT was defined as the minimum intensity (in mA) required to evoke a visible twitch in the APB muscle belly. Fifty stimuli were delivered and the peak-to-peak amplitude of the averaged SNAP was quantified. This procedure continued in stepwise increments of 2 mA until SNAP_{max} was achieved. The SNAP_{max} was defined as the intensity (in mA) at which the SNAP ceased to increase by 10% in three consecutive blocks of fifty trials. Following the acquisition of SNAP_{max} , the current was lowered until the following amplitudes of SNAP were found: 25%, 50%, and 75% SNAP_{max} (i.e. until the averaged SNAP amplitude after fifty trials matched the amplitude corresponding to approximately 25%, 50%, or 75% SNAP_{max}). Following this procedure, participants rated the sensation of the nerve stimulus on a scale of mild, moderate, strong, or painful for each of the four intensities (25%, 50%, 75%, 100% SNAP_{max}). If the sensation was deemed painful, they were asked to rate the pain on a scale of 0 to 10 according to the Numeric Rating Scale (NRS) (Hawker et al. 2011). If participants rated pain greater than 7 on the scale then the stimulation intensity was not increased further. This ensured that participants never received painful stimulation since LAI is reduced 15 minutes following the resolution of a painful stimulus (Burns et al. 2016).

For DN stimulation, SNAPs were elicited using ring electrodes placed around the proximal and middle segments of digit 2 (index finger) with the cathode proximal (Digitimer DS7AH; square wave pulses 0.5 ms, 2 Hz). To determine SNAP_{max} , the starting nerve stimulus intensity was set to sensory threshold (ST) defined as the minimum current (in mA) required for the participant to detect the presence of the electrical stimulus. The peak-

to-peak SNAP was quantified as the average of the 100 stimuli and this procedure was repeated at stepwise increments of 1 mA until SNAP_{max} was achieved (as defined above). Again, following the acquisition of SNAP_{max} , the current was lowered until the following amplitudes of SNAP were found: 25%, 50%, and 75% SNAP_{max} . The aforementioned pain rating was performed as described above.

Experiment 1: Contralateral LAI

LAI was tested at two TMS intensities whereby the TMS intensity was set to elicit an averaged MEP with peak-to-peak amplitude of ~1 mV or 0.5 mV in the right FDI muscle. EMG was recorded from the FDI and APB muscles. For each TMS intensity, twenty unconditioned MEPs (i.e. TMS only) and twenty conditioned MEPs were acquired (i.e. nerve stimulation – TMS) for each SNAP percentage (25%, 50%, 75%, 100% SNAP_{max}). The order of SNAP percentage delivery was randomized using a William's square design for each nerve. The orders of TMS intensity (1 mV, 0.5 mV) and nerve stimulated (MN, DN) were pseudo-randomized across participants.

Experiment 2: Ipsilateral LAI

TMS intensity was maintained to evoke an unconditioned MEP of 1 mV. The TMS coil was positioned over the FDI motor hotspot in the left hemisphere for acquiring MEPs from the FDI muscle of the right hand. The ipsilateral (left) arm received DN or MN stimulation in an order pseudo-randomized across participants. EMG recordings were recorded from the FDI muscle. SNAPs were acquired as outlined above to obtain 25%, 50%, 75%, and

100% SNAP_{max}. Twenty unconditioned MEPs were acquired (i.e. TMS alone), and for each SNAP amplitude, twenty conditioned MEPs were acquired.

Statistical Analyses

All MEP data were visually inspected and any trials that were contaminated with EMG activity prior to the TMS artefact were discarded. Specifically, a trial was discarded if the peak-to-peak EMG signal within a 160 ms window between the nerve and TMS stimuli was greater than twice the peak-to-peak EMG signal in a 20 ms window prior to the nerve stimulus. Data for a given participant at a particular SNAP percentage was only included if more than 75% of trials remained following visual inspection. Table 1 shows the number of participants whose data sets were included in the analyses for each SNAP percentage. Group level analysis included outlier analysis and normality testing via Shapiro-Wilk test. For all normally distributed data, an ANOVA was performed and post-hoc tests used Tukey's tests. For non-normally distributed data, the data were ranked data and a Conover's ANOVA was performed whereby post-hoc testing used Wilcoxon-signed ranks tests (WSRT) (Conover and Iman 1982). The following statistical analyses were based on the results of the above normality tests. For the analysis of SNAPs, first, the actual SNAP amplitudes recorded corresponding to the intended 25%, 50%, 75% and 100% SNAP_{max} bins were computed. The group-averaged SNAP amplitude at each percentage of SNAP_{max} was compared against neighbouring SNAP percentages via WSRT. This analysis was used to determine whether SNAP amplitudes within each percentage bin were statistically different from their neighbouring bins. Next, the absolute amplitude of SNAP_{max} (in μV)

was compared between the MN and DN using a two-tailed paired t-test to confirm the larger SNAPs associated with MN as shown previously (Bailey et al. 2016). Finally, the percentage growth of SNAPs was calculated for each bin (25-50%, 50-75% and 75-100% SNAP_{max}) and subject to a two-way Conover's ANOVA using within-subjects factor INTERVAL (3 levels: 25-50%, 50-75%, 75-100%) and NERVE (2 levels; DN, MN).

For Experiment 1, a three-way repeated measures Conover's ANOVA was performed using within-subjects factors NERVE (2 levels: DN, MN), MUSCLE (2 levels: FDI, APB), and SNAP (5 levels: TMS alone, 25%, 50%, 75%, 100% SNAP_{max}) for each of TMS intensity 1 mV and 0.5 mV. Separate ANOVAs were performed for each TMS intensity (0.5 mV and 1 mV) in order to assess the LAI and SNAP relationship within a specific TMS intensity. No statistical comparisons were made between TMS intensities. For Experiment 2, a two-way repeated measure Conover's ANOVA was performed using within-subjects factors NERVE (2 levels: DN, MN) and SNAP (5 levels: TMS alone, 25%, 50%, 75%, 100% SNAP_{max}).

Finally, the unconditioned and conditioned MEP amplitudes from the contralateral 0.5 mV TMS condition were plotted and a second-order polynomial trend line was fitted to the data. For all analyses, significance was set to $\alpha < 0.05$. Table 1.2 provides the results of all statistical analyses.

3.3 Results

Experiment 1: Contralateral LAI

In total, data from twenty and nineteen participants were collected for the MN and DN, respectively. One individual opted to not partake in the DN component of this experiment. The precise number of data sets included in the analyses (following trials discarded due to excessive EMG) is listed in Table 3.1. The actual group-averaged SNAP percentages (\pm standard deviation) for MN were 25% (\pm 2.2%), 49% (\pm 1.9%), 75% (\pm 2.4%), and 100% SNAP_{max} and for DN were 29% (\pm 6.9%), 51% (\pm 4.3%), 73% (\pm 4.5%), and 100% SNAP_{max}, and each SNAP amplitude was significantly different from neighbouring percentages (WSRT, all $p < 0.001$). For simplicity, we have used the labels of 25%, 50%, 75% and 100% on the plots and in our discussion of the results. Three participants for both MN and DN rated the 100% SNAP_{max} as mild according to the NRS pain scale (NRS average 3.3). No participant rated nerve stimulation as severe (i.e. greater than 7 on the NRS scale). Sample SNAPs from one individual are shown in Figure 3.1A following MN (left) and DN (right) stimulation. The MN SNAP_{max} was significantly greater than DN SNAP_{max} as shown in Figure 3.1B (two-tailed paired t-test, $p < 0.001$). Figure 3.1C displays the percentage change in SNAP amplitude with nerve stimulation intensities. A two-way Conover's ANOVA revealed a main effect of INTERVAL ($F_{(2,30)} = 72.33$, $p < 0.001$) and NERVE ($F_{(1,15)} = 5.20$, $p = 0.038$). However, post-hoc tests indicate no significant difference between nerves (WSRT, $p = 0.195$). For the main effect of INTERVAL, the largest growth in the SNAP occurred between \sim 25-50% of SNAP_{max} (WSRT, $p < 0.001$). The change in SNAP amplitude, while still significant, was much less between 50% and

75% SNAP_{max} (WSRT, $p < 0.001$). Similarly, the change in SNAP amplitude between 75% and 100% SNAP_{max} was significantly less than the change between 50% and 75% SNAP_{max} (WSRT, $p < 0.001$). Therefore, despite the difference in the absolute amplitude of the DN versus MN evoked SNAP, both nerve types display similar growth patterns with the largest changes occurring between 25% and 50% SNAP_{max}.

Table 3.1: Data sets included within each condition.

Condition	FDI					APB				
	TMS alone	25%	50%	75%	100%	TMS alone	25%	50%	75%	100%
Contralateral										
1 mV MN	20	20	20	19	20	19	18	17	18	18
1 mV DN	19	19	19	19	17	18	18	18	18	18
0.5 mV MN	20	20	20	20	20	19	19	18	19	19
0.5 mV DN	19	19	19	19	19	19	18	19	18	19
Ipsilateral										
MN	16	16	16	16	16					
DN	15	15	15	15	15					

FDI, first dorsal interosseous muscle; APB: abductor pollicis brevis muscle; TMS, transcranial magnetic stimulation; MN, median nerve; DN, digital nerve.

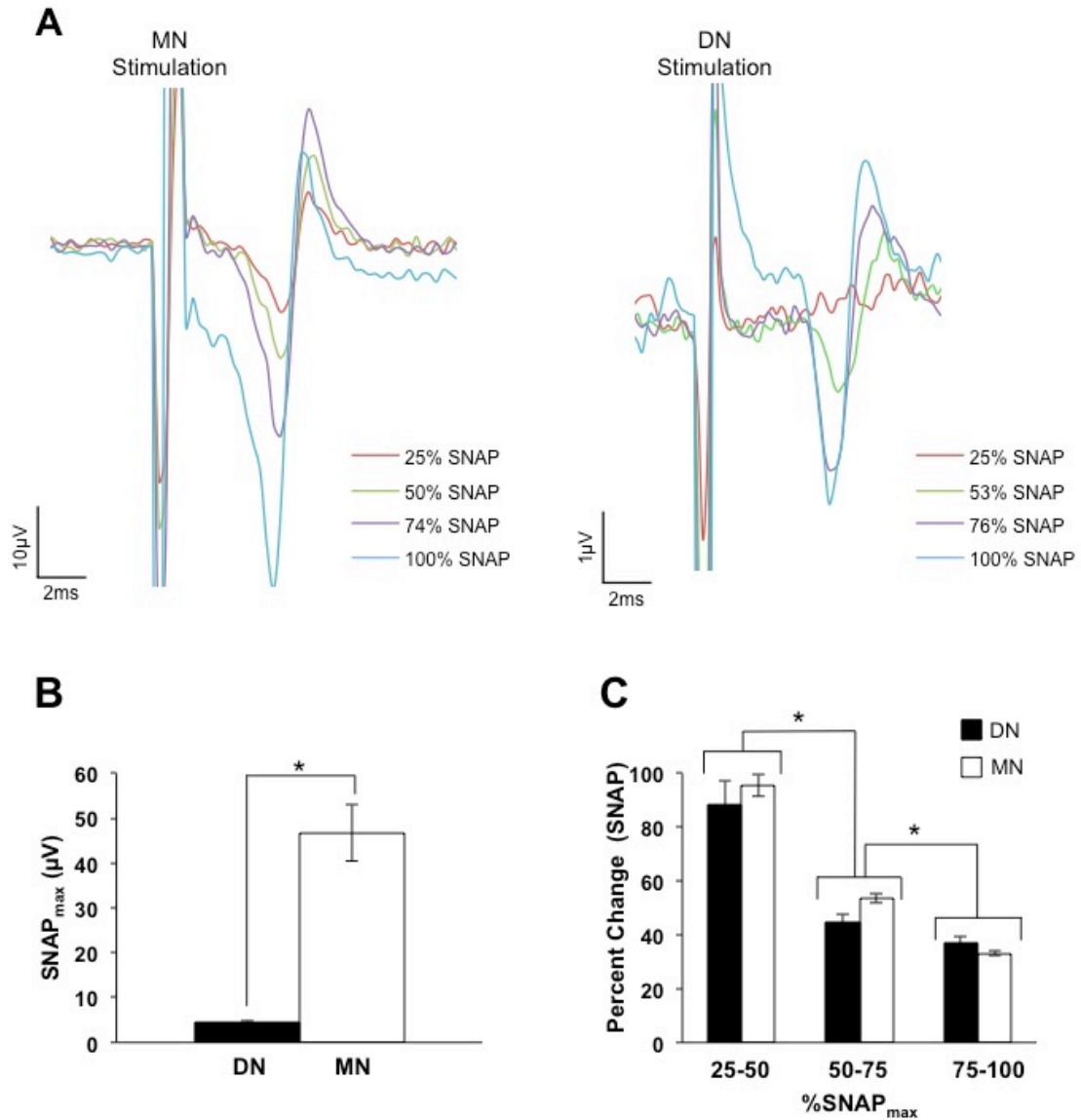


Figure 3.1: Contralateral Sensory Nerve Action Potential

A) Average sensory nerve action potential (SNAP) recorded from one participant at each percentage of SNAP_{max} following MN (left) or DN (right) stimulation. The percentages of SNAP_{max} correspond to that individual's data and are not the group-averaged percentages of SNAP_{max}. **B)** The absolute values (in μV) of group-averaged 100% SNAP_{max} recorded from the median nerve and digital nerve. * indicates a significant difference between nerves (Cohen's $d = 2.08$). **C)** The group-averaged percent change of the SNAP for each interval of % SNAP_{max}. * indicates a significant difference between intervals of % SNAP_{max}. A significantly greater change in SNAP was seen between 25-50% SNAP_{max} compared to 50-75% SNAP_{max} (Cohen's $d = 1.89$). Additionally, the change in SNAP amplitude between 50-75% SNAP_{max} was significantly greater than the change between 75-100% SNAP_{max}

(Cohen's $d = 1.54$). Furthermore, the SNAP grows similarly for each increment of change between both nerves.

TMS 1 mV

Table 3.2 shows the complete statistical analyses. Figure 3.2A (left) shows the group-averaged MEPs (with standard errors) for each nerve and muscle. Conover's ANOVA revealed a main effect of NERVE ($F_{(1,13)} = 5.81, p = 0.031$), MUSCLE ($F_{(1,13)} = 5.04, p = 0.043$), SNAP ($F_{(4,52)} = 21.12, p < 0.001$) and a NERVE*SNAP interaction ($F_{(4,52)} = 8.74, p < 0.001$) as plotted in Figure 3.2A (right). The main effect of muscle revealed that the MEP amplitude from the APB muscle was greater than that of the FDI muscle (WSRT, $p < 0.001$). The interaction revealed differences between the two nerves at 25% SNAP_{max} (shown as #, WSRT, $p < 0.001$). Other than at 25% SNAP_{max}, there was no difference in the magnitude of LAI obtained between nerves. Further, for the MN, LAI existed at all percentages of SNAP_{max} (shown as *, WSRT, all $p < 0.001$) and the maximum depth of LAI was observed by 25% SNAP_{max}. For the DN, LAI was present at 50%, 75%, and 100% SNAP_{max} (shown as *, WSRT, all $p < 0.01$) and was not increased beyond 50% SNAP_{max}. Therefore, for both nerve types, once LAI was present it did not increase significantly with additional gains in the SNAP amplitude. Collectively, the data obtained at a TMS intensity of 1 mV indicate that MN and DN LAI do not continue to increase despite the increase in the amplitude of the SNAP.

Table 3.2: Conover’s ANOVA statistics.

Condition	Degrees of freedom	<i>F</i> -statistic	<i>P</i> value	Effect size (partial η^2)
Contralateral TMS 1mV*				
Nerve	1, 13	5.81	0.031	0.31
Muscle	1, 13	5.04	0.043	0.28
SNAP	4, 52	21.12	<0.001	0.62
Nerve × Muscle	1, 13	0.28	0.604	0.02
Nerve x SNAP	4, 52	8.74	<0.001	0.40
Muscle x SNAP	4, 52	1.07	0.361	0.07
Nerve x Muscle x SNAP	4, 52	1.12	0.354	0.08
Contralateral TMS 0.5mV*				
Nerve	1, 15	0.78	0.390	0.07
Muscle	1, 15	5.64	0.031	0.27
SNAP	4, 60	11.16	>0.001	0.43
Nerve x Muscle	1, 15	2.12	0.16	0.12
Nerve x SNAP	4, 60	3.45	0.013	0.19
Muscle x SNAP	4, 60	0.86	0.439	0.05
Nerve x Muscle x SNAP	4, 60	0.41	0.718	0.03
Ipsilateral**				
Nerve	1, 13	4.72	0.049	0.267
SNAP	4, 52	2.86	0.032	0.181
Nerve x SNAP	4, 52	0.89	0.476	0.064
DN ipsilateral***				
SNAP	4, 56	1.51	0.228	0.098
MN ipsilateral***				
SNAP	4, 60	2.61	0.044	0.149

SNAP, sensory nerve action potential. * Three-way Conover’s ANOVA (ranked data). ** Two-way Conover’s ANOVA (ranked data). *** One-way Conover’s ANOVA (ranked data). Bolded values indicate significance as shown.

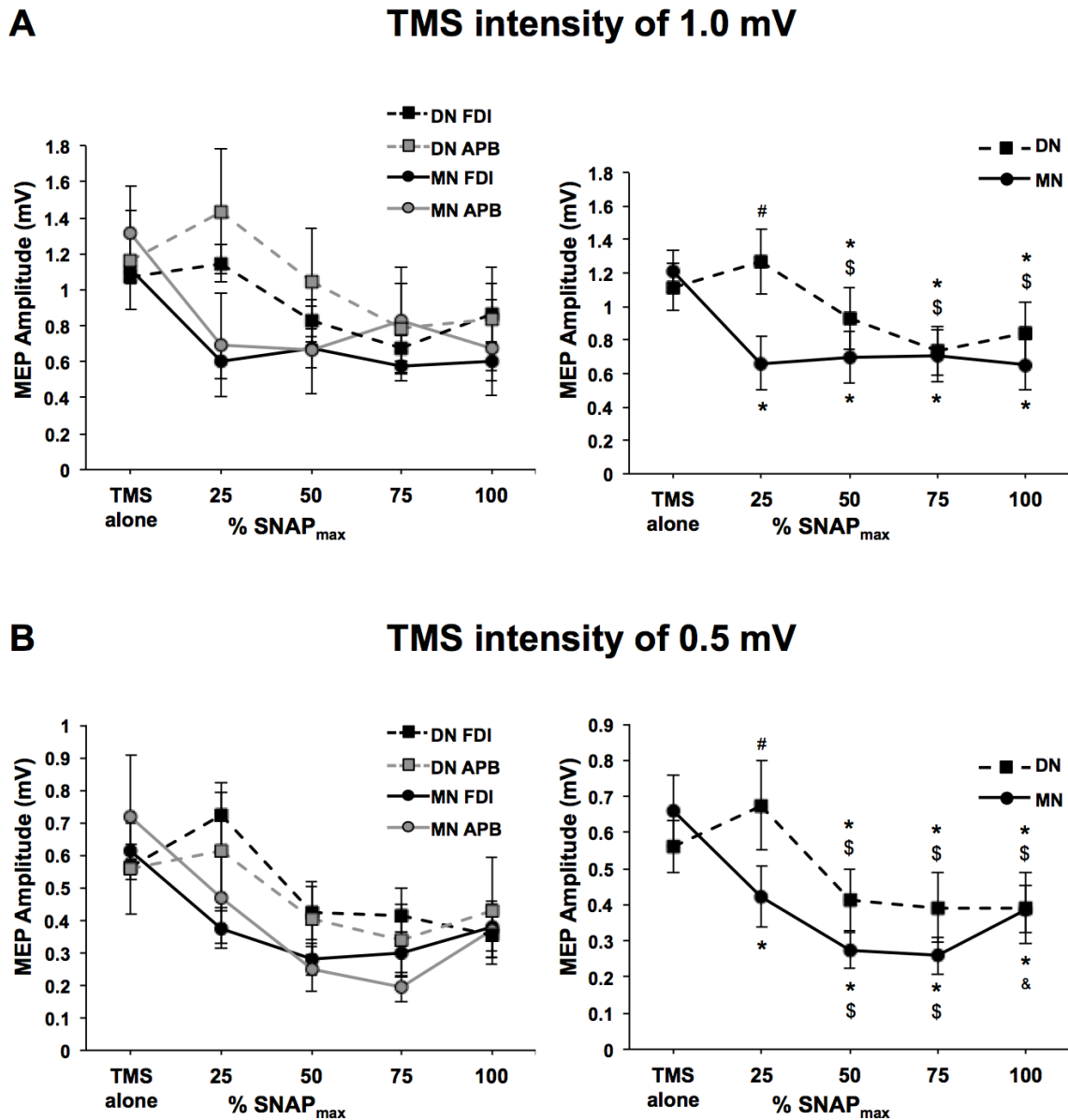


Figure 3.2: Contralateral LAI.

A) TMS 1 mV condition: three-way Conover's ANOVA plot (left) and the NERVE*SNAP interaction (right). Both graphs show the group-averaged MEP amplitude (\pm standard error) in each condition. # indicates that the conditioned MEP amplitude is greater for DN than MN (Cohen's $d = 0.78$). * indicates the presence of LAI (i.e. significance difference from TMS alone). \$ indicates inhibition greater than that seen at 25% $SNAP_{max}$. For the MN, LAI was present at all percentages of $SNAP_{max}$ (Cohen's $d = 0.85, 0.82, 0.79, 0.89$, respectively). For the DN, LAI was present at 50%, 75%, and 100% $SNAP_{max}$ (Cohen's $d = 0.26, 0.62, 0.38$, respectively). For the DN, LAI observed at 25% $SNAP_{max}$ is significantly smaller than at 50%, 75%, and 100% $SNAP_{max}$ (Cohen's $d = 0.41, 0.71, 0.51$, respectively).

B) TMS 0.5 mV condition: three-way ANOVA plot (left) and the NERVE*SNAP

interaction (right). Both graphs show the group-averaged MEP amplitude (\pm standard error) in each condition. # indicates that the conditioned MEP amplitude is greater for DN than MN (Cohen's $d = 0.55$). * indicates the presence of LAI (i.e. significant difference from TMS alone). \$ indicates inhibition greater than that seen at 25% SNAP_{max}. The '&' indicates that, for the MN, the conditioned MEP amplitude at 100% SNAP_{max} is greater than at 75% SNAP_{max} (Cohen's $d = 0.49$). For the MN, LAI was present at all percentages of SNAP_{max} (Cohen's $d = 0.59, 1.12, 1.15, 0.74$, respectively). For the DN, LAI was present at 50%, 75%, and 100%SNAP_{max} (Cohen's $d = 0.42, 0.43, 0.46$, respectively). For the MN, LAI observed at 25% SNAP_{max} is significantly smaller than at 50% and 75% SNAP_{max} (Cohen's $d = 0.49, 0.52$, respectively). For the DN, LAI observed at 25% SNAP_{max} is significantly smaller than at 50%, 75%, and 100% SNAP_{max} (Cohen's $d = 0.57, 0.59, 0.59$, respectively).

TMS 0.5 mV

Figure 3.2B (left) plots the group-averaged MEPs (with standard errors) for each nerve and muscle. Conover's ANOVA revealed main effects of MUSCLE ($F_{(1,15)} = 5.64, p = 0.031$), and SNAP ($F_{(3,60)} = 11.16, p < 0.001$) and a NERVE*SNAP interaction ($F_{(4,60)} = 3.45, p = 0.013$) shown in Figure 3.2B (right). The main effect of muscle revealed that the MEP amplitude from the FDI muscle was greater than that of the APB muscle (WSRT, $p < 0.001$). The interaction revealed differences between the two nerves at 25% SNAP_{max} (shown as #, WSRT, $p < 0.01$). Other than at 25% SNAP_{max}, there were no differences in between the nerves. For MN, the interaction revealed that LAI existed at all percentages of SNAP_{max} (shown as *, WSRT, all $p < 0.001$) similar to the TMS 1 mV data described above. Additionally, the maximum depth of LAI was observed at 50% SNAP_{max} and LAI did not grow beyond this intensity. However, in contrast to the TMS 1 mV data above, the depth of MN LAI increased from 25% to 50% SNAP_{max} (different from 25% shown as \$, WSRT, $p < 0.01$) indicating that the additional contribution of sensory fibers leads to further increases in the magnitude of LAI in this range. Last, for MN stimulation, we note that LAI is decreased from 75% to 100% SNAP_{max} (shown as &, WSRT, $p < 0.01$). For DN

LAI, the results were similar to the TMS 1 mV data. Specifically, LAI was present at 50%, 75%, and 100% SNAP_{max} (shown as *, WSRT, all $p < 0.01$) with no further increases in LAI beyond 50% SNAP_{max}.

To examine the trend in LAI as a function of current intensity and percentage of SNAP_{max}, second-order polynomial trend lines were plotted (Figure 3.3) for each nerve. Polynomial trends lines were made for the 0.5 mV TMS intensity only since MN LAI in this condition showed a dose-dependent relationship. MT and multiples of ST commonly used in the literature are plotted for comparison. For the MN, MT corresponds with ~50% SNAP_{max} while for DN, ST corresponds to ~25% SNAP_{max}. Two and three times ST correspond to ~50% and 75% SNAP_{max}.

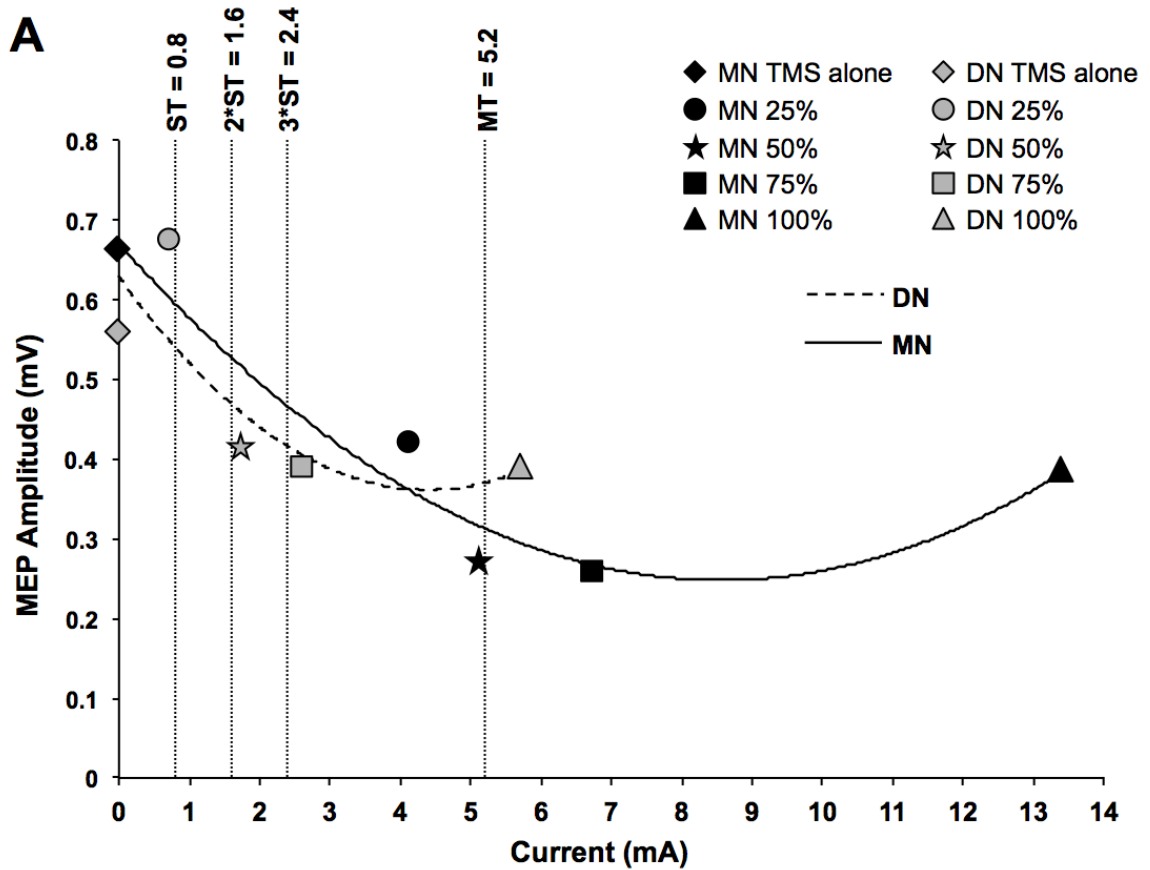


Figure 3.3: Contralateral Polynomial Trends (TMS intensity 0.5 mV).

A) Data averaged across muscles for LAI following contralateral nerve stimulation. Second-order polynomial trend lines show the conditioned MEP amplitude changes following increases in SNAP for each nerve. The conditioned MEP amplitude decreases (i.e. more inhibition) and trends towards a maximum at 50% SNAP_{max} for both MN and DN. Shown on this graph is the average motor threshold (MT), sensory threshold (ST), 2 x ST and 3 x ST.

Experiment 2: Ipsilateral LAI

Data from seventeen participants was collected in Experiment 2. One participant opted not to partake in the MN component and another did not partake in the DN component of this experiment. Therefore, in total, sixteen data sets were collected for each nerve. However, Table 3.1 displays the precise number of data sets included in each level of the analyses following exclusion of trials based on the inclusion criteria. The actual group-averaged

SNAP percentages for MN were 25% ($\pm 1.8\%$), 51% ($\pm 2.0\%$), 75% ($\pm 2.5\%$), and 100% SNAP_{max} and for DN were 28% ($\pm 5.7\%$), 49% ($\pm 4.7\%$), 75% ($\pm 4.5\%$), and 100% SNAP_{max}. Each SNAP amplitude was significantly different from neighbouring percentages (WSRT, all $p < 0.001$). Two and three participants rated MN and DN 100% SNAP_{max} as moderate on the NRS pain scale, respectively (NRS average 5.9). No participants rated nerve stimulation as severe (i.e. > 7 on the NRS scale).

Figure 3.4 plots the group-averaged MEP amplitudes (with standard errors) at each percentage of SNAP_{max}. Conover's ANOVA revealed a main effect of NERVE ($F_{(1,13)} = 4.72$, $p = 0.049$) such that the MEP amplitude averaged across stimulus intensities for DN was greater than that observed for MN (WSRT, $p = 0.041$). Therefore, one-way Conover's ANOVAs were performed for each nerve separately. For the MN, there was a main effect of SNAP ($F_{(4,60)} = 2.61$, $p = 0.044$) such that LAI occurs at 50%, 75%, and 100% SNAP_{max} (WSRT, all $p < 0.05$). However, the magnitude of inhibition is smaller following ipsilateral stimulation compared to contralateral stimulation ($\sim 15\%$ ipsilateral versus $\sim 40\%$ contralateral). For the DN, there was no effect of SNAP indicating that LAI does not occur following ipsilateral DN stimulation.

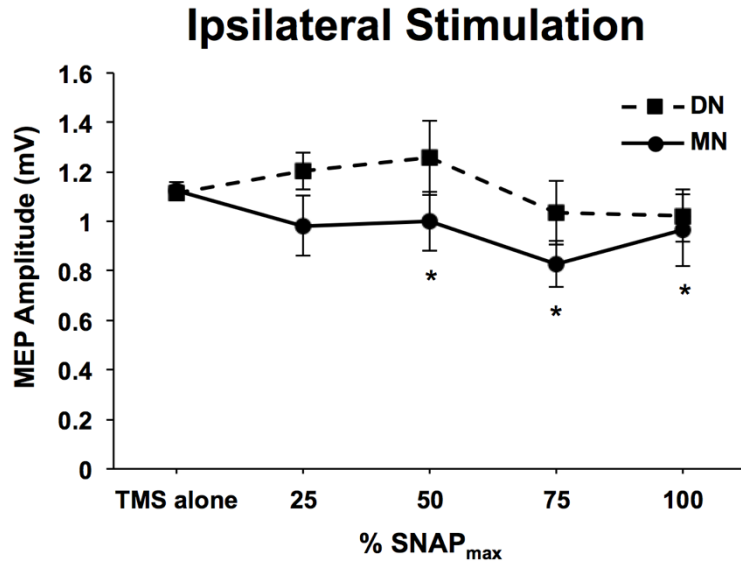


Figure 3.4: Ipsilateral stimulation (FDI only).

Graph of both one-way Conover’s ANOVAs, one for each nerve. Group-averaged MEP amplitude (\pm standard error) for each nerve at each percentage of SNAP_{max}. * indicates the presence of LAI (i.e. significance difference from TMS alone) for ipsilateral MN stimulation at 50%, 75%, and 100% SNAP_{max} (Cohen’s $d = 0.35, 1.07, 0.39$, respectively). LAI was not present at any SNAP amplitude following ipsilateral DN stimulation.

3.4 Discussion

This study examined the relationship between the sensory afferent volley and the depth of LAI. Novel findings include the observation that LAI reflects increases in the volume of the afferent volley up until $\sim 50\%$ SNAP_{max} for the mixed MN, indicating that LAI increases until presumably all sensory fibers are recruited (see below). Notably, this was only observed for the TMS intensity of 0.5 mV. For the DN, LAI appeared at $\sim 50\%$ SNAP_{max} and further increases in SNAP did not yield changes in LAI. We also observed that ipsilateral MN but not DN stimulation evokes LAI, although the magnitude of inhibition is quite small compared to the contralateral stimulation (MN: $\sim 15\%$ ipsilateral versus $\sim 40\%$

contralateral). We discuss these findings and their practical implications to basic and clinical research below.

Median Nerve LAI

The MN is a mixed nerve bundle containing both motor efferent and sensory afferent nerve fibers. A previous study examining SNAPs and somatosensory evoked potentials (SEPs) showed that SEPs plateaued at 50% of the MN SNAP_{max} but continued to increase until 100% of the DN SNAP_{max} (Bailey et al. 2016). It was speculated that for MN, all sensory afferent fibers were recruited by 50% SNAP_{max} and subsequent increases in SNAP were contributed by motor efferents (Bailey et al. 2016). Therefore, in this study we speculate that sensory afferents contribute to the MN SNAP until ~50% of the SNAP_{max}, after which further increases in SNAP may result from the addition of antidromic efferent fibers. Following MN stimulation, we observed LAI at all percentages of SNAP_{max}, irrespective of TMS intensity. For the TMS intensity of 0.5 mV, the depth of LAI grew from 25% to 50% SNAP_{max}. It is notable that it is within this range of 25% to 50% SNAP_{max} when the SNAP itself demonstrated the largest increase (Figure 1.1C). That is, where the contribution of sensory afferents was greatest, an increase in LAI was observed. Therefore, we conclude that the magnitude of LAI increases with the added recruitment of sensory afferent fibers. Of note, we did not observe this effect using the stronger 1 mV TMS protocol, which may have masked the subtle effects of the sensory afferent volley that are observable at lower TMS intensities. One explanation is that a TMS intensity that evoked ~1 mV MEP would activate a larger number of corticospinal neurons compared to an intensity that evoked MEP

of 0.5 mV. The afferent volley at a set nerve intensity will activate a given population of neurons within M1. Therefore, for 25% SNAP_{max}, TMS set to 1 mV may result in the activation of a larger number of neurons that are influenced by the peripheral afferent volley compared to 0.5 mV, thereby leading to maximum LAI for the 1 mV intensity. Increasing TMS intensity from 0.5 mV to 1 mV would lead to the recruitment of late I-waves but also increase the amplitude of early I waves (Di Lazzaro et al. 2012b). While SAI predominately inhibits late I-waves (Di Lazzaro et al. 2012b; Ni et al. 2011), it is not known whether LAI predominately inhibits early or late I-waves. How the effects of LAI on different I waves influence the effects of TMS intensity requires further study. Collectively, these data suggest that maximal MN LAI occurs via 1) a TMS intensity to recruit a large population of neurons that are influenced by the sensory afferent volley (i.e. ~1 mV MEP), and by 2) increasing the volume of sensory afferents to achieve the maximum influence on a set population of motor neurons, which may explain the increase in LAI from 25% to 50% for TMS at 0.5 mV.

We observed that the conditioned MEP increased from 75% to 100% SNAP_{max} (i.e. less inhibition). One explanation for this change may relate to the ascending re-afferent signal that occurs following the muscle twitch in APB. Such input may have interfered with the opportunity to observe inhibition. In support of this idea, LAI in the APB muscle is reduced immediately following 15 minutes of muscle vibration (Lapole and Tindel 2015). It is notable that this occurred for the MN but not the DN stimulation that did not produce muscle twitch. Therefore, the relationship between MN LAI and the sensory afferent volley

appears to be very similar to that reported for the SAI circuit whereby SAI increases to ~50% SNAP_{max} and demonstrates a U-shaped function with modest decreases in SAI beyond 75% SNAP_{max} (Bailey et al. 2016). Further, we observed that MN stimulation leads to ~40% inhibition of the MEP for LAI circuit and this is similar to the maximum magnitude of MN SAI (Bailey et al. 2016).

Finally, we observed that LAI occurs following stimulation of the ipsilateral MN at 50% SNAP_{max} and greater. This is consistent with previous research that showed ipsilateral MN stimulation set to MT is able to elicit LAI (Chen et al. 1999), and in our study 50% SNAP_{max} aligned with MT (Figure 3.4). Chen et al. (1999) showed ~20% inhibition in the FDI muscle at this ipsilateral nerve stimulation intensity and our data demonstrates ~10% inhibition at 50% SNAP_{max}. Slight differences in the amount of inhibition may be attributed to the muscle hotspot targeted (FDI here versus APB in Chen et al. (1999)).

Digital Nerve LAI

DN is composed of purely sensory fibers that determine the SNAP amplitude until presumably SNAP_{max} is achieved (Bailey et al. 2016). Following DN stimulation, LAI was present at ~50% SNAP_{max} and beyond for both TMS intensities tested. It is notable that ~50% of SNAP_{max} equated with 2 x ST (Figure 3.4), and one study demonstrated that 2 x ST was the minimum intensity to observe DN LAI (Chen et al. 1999). Activation of nerve fibers is dependent on stimulation intensity, such that larger diameter fibers have lower activation threshold (Hennings et al. 2005). Lower stimulation intensities activate large

diameter fibers such as the $A\alpha$ and $A\beta$ afferent fibers, and smaller diameter fibers, such as the sensory $A\delta$ and C fibers, are recruited with increasing stimulus intensities (Boyd and Kalu 1979). It is likely that DN stimulation causes activation of lower threshold (i.e. larger diameter) sensory fibers, leading to DN LAI mediated by these fibers.

Despite the growth in SNAP that was contributed by the recruitment of sensory afferent fibers up to 100% SNAP_{max}, the depth of LAI did not increase beyond its first appearance at ~50% SNAP_{max}, a finding that occurred irrespective of TMS intensity. These data indicate that the sensory afferent volley dictates the appearance of LAI such that a certain volume of sensory afferent fibers is required to evoke the circuit (i.e. ~50% SNAP_{max} and 2 x ST). Therefore, the addition of sensory fibers does not yield concomitant changes in the magnitude of LAI beyond its first appearance. However, we note that DN LAI is reported to be maximum at 3 x ST (Chen et al. 1999), which corresponds to ~75% SNAP_{max} in our study. Therefore, we conclude that DN LAI is maximum in the range of 2-3 x ST and is not impacted by further recruitment of sensory fibers that act to increase the amplitude of the SNAP. We also note that DN LAI has a different relationship with the sensory afferent volley compared to the DN SAI circuit. DN SAI increases until 100% SNAP_{max} is achieved (i.e. all cutaneous afferent fibers are recruited) (Bailey et al. 2016). Our data indicates that DN LAI is less reliant on the sensory afferent volley once a minimum afferent volley to activate the circuit is achieved. We did not observe LAI following ipsilateral DN stimulation at any SNAP percentage.

Comparison of LAI between Nerves

For contralateral nerve stimulation, we did not observe a difference in the magnitude of LAI between the nerve types. That is, when LAI existed for DN, its depth was not different for the MN. This was somewhat surprising since the stimulated MN includes proprioceptive afferents and is responsible for the cutaneous innervation of digits 1, 2 and 3 while our DN stimulation was selective for the cutaneous innervation of digit 2 only (Tubbs et al. 2011). However, there were differences between nerves that may indeed be attributed to the difference in sensory afferent volume. First, MN LAI was observed at 25% SNAP_{max} while a greater afferent volley was required of the DN to reach the threshold for LAI appearance (~50% SNAP_{max}). Differences in the induction of LAI between the nerves may also be attributed to differences in the composition of the nerve fibers, such as the contributions of muscle spindle afferent fibers in the MN but not in the DN. Muscle spindle afferents provide proprioceptive input that projects directly to M1 from the thalamus or relayed through area 3a (Huffman and Krubitzer 2001). It is likely that this proprioceptive information will reach M1 quicker than the sensory information obtained by the DN that first project to S1. The differences in timing or path traversed between the nerve types may account for the observation that DN does not demonstrate LAI at 25% SNAP_{max}. We studied four increments of SNAP_{max}, and it is possible that smaller increments may have exposed the stimulus-response relationship more precisely for the DN LAI between 25% and 50% SNAP_{max} (i.e. 35% and 45% SNAP_{max}). Second, once present, DN LAI does not demonstrate evidence of a response contingent on the sensory afferent volley while MN LAI is increased from 25% to 50% SNAP_{max} (as described above). Last, we observed

ipsilateral MN LAI but not DN LAI, a finding that may be explained by the wider spread cortical termination of the MN versus DN afferent volley whereby the MN activates somatosensory loci responsive to inputs derived from cutaneous and proprioceptive sources, and their combination.

Practical Implications

This study provides practical methodological implications for future studies aiming to evoke LAI. The first implication of this research stems from the stimulus-response relationship between the depth of LAI and the SNAP amplitude. For MN stimulation, LAI grew up until 50% SNAP_{max}, which equated to the stimulus intensity required to obtain MT in the APB muscle (Figure 1.3). Therefore, stimulation at MT would be expected to evoke the maximum LAI. Furthermore, studies using DN stimulation to evoke LAI would benefit from nerve stimulation intensities at 50% SNAP_{max} or greater, as no LAI was observed at 25% SNAP_{max} in this study. Therefore, based on our results, stimulation at the ST in the index finger would not be expected to evoke LAI. Rather, stimulation at 2-3 xST would be expected to evoke maximum LAI. A second implication is the use of LAI as marker for recovery following neurological disease or injury. To reveal changes in the magnitude of MN LAI, MN stimulation should be set between 25% and 50% SNAP_{max}, with a TMS intensity adjusted to a 0.5 mV MEP. For DN LAI, one might consider delivering smaller incremental changes in nerve intensity to achieve SNAPs between 25% and 50%, or alternatively, test both 25% SNAP_{max} and 50% SNAP_{max}. In a healthy young population, this would demonstrate the emergence of LAI.

Limitations

We studied LAI using an ISI of 200 ms since this was previously shown to evoke the maximum amount and most consistent magnitude of LAI in the FDI muscle (Chen et al. 1999; Sailer et al. 2002). However, LAI can be evoked from ISIs ranging from 200-1000 ms (Chen et al. 1999). Therefore, these findings may or may not extend to other ISIs. Next, our population tested consisted of healthy young adults, and it is unclear whether the same results would exist in older or special populations. Finally, the majority of our participants were females. While the effects of biological sex on LAI are unknown, it is possible that our observations are driven largely by the female population.

3.5 Rationale for Study 2

Prior to the initiation of this thesis, it was clear that there was a large volume of research in this field attempting to optimize SAI acquisition and understand the pharmacology underlying this TMS measure. However, there was a notable paucity of research dedicated to LAI. In Study #1, I was able to address this gap in the field by characterizing the relationship between LAI and sensory afference. However, there is a lack of research investigating the pharmacology of LAI. Therefore, the purpose of Study #2 was to address another large gap of knowledge in the field by determining whether LAI was also related to GABAergic neurotransmission.

Chapter 4: Study 2

Effects of Lorazepam and Baclofen on Short- and Long-latency Afferent Inhibition

Turco, C.V., El-Sayes, J., Locke, M.B., Chen, R., Baker, S., & Nelson, A.J. (2018). Effects of lorazepam and baclofen on short- and long-latency afferent inhibition. *Journal of Physiology*, 529(21), 5267-5280.

4.1 Introduction

The afferent volley evoked by peripheral nerve stimulation is capable of modifying the neural output of the primary motor cortex (M1), as assessed using transcranial magnetic stimulation (TMS). This phenomenon, known as afferent inhibition, occurs at short (i.e. short-latency afferent inhibition, SAI) and long latencies (i.e. long-latency afferent inhibition, LAI). SAI occurs when the nerve stimulus precedes a TMS pulse by an interval approximately equal to the time required for the sensory afferent input to reach the somatosensory cortex (~20-25 ms) (Tokimura et al. 2000), while LAI occurs between 200-1000 ms (Chen et al. 1999). SAI is reduced in populations with cognitive deficits such as Alzheimer's disease (Nardone et al. 2006, 2008a) and mild cognitive impairment (Nardone et al. 2012a; Yarnall et al. 2013). Abnormal LAI is seen in individuals with sensorimotor deficits including Parkinson's disease (Sailer et al. 2003) and complex regional pain syndrome (Morgante et al. 2017). Further, the magnitude of SAI and LAI decline with age (Bhandari et al. 2016; Young-Bernier et al. 2012, 2014, 2015), possibly reflecting an age-related decline in sensorimotor function (He et al. 2017). Therefore, measures of afferent inhibition can be used to assess the integrity of the sensorimotor system and probe sensorimotor function. For a detailed review of this topic, see Turco et al. (2018b).

Pharmacological studies have provided insight into the neural genesis of SAI (Ziemann et al. 2015). SAI is reduced following intravenous injection of scopolamine, a muscarinic antagonist (Di Lazzaro et al. 2000b), leading to the conclusion that SAI is mediated by cholinergic transmission. This is further supported by findings of reduced SAI in disorders of cognition, which have underlying cholinergic deficits (Nardone et al. 2006, 2008a). SAI is also reduced by lorazepam, a positive allosteric modulator of the GABA_A receptor, indicating a role for GABAergic neurotransmission in the genesis of SAI (Di Lazzaro et al. 2005a, 2005b, 2007a). In contrast to SAI, the neural mechanisms that mediate LAI are less understood. LAI was unaltered by GABA_A agonists lorazepam and zolpidem in a double-blinded, non-placebo-controlled study (Teo et al. 2009). However, in this study LAI was tested with the interstimulus interval of 100 ms when inhibition is not always present (Chen et al. 1999).

The present study aimed to explore the role of GABAergic neurotransmission in the genesis of LAI. In a double-blinded, placebo-controlled study, we assessed LAI in response to lorazepam (positive allosteric modulator of the GABA_A receptor) and baclofen (GABA_B agonist), and investigated SAI for comparison with other reports. Our novel findings indicate that LAI was reduced in the presence of lorazepam, which enhanced GABA_A transmission, but not by the GABA_B agonist, baclofen. Consistent with previous findings, SAI was also reduced in the presence of lorazepam (Di Lazzaro et al. 2005a, 2005b, 2007a).

4.2 Methods

Ethical Approval

This study was approved by the Hamilton Integrated Research Ethics Board (HIREB 2731). The research conformed to the standards set by the latest revision of the declaration of Helsinki, except for registration in a database. After explanation of the study protocol, the usual action and potential side-effects of lorazepam and baclofen, all participants provided written informed consent prior to participation.

Participants

Fourteen healthy, right-handed males (mean age: 22.7 ± 1.9 years) participated in Experiment 1 and ten of these individuals (mean age: 23.1 ± 1.7 years) returned to participate in Experiment 2. All participants were screened for contraindications to TMS, lorazepam and baclofen. Right-hand dominance was confirmed by a modified handedness questionnaire (Oldfield 1971). All pharmaceuticals and the randomization schedules were prepared by the McMaster University Medical Centre (MUMC) pharmacy. All experiments and data analyses were performed by experimenters blinded to the drug administered (CT, JE, ML).

Electromyography

Electromyography (EMG) was recorded with surface electrodes (9 mm Ag-AgCl) placed over the first dorsal interosseous (FDI) muscle of the right hand. A wet ground was secured around the forearm. All EMG recordings were amplified 1000x (Intronix Technologies

Corporation Model 2024F, Bolton, Canada) and band-pass filtered between 20 Hz and 2.5 kHz. Data was digitized at 5 kHz using an analog-to-digital interface (Power 1401; Cambridge Electronics Design, Cambridge, UK) and analyzed using commercial software (Signal v6.02; Cambridge Electronics Design).

Transcranial Magnetic Stimulation

TMS was performed with a customized figure-of-eight branding iron style coil (50 mm diameter) connected to a Magstim 200² stimulator (Magstim, Whitland, UK). The TMS coil was positioned over the left M1 at the optimal location to elicit a motor-evoked potential (MEP) in the right FDI muscle (i.e. motor hotspot). The coil was oriented at a 45-degree angle from the sagittal plane to induce a posterior-anterior current in the cortex. The location and orientation of the coil was digitally registered using Brainsight Neuronavigation (Rogue Research, Montreal, Canada). Resting motor threshold (RMT) was taken as a measure of baseline cortical excitability (Siebner and Rothwell 2003) before and after drug administration. RMT was determined using ML-PEST, a systematic predictive algorithm that determines the next TMS intensity predicted to yield a 50% probability of generating a MEP (TMS Motor Threshold Assessment Tool (MTAT 2.0), <http://www.clinicalresearcher.org/software.html>). *A priori* information was selected, and the starting TMS intensity was set to 37%. Twenty stimuli were delivered to accurately determine RMT (Ah Sen et al. 2017; Siebner and Rothwell 2003).

Short- and Long-latency Afferent Inhibition

The latency of the N20 component of the somatosensory evoked potential (SEP) was first obtained in each individual. To record SEPs, electroencephalography (EEG) electrodes were positioned on the scalp over the primary somatosensory cortex (S1) at C3' located 2 cm posterior to C3 and referenced to Fz (International 10-20 system). Nerve stimulation was performed with a surface bar electrode positioned over the median nerve at the wrist (cathode proximal). A constant current stimulator (Digitimer DS7AH) delivered square wave pulses (200 μ s pulse width) at the minimum intensity to evoke a visible twitch in the right abductor pollicis brevis (APB) muscle. Five hundred stimuli were delivered at a rate of 3 Hz, and time-locked averaged to determine the latency of the N20.

SAI was measured using two interstimulus intervals (ISIs) between nerve stimulation and the TMS pulse based on the latency of the N20 potential: N20 + 4 ms and N20 + 6 ms. Fifteen unconditioned MEPs were recorded (i.e. TMS alone) and randomized among fifteen conditioned MEPs (nerve stimulation-TMS) for each ISI with a 6 second inter-trial interval. LAI was obtained at ISIs of 200, 400 or 600 ms. Similar to SAI, fifteen unconditioned MEPs were randomized among 45 conditioned MEPs (15 each for ISI) and 6 seconds elapsed between trials. Trial sweeps recorded through Signal software were 0.3 seconds and 1 second long for collection of SAI and LAI data, respectively. SAI and LAI were assessed pre- and post-drug administration (Figure 4.1). The intensity of TMS was set to evoke a MEP of \sim 1 mV peak-to-peak amplitude prior to the collection of data before and after drug administration. For the collection of SAI and LAI, the nerve stimulation intensity was maintained at the minimum intensity to evoke a visible twitch in the right APB muscle.

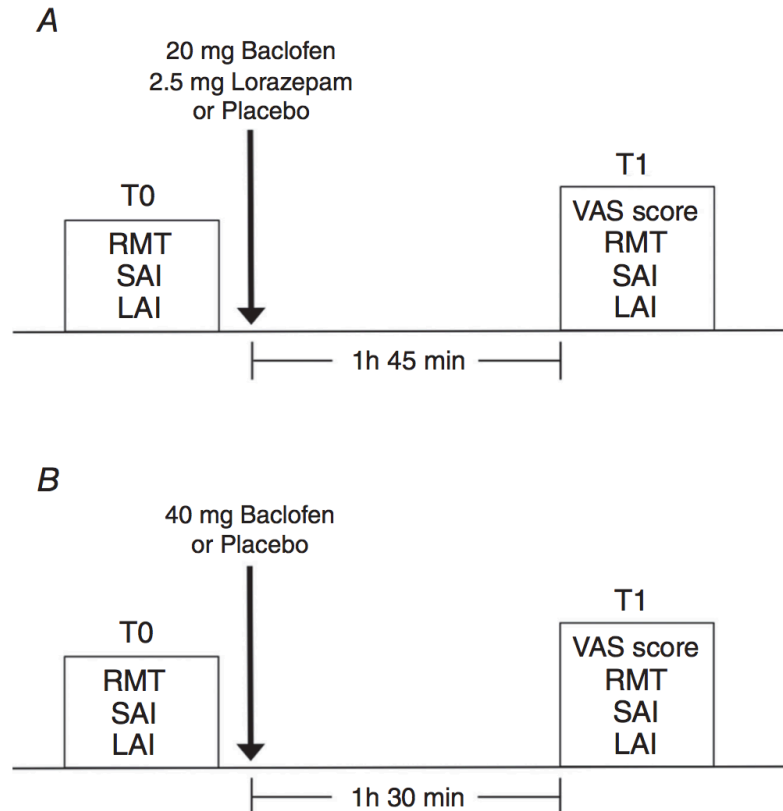


Figure 4.1: Experimental design

Study design for (A) Experiment 1 and (B) Experiment 2. Timeline for experimental sessions with two time points corresponding to baseline (T0) and peak plasma concentration of baclofen/lorazepam (T1).

Experimental Design

Experiment 1 (Figure 4.1A) was double-blinded and placebo-controlled. Participants were tested in three sessions, each separated by a minimum of one week. Within a session, participants were administered either 2.5 mg of lorazepam, 20 mg of baclofen or a placebo. The dosage of lorazepam was chosen because it has been previously shown to reduce SAI (Di Lazzaro et al. 2005a, 2005b, 2007a). The dosage for baclofen that has been previously shown to alter TMS measures of intracortical inhibition is 50 mg (McDonnell et al. 2006). However, to minimize possible risks associated with this dosage, we delivered 20 mg in Experiment 1. Dependent measures were acquired prior to (T0) and at 1 hour and 45

minutes (T1) following drug administration. The timing of T1 was based on the peak plasma concentrations of both lorazepam (1.5-2.5 hours) and baclofen (1-2 hours) (Kyriakopoulos et al. 1978; Ziemann et al. 1996).

In Experiment 1, we did not observe any influence of baclofen on sedation levels or physiological measures. We considered that our dosage of baclofen may have been insufficient to observe an effect. Therefore, in Experiment 2 (Figure 4.1B) (double-blinded and placebo-controlled), participants were administered either 40 mg of baclofen or a placebo, in two sessions separated by a minimum of one week. All TMS measures were acquired prior to (T0) and at 1 hour and 30 minutes (T1) following drug administration, based on the timing of the peak concentration of baclofen (1-2 hours) (Kyriakopoulos et al. 1978; Ziemann et al. 1996).

For both experiments, the order of dependent measures (SAI, LAI) was pseudo-randomized across participants using a William's square design. To evaluate the sedative effects of lorazepam and baclofen, a measure of sedation was performed independently by both experimenters present at T1 using a Visual Analogue Scale (VAS) (Di Lazzaro et al. 2005a, 2005b). This scale consisted of a 100 mm line, with 0 mm indicating that the participant was "alert" and 100 mm indicated "very sedated".

Data and Statistical Analyses

To avoid contamination of the MEP by background muscle activity, EMG trials were discarded if the peak-to-peak amplitude of the signal 50 ms before the TMS artefact was greater than 50 μ V.

The following analyses were performed on data obtained from both Experiment 1 and Experiment 2. Normality for all variables was assessed using the Shapiro-Wilks test. If normality was not reached, a square root transformation was applied to the data.

Paired t-tests were used to assess changes in RMT following drug administration. For SAI and LAI, the mean peak-to-peak MEP amplitude was obtained for the conditioned and unconditioned stimuli separately. Two-tailed paired t-tests were used to compare the conditioned MEP amplitude to the unconditioned MEP amplitude to determine if significant SAI and LAI were obtained at T0 and T1. Next, inhibition was calculated as a ratio of the mean conditioned to mean unconditioned MEP.

$$\text{SAI/LAI} = \frac{\text{MEP}_{\text{nerve-TMS}}}{\text{MEP}_{\text{TMS}}} = \frac{\text{MEP}_{\text{conditioned}}}{\text{MEP}_{\text{unconditioned}}}$$

A two-way ANOVA was performed on SAI and LAI data separately for each drug condition using the within-subject factors TIME (2 levels: T0, T1) and ISI (N20 + 4 ms, N20 + 6 ms for SAI or 200, 400, 600 ms for LAI). Post-hoc testing was performed with Tukey's HSD.

The Mann-Whitney U test was used to compare VAS scores between raters, and the Wilcoxon signed-rank test was used to compare VAS scores between drugs. To determine if changes in afferent inhibition were related to changes in sedation, the percent change in SAI/LAI was correlated with the VAS scores using Spearman's rho. For all analyses, significance was set to $p < 0.05$. Effect sizes were calculated using Cohen's d.

4.3 Results

Experiment 1

No serious adverse events were observed following administration of any drug. One participant experienced nausea and vomiting approximately 2.5 hours following lorazepam ingestion but recovered fully by the next morning. For SAI and LAI, <1% of the total number of trials were removed due to excessive EMG activity. Table 4.1 displays all group-averaged data from Experiment 1.

Table 4.1: Experiment 1 group-averaged measures (with standard deviations)

Measure	Placebo		Baclofen		Lorazepam	
	T0	T1	T0	T1	T0	T1
RMT (%MSO)	41.6 ± 7.1	42.4 ± 7.6	40.6 ± 6.3	40.6 ± 6.6	41.9 ± 7.6	40.0 ± 7.2
<i>Somatosensory evoked potentials</i>						
APB motor threshold (mA)	12.6 ± 3.3		11.3 ± 2.6		11.3 ± 3.3	
N20 latency (ms)	19.4 ± 0.7		19.7 ± 0.6		19.5 ± 0.6	
<i>Short-latency afferent inhibition</i>						
APB motor threshold (mA)	12.2 ± 3.4	11.9 ± 2.7	12.0 ± 3.1	11.9 ± 2.9	11.4 ± 3.3	11.0 ± 2.9
1 mV MEP (%MSO)	51.9 ± 8.9	53.3 ± 9.7	52.1 ± 10.2	50.3 ± 8.7	54.8 ± 7.6	53.2 ± 9.8
N20 + 4 ms	0.63 ± 0.18	0.59 ± 0.24	0.58 ± 0.24	0.64 ± 0.39	0.62 ± 0.20	0.71 ± 0.24
N20 + 6 ms	0.80 ± 0.26	0.84 ± 0.31	0.82 ± 0.26	0.94 ± 0.43	0.75 ± 0.26	0.92 ± 0.30
Averaged ISI	0.71 ± 0.21	0.71 ± 0.25	0.70 ± 0.23	0.79 ± 0.39	0.69 ± 0.22	0.81 ± 0.23
<i>Long-latency afferent inhibition</i>						
APB motor threshold (mA)	12.3 ± 3.6	12.2 ± 2.9	11.9 ± 2.8	12.0 ± 2.7	11.5 ± 3.3	11.0 ± 3.1
1 mV MEP (%MSO)	52.7 ± 8.6	52.4 ± 9.5	53.2 ± 11.2	50.2 ± 9.7	54.4 ± 9.5	53.3 ± 8.6
200 ms	0.57 ± 0.22	0.76 ± 0.55	0.56 ± 0.31	0.55 ± 0.34	0.60 ± 0.31	0.86 ± 0.38
400 ms	0.58 ± 0.22	0.66 ± 0.30	0.60 ± 0.31	0.60 ± 0.29	0.55 ± 0.28	0.77 ± 0.30
600 ms	0.66 ± 0.22	0.72 ± 0.32	0.70 ± 0.28	0.63 ± 0.26	0.62 ± 0.24	0.85 ± 0.47
Averaged ISI	0.61 ± 0.19	0.72 ± 0.35	0.62 ± 0.27	0.60 ± 0.25	0.59 ± 0.25	0.83 ± 0.33

RMT was not significantly modified by lorazepam, baclofen or placebo (two-tailed paired t-tests, all $p > 0.05$), as reported elsewhere (Di Lazzaro et al. 2005a, 2005b, 2007a; McDonnell et al. 2006; Teo et al. 2009). VAS rating of sedation was not different between raters following baclofen, lorazepam or placebo (Mann-Whitney U, $p > 0.05$), therefore the VAS score was averaged across raters. The mean VAS score was significantly greater following lorazepam (60.8 ± 16.5) compared to baclofen (23.5 ± 17.7) and placebo (26.2 ± 11.6) (Wilcoxon signed-rank test, all $p < 0.05$).

Table 4.2 displays the statistics from the ANOVAs performed on normalized LAI and SAI data from Experiment 1. A two-way ANOVA using within-subject factors of ISI and TIME revealed a main effect of TIME ($F_{(1,13)} = 6.190$, $p = 0.027$) for LAI in the lorazepam condition, such that LAI was significantly reduced by lorazepam (40.40% reduction) (Figure 4.2A, 4.2B). Two-way ANOVAs for the baclofen and placebo conditioned revealed

no main effects or interactions for LAI (Figure 4.2C, 4.2D). No correlation between VAS scores and percent change in LAI following lorazepam was observed (Spearman's rho, $r = 0.297$, $p > 0.05$), indicating that sedation was not associated with the reduction in LAI. Individual effects of lorazepam on LAI are shown in Figure 4.3A. Ten individuals (shown with asterisk) demonstrate a reduction of LAI following lorazepam while the remainder show an increase ($n = 3$) or no LAI at baseline ($n = 1$). Figures 4.3B and 4.3C show individual responses to baclofen and placebo, respectively. For all drug conditions, LAI was present at T0 ($MEP_{conditioned}$ vs $MEP_{unconditioned}$, two-tailed paired t-test, all $p < 0.001$) and T1 ($MEP_{conditioned}$ vs $MEP_{unconditioned}$, two-tailed paired t-test, all $p < 0.05$). In summary, the data indicates that LAI is reduced by lorazepam and not baclofen.

Table 4.2: Experiment 1 two-way ANOVA statistics

Dependent Measure	ANOVA
Long-latency afferent inhibition	
Lorazepam	ISI _(2,26) = 0.769, p = 0.474 TIME_(1,13) = 6.190, p = 0.027 ISI × TIME _(2,26) = 0.118, p = 0.889
Baclofen	ISI _(2,26) = 2.435, p = 0.107 TIME _(1,13) = 0.110, p = 0.745 ISI × TIME _(2,26) = 0.273, p = 0.763
Placebo	ISI _(2,26) = 0.793, p = 0.463 TIME _(1,13) = 1.252, p = 0.283 ISI × TIME _(2,26) = 0.638, p = 0.536
Short-latency afferent inhibition	
Lorazepam	ISI_(1,13) = 20.634, p = 0.001 TIME_(1,13) = 5.233, p = 0.040 ISI × TIME _(1,13) = 0.495, p = 0.494
Baclofen	ISI_(1,13) = 41.920, p < 0.001 TIME _(1,13) = 1.116, p = 0.310 ISI × TIME _(1,13) = 0.532, p = 0.479
Placebo	ISI_(1,13) = 19.710, p = 0.001 TIME _(1,13) = 0.000, p = 0.989 ISI × TIME _(1,13) = 1.713, p = 0.213

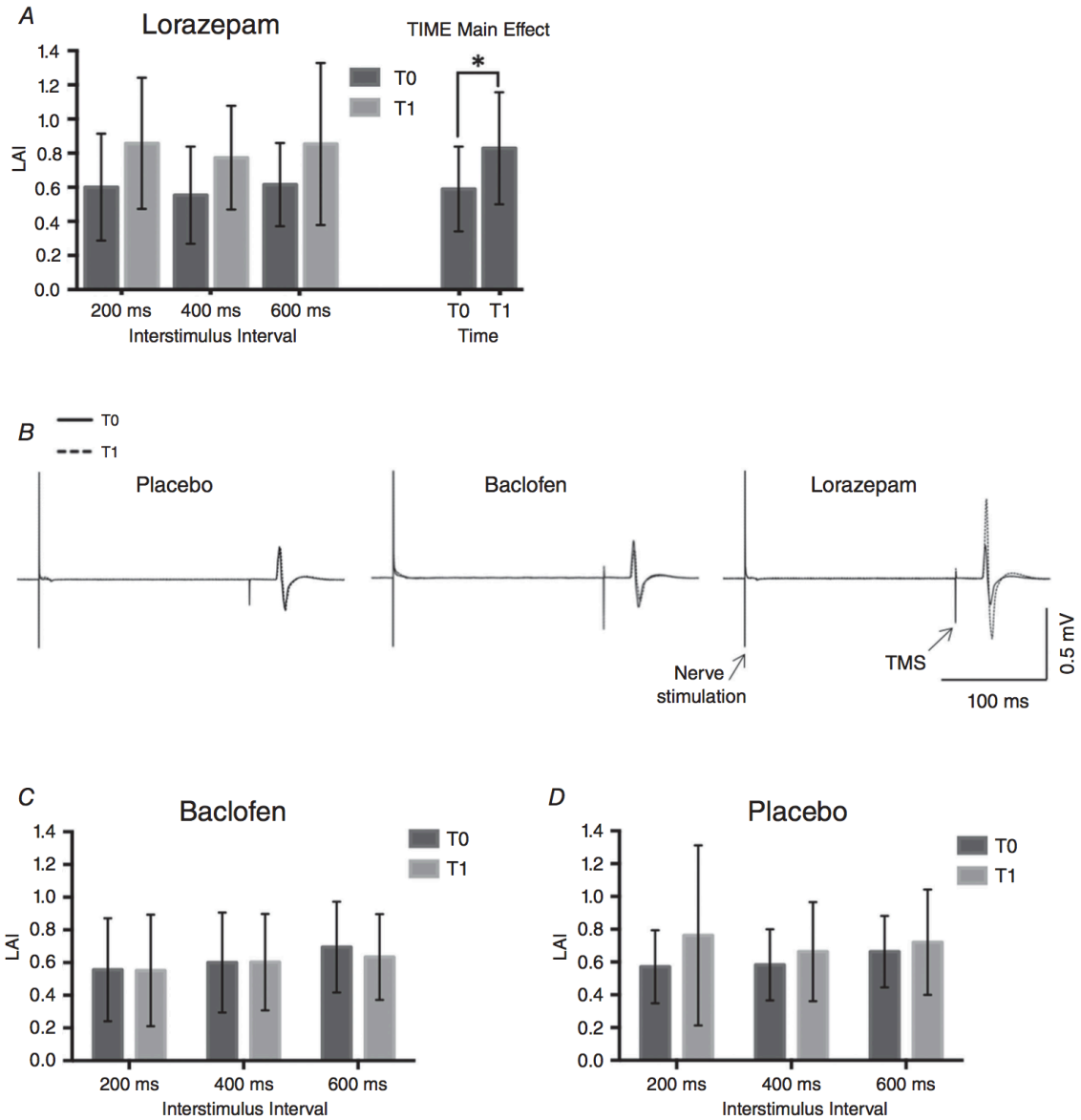


Figure 4.2: Experiment 1, LAI.

(A) Mean LAI (\pm SD) expressed as a ratio of the conditioned MEP (nerve stimulation preceding TMS) to the unconditioned MEP (TMS alone) before (T0) and after (T1) administration of lorazepam. A main effect of TIME is shown on the right, where LAI was significantly reduced following lorazepam administration (significance denoted by asterisk). (B) LAI in one participant before (T0, solid line) and after (T1, dashed line) administration of placebo, lorazepam or baclofen. Traces show the time-locked averaged conditioned MEP for participant 14. (C) Mean LAI (\pm SD) before and after administration of baclofen. (D) Mean LAI (\pm SD) before and after administration of placebo.

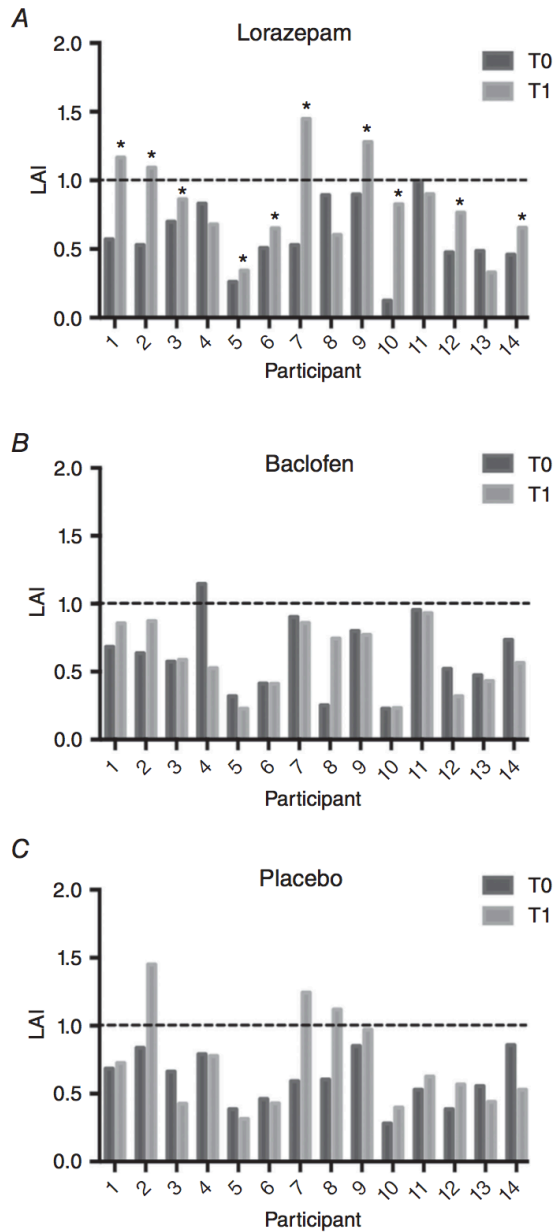


Figure 4.3: Experiment 1, individual LAI.

LAI (averaged across ISIs) in individual participants before (T0) and after (T1) (A) lorazepam intake, (B) baclofen intake, or (C) placebo intake. Asterisks indicate individuals who demonstrated reduction in LAI following lorazepam intake, reflecting the TIME main effect found in the two-way ANOVA.

For SAI in the lorazepam condition (Figure 4.4A, 4.4B), a two-way repeated measures ANOVA revealed a main effect of ISI ($F_{(1,13)} = 20.634$, $p = 0.001$), such that the magnitude of SAI (\pm SD) was stronger at N20 + 4 ms (0.67 ± 0.20) than N20 + 6 ms (0.84 ± 0.22). A main effect of TIME was also revealed ($F_{(1,13)} = 5.233$, $p = 0.040$), such that SAI was significantly reduced by lorazepam (18.73% reduction). For SAI in the baclofen condition (Figure 4.4C), a two-way ANOVA showed a main effect of ISI ($F_{(1,13)} = 41.920$, $p < 0.001$), such that the magnitude of SAI (\pm SD) was stronger at N20 + 4 ms (0.61 ± 0.26) than N20 + 6 ms (0.88 ± 0.32). Finally, for SAI in the placebo condition (Figure 4.4D), a two-way ANOVA revealed a main effect of ISI ($F_{(1,13)} = 19.710$, $p = 0.001$), such that the magnitude of SAI (\pm SD) was stronger at N20 + 4 ms (0.61 ± 0.18) than N20 + 6 ms (0.82 ± 0.25). The reduction of SAI was unrelated to sedation caused by lorazepam (Spearman's rho, $r = 0.024$, $p > 0.05$). Individual data for lorazepam effects show that at N20 + 4 ms (Figure 4.5A, left), ten individuals showed a reduction following lorazepam, while others showed no change ($n = 1$) or an increase ($n = 3$). SAI at N20 + 6 ms (Figure 4.5A, right) was reduced in eight participants (shown with asterisk) while others showed no change ($n = 1$), an increase ($n = 3$) or no SAI at baseline ($n = 2$). Figures 4.5B and 4.5C show individual responses to baclofen and placebo, respectively. For all drug conditions, SAI was present at T0 ($MEP_{\text{conditioned}}$ vs $MEP_{\text{unconditioned}}$, two-tailed paired t-test, all $p < 0.001$). At T1, SAI was present following lorazepam ($MEP_{\text{conditioned}}$ vs $MEP_{\text{unconditioned}}$, two-tailed paired t-test, $p < 0.01$) and placebo ($MEP_{\text{conditioned}}$ vs $MEP_{\text{unconditioned}}$, two-tailed paired t-test, $p < 0.001$), but not following baclofen ($MEP_{\text{conditioned}}$ vs $MEP_{\text{unconditioned}}$, two-tailed paired t-test, $p = 0.06$). Of note, although the unconditioned MEP is not different from the conditioned MEP

at T1 following baclofen, the ANOVA shows no main effect of TIME indicating that SAI is not significantly modulated by baclofen. In summary, the data indicates that SAI is reduced by lorazepam and not baclofen.

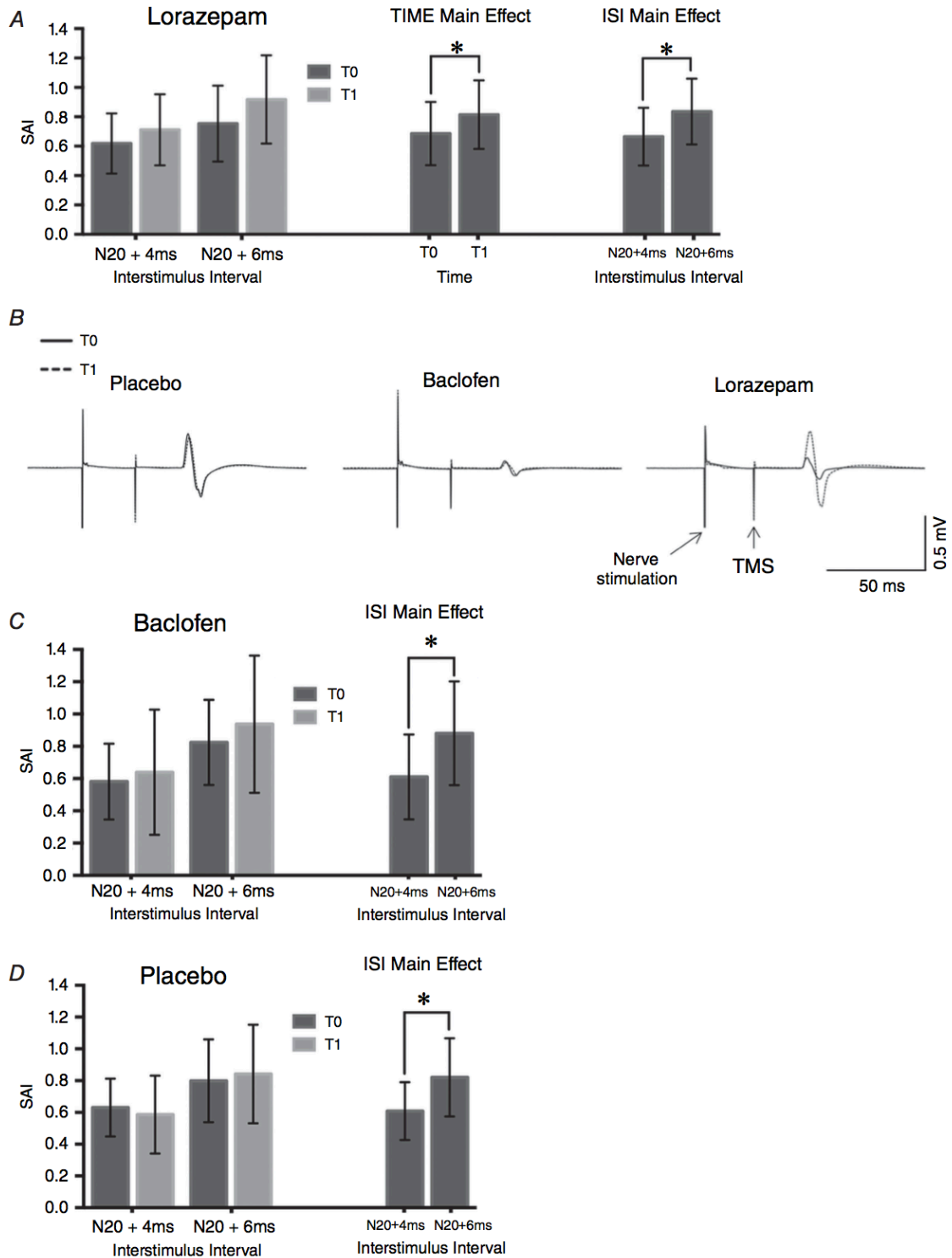


Figure 4.4: Experiment 1, SAI.

(A) Mean SAI (\pm SD) expressed as a ratio of the conditioned MEP (nerve stimulation preceding TMS) to the unconditioned MEP (TMS alone) before (T0) and after (T1)

administration of lorazepam. Main effects of ISI and TIME are shown on the right, where SAI was stronger for N20 + 4 ms compared to N20 + 6 ms, and SAI was reduced by lorazepam (significance denoted by asterisk). **(B)** SAI in one participant before (T0, solid line) and after (T1, dashed line) administration of placebo, lorazepam or baclofen. Traces show the time-locked averaged conditioned MEP for a participant 9. **(C)** Mean SAI (\pm SD) before and after administration of baclofen. A main effect of ISI is shown on the right, where SAI was significantly stronger for N20 + 4 ms compared to N20 + 6 ms. **(D)** Mean SAI (\pm SD) before and after administration of placebo. A main effect of ISI is shown on the right, where SAI was significantly stronger for N20 + 4 ms compared to N20 + 6 ms.

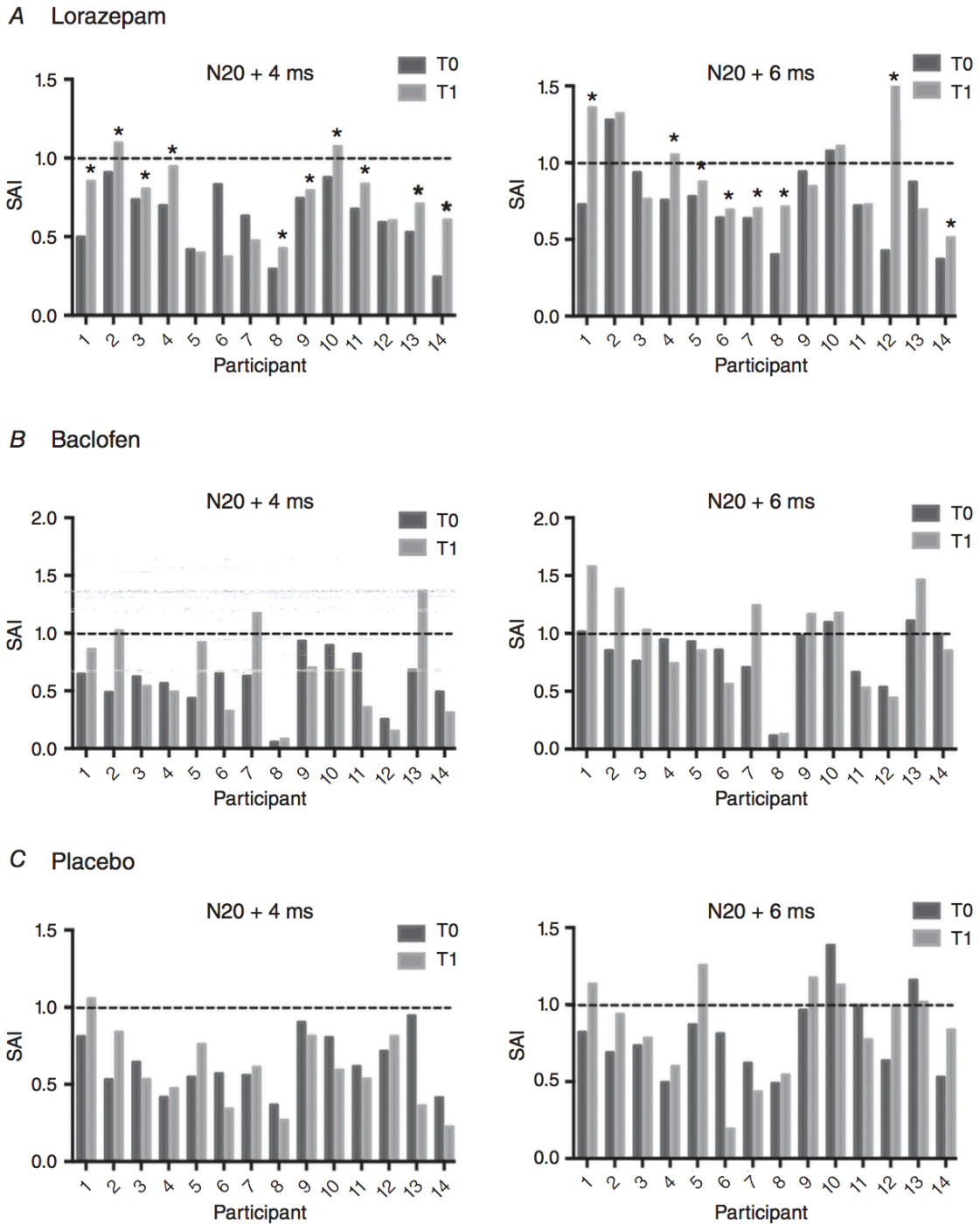


Figure 4.5: Experiment 1, SAI individual

SAI at N20 + 4 ms (*left*) and N20 + 6 ms (*right*) observed in individual participants before (T0) and after (T1) (A) lorazepam intake, (B) baclofen intake, or (C) placebo intake. Asterisks indicate individuals who demonstrated reduction in SAI following lorazepam intake, reflecting the TIME main effect found in the two-way ANOVA.

Experiment 2

No serious adverse events were observed following administration of 40 mg of baclofen. For SAI and LAI, <1% of trials were removed due to excessive EMG activity. Table 4.3 displays all group-averaged data from experiment 2. RMT was not significantly modified by baclofen or the placebo (two-tailed paired t-test, both $p > 0.05$). VAS rating of sedation was not different between raters (Mann-Whitney U, $p > 0.05$) and the mean VAS scores did not differ following baclofen (23.4 ± 9.9) and placebo (24.5 ± 12.5) (Wilcoxon signed-rank test, $p > 0.05$).

Table 4.3: Experiment 2 group-averaged measures (with standard deviations)

Measure	Placebo		Baclofen	
	T0	T1	T0	T1
RMT (%MSO)	43.3 ± 7.7	41.6 ± 8.0	44 ± 9.2	43.4 ± 9.7
<i>Somatosensory evoked potentials</i>				
APB motor threshold (mA)	8.8 ± 2.4		9.3 ± 3.1	
N20 latency (ms)	19.3 ± 1.1		19.5 ± 0.9	
<i>Short-latency afferent inhibition</i>				
APB motor threshold (mA)	9.4 ± 2.5	9.7 ± 3.2	9.1 ± 3.2	9.0 ± 3.1
1 mV MEP (%MSO)	54.0 ± 12.7	55.1 ± 12.5	57.2 ± 14.0	52.2 ± 10.4
N20 + 4 ms	0.80 ± 0.46	0.72 ± 0.35	0.75 ± 0.37	0.66 ± 0.46
N20 + 6 ms	0.79 ± 0.36	0.81 ± 0.30	0.84 ± 0.23	0.82 ± 0.39
Averaged ISI	0.79 ± 0.39	0.77 ± 0.31	0.79 ± 0.28	0.74 ± 0.32
<i>Long-latency afferent inhibition</i>				
APB motor threshold (mA)	9.6 ± 2.4	9.9 ± 3.3	9.1 ± 3.2	9.2 ± 3.0
1 mV MEP (%MSO)	55.6 ± 12.6	55.4 ± 13.1	54.6 ± 13.2	53.5 ± 10.7
200 ms	0.81 ± 0.47	0.73 ± 0.58	0.60 ± 0.30	0.66 ± 0.45
400 ms	0.78 ± 0.54	0.58 ± 0.30	0.51 ± 0.26	0.56 ± 0.26
600 ms	0.75 ± 0.29	0.73 ± 0.26	0.53 ± 0.24	0.68 ± 0.28
Averaged ISI	0.78 ± 0.39	0.68 ± 0.28	0.55 ± 0.22	0.64 ± 0.27

Table 4.4 displays the statistics from the ANOVAs performed on the normalized LAI and SAI data from experiment 2. Two-way ANOVAs with factors of ISI and TIME were performed on LAI data separately for each drug, and no main effects or interactions were found (Figure 4.6A). For SAI, two-way ANOVAs with factors of ISI and TIME were performed for each drug separately and showed no main effects or interactions (Figure 4.6B).

Table 4.4: Experiment 2 ANOVA statistics

Dependent Measure	ANOVA
Long-latency afferent inhibition	
Baclofen	ISI _(1,9) = 0.631, p = 0.543 TIME _(2,18) = 1.497, p = 0.252 ISI × TIME _(2,18) = 1.125, p = 0.346
Placebo	ISI _(1,9) = 0.509, p = 0.610 TIME _(2,18) = 0.896, p = 0.369 ISI × TIME _(2,18) = 0.548, p = 0.588
Short-latency afferent inhibition	
Baclofen	ISI _(1,9) = 1.299, p = 0.284 TIME _(1,9) = 0.884, p = 0.372 ISI × TIME _(1,9) = 0.279, p = 0.610
Placebo	ISI _(1,9) = 0.297, p = 0.599 TIME _(1,9) = 0.093, p = 0.767 ISI × TIME _(1,9) = 2.557, p = 0.144

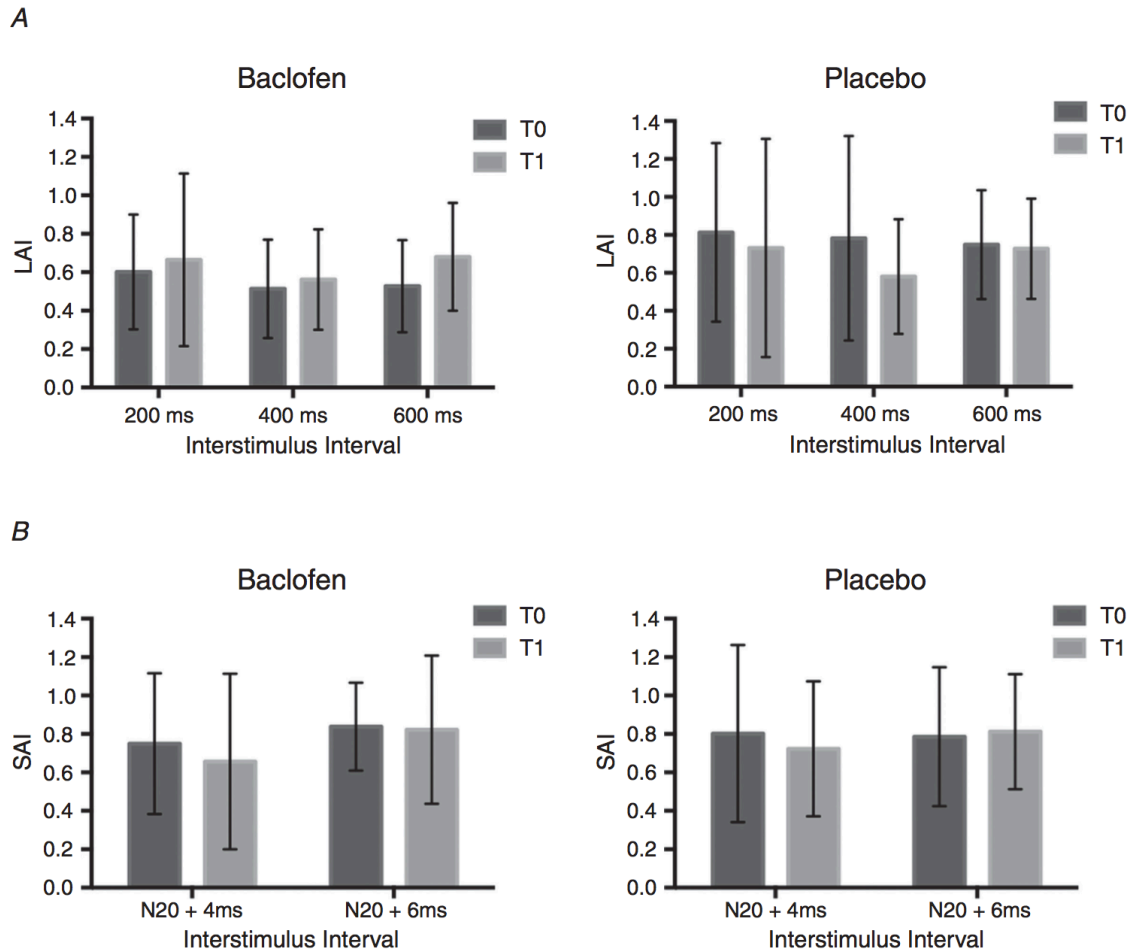


Figure 4.6: Experiment 2, LAI and SAI.

(A) Mean LAI (\pm SD) expressed as a ratio of the conditioned MEP (nerve stimulation preceding TMS) to the unconditioned MEP (TMS alone). LAI was not significantly modified by baclofen (*left*) or placebo (*right*). (B) Mean SAI (\pm SD) expressed as a ratio of the conditioned MEP (nerve stimulation preceding TMS) to the unconditioned MEP (TMS alone). SAI was not significantly modified by baclofen (*left*) or placebo (*right*).

4.4 Discussion

The present study examined the pharmacological influence of GABA_A and GABA_B receptor modulators on SAI and LAI. We report the novel finding that LAI is reduced by lorazepam but not by baclofen, suggesting that LAI is GABA_A but not GABA_B receptor-modulated. We support previous research indicating that SAI is reduced by

benzodiazepines that are positive allosteric modulators of the GABA_A receptor (Di Lazzaro et al. 2005a, 2005b, 2007a; Teo et al. 2009), and extend this knowledge to indicate that SAI is not modulated by the GABA_B agonist baclofen. We discuss these findings and their putative neural mechanisms below.

In this study, we observed a ~40% decrease in LAI following administration of lorazepam. One study examined the effect of 2.5 mg of lorazepam and 10 mg of zolpidem (a benzodiazepine) and observed no change in LAI (Teo et al. 2009). Of note, we did not test LAI at the same ISI (100 ms) used by Teo et al. (2009), due to the low level of inhibition they observed at baseline (~15%). Our LAI data revealed ~41% inhibition at baseline in line with previous work (Chen et al. 1999), allowing for a greater opportunity for the reduction in LAI should it occur following drug ingestion. Next, we observed a ~19% decrease in SAI following lorazepam. This reduction is consistent with previous findings that range from ~15 to 40% SAI reduction following lorazepam or zolpidem administration (Di Lazzaro et al. 2005a, 2005b, 2007a; Teo et al. 2009). SAI is only modulated by benzodiazepines that target GABA_A receptors bearing the α 1 subunit, including zolpidem and lorazepam (Di Lazzaro et al. 2007a).

How does lorazepam reduce SAI and LAI?

Lorazepam appears to reduce inhibition in S1 while increasing inhibition in neighbouring M1. Lorazepam reduces inhibition in S1 as evidenced by a decrease in the paired pulse suppression of the SEP components recorded from S1 (Huttunen et al. 2008; Stude et al.

2016). In contrast, lorazepam reduces late I-waves recorded epidurally following TMS over M1 (Di Lazzaro et al. 2000a), an outcome consistent with increasing the inhibitory effect of GABAergic interneurons within M1. The opposing effects of lorazepam observed in S1 versus M1 may be due simply to the differing composition of these two cortical areas. Inhibition plays a large role in S1 to modulate receptor response profiles, where networks of inhibitory interneurons shape the spatial and temporal profiles of excitatory pyramidal neurons (DiCarlo and Johnson 2000; Wood et al. 2017). M1 is governed by a balance of excitation and inhibition, with excitation mainly governing motor output (Werhahn et al. 2007).

What then, are the potential mechanisms by which SAI and LAI are reduced by lorazepam? While lorazepam acts globally within the cortex, lorazepam may increase GABA_A receptor transmission on the dense inhibitory interneuron population within S1 that ultimately act to disinhibit pyramidal neurons (DiCarlo and Johnson 2000; Wood et al. 2017). Disinhibition of S1 pyramidal neurons would allow for excitation of M1 pyramidal neurons via long-range connections throughout layers II/III (Amassian et al. 1987) and V (Aronoff et al. 2010; Ferezou et al. 2007). In M1, however, we would expect that lorazepam would inhibit MEPs relative to baseline by increasing the inhibitory influence of GABAergic interneurons, and although this may be the case, the net influence from the arrival of the afferent volley in M1 is to increase the output of corticospinal pyramidal neurons.

This is the first report to examine the effect of the GABA_B agonist baclofen on LAI and SAI and we did not observe any induced effects using a single 20 mg or 40 mg dose. Although SAI and LAI are not influenced by baclofen, other TMS evoked circuits are modulated by baclofen. Baclofen increases long-interval intracortical inhibition (LICI) (McDonnell et al. 2006; Müller-Dahlhaus et al. 2008) and reduces intracortical facilitation (ICF) (Ziemann et al. 1996). For short-interval intracortical inhibition (SICI), baclofen does not change (McDonnell et al. 2007), reduces (McDonnell et al. 2006) or increases (Ziemann et al. 1996) inhibition. Although it is unclear why GABA_B receptors are modulators of the aforementioned circuits but not SAI and LAI, the obvious difference relates to the transmission of the afferent volley that is essential for afferent inhibition.

Functional relevance of afferent inhibition

The reduction of both SAI and LAI by lorazepam provides evidence that they are more similar than originally thought. This is consistent with a study showing that chronic subthalamic nucleus deep brain stimulation normalized both SAI and LAI in Parkinson's disease (Wagle Shukla et al. 2013). However, the functional relevance of these two phenomena may be entirely different. SAI is impaired in a variety of clinical populations (for review, see Turco et al. 2018). Most often shown is reduced SAI in disorders of cognition such as Alzheimer's disease (Celebi et al. 2012; Di Lazzaro et al. 2002, 2006, 2007b, 2008; Di Lorenzo et al. 2013; Marra et al. 2012; Martorana et al. 2009; Nardone et al. 2013, 2006, 2008a; Sakuma et al. 2007; Terranova et al. 2013; Yarnall et al. 2013) and in those with mild cognitive impairment (Nardone et al. 2012a; Tsutsumi et al. 2012a). In

those with REM sleep behavior disorder, SAI is positively correlated with greater executive function, verbal memory, and visuospatial abilities (Nardone et al. 2012b, 2013). Further, in healthy individuals, SAI has been shown to be enhanced only during the retrieval phase and not encoding or consolidation phase of memory (Bonni et al. 2017). Therefore, it is clear that SAI plays a role in various aspects of human cognition. Previous work also shows that SAI can be used to quantify neurophysiological changes. SAI is reduced in those with chronic incomplete spinal cord injury, reflecting impaired transmission of afferent input to M1 (Bailey et al. 2015). Further, following ischemic stroke, those showing greater reductions in SAI also show greater improvement in symptoms 6 months post-injury (Di Lazzaro et al. 2012a). Therefore, SAI may potentially be used as a biomarker of functional recovery following neurological injury, however further research is necessary to confirm this notion.

There is a paucity of research investigating LAI in relation to human behavior. In clinical populations, LAI is most often abnormal in those displaying deficits in sensorimotor abilities such as Parkinson's disease (Sailer et al. 2003), complex regional pain syndrome (Morgante et al. 2017), and focal hand dystonia (Richardson et al. 2009). It is unknown if, similar to SAI, LAI is also related to human cognition. Next, it is unknown if afferent inhibition is related to basic aspects of sensation and movement. However, it is commonly assumed that both SAI and LAI are indirect assessments of sensorimotor integration based on the cortical loci that are targeted by the afferent signal, mainly S1 and M1, and reports that afferent inhibition is modulated during movement and movement planning (Asmussen

et al. 2013, 2014; Cho et al. 2016; Ni et al. 2011; Richardson et al. 2008; Voller et al. 2005, 2006). We recently reported that there is no significant relationship between afferent inhibition and tactile or motor performance (Turco et al. 2018c). Further research is needed to expose behavioral correlates of afferent inhibition, in order to improve our understanding of this phenomenon.

Limitations & Future Considerations

Our sample size was determined based on estimates from previous literature (Di Lazzaro et al. 2005a, 2005b, 2007a). However, we note that post-hoc power analyses of our data reveal a power of 0.64 and 0.51 for the reduction in LAI and SAI by lorazepam, respectively. Therefore, to achieve a higher power of 0.8, we would need to test 26 participants. Baclofen did not demonstrate significant sedative effects as assessed with the VAS at either the 20 mg or 40 mg dosages. It is possible that a higher baclofen dosage would induce sedative effects and alter SAI/LAI, although higher dosages were beyond the safety limitations of the research. We only examined the effect of GABAergic modulators on afferent inhibition. Future studies should consider other neuromodulators that may play a role in shaping afferent inhibition. SAI is modulated by cholinergic drugs (Di Lazzaro et al. 2000b), however the role of acetylcholine in LAI is unknown. Serotonin, a neuromodulator that excites GABAergic interneurons (Abi-Saab et al. 1999) and reduces the responsiveness of neurons in the somatosensory cortex to afferent input (Waterhouse et al. 1986), may also modulate afferent inhibition.

Conclusions

We have shown for the first time that LAI is modulated by GABA_A receptor activity. SAI was reduced by lorazepam, confirming previous studies that GABA_A receptors modulate SAI. Further, LAI and SAI are not influenced by baclofen, suggesting that GABA_B receptor activity does not modulate these phenomena. These findings advance our understanding of the pharmacological basis of afferent inhibition in humans.

4.5 Rational for Study 3

Although the stimulation parameters and pharmacology for evoking maximal SAI and LAI have been determined, it is important to investigate whether these stimulation parameters allow for a reliable assessment of these variables. Evidence about the reliability of afferent inhibition is sparse. However, reliability metrics provide insights on the ability for an outcome to detect differences between groups or to track change within an individual or group. As such, reliability metrics help improve the interpretation of studies using within and between-group experimental designs. Therefore, the purpose of Study #3 is to provide a comprehensive reliability analysis of SAI and LAI to quantify the relative and absolute reliability of these measures.

Chapter 5: Study 3

Reliability of Transcranial Magnetic Stimulation Measures of Afferent Inhibition

Turco, C.V., Pesevski, A., McNicholas, P.D., Beaulieu, L.D., & Nelson, A.J. (2019). Reliability of transcranial magnetic stimulation measures of afferent inhibition. *Brain Research*, 1723(146394).

5.1 Introduction

Afferent inhibition is a phenomenon whereby the motor evoked potential (MEP) elicited by transcranial magnetic stimulation (TMS) is suppressed when preceded by peripheral nerve stimulation. The resulting suppression is known as short-latency afferent inhibition (SAI) when the interstimulus interval (ISI) is ~20-25 ms (Tokimura et al. 2000), and known as long-latency afferent inhibition (LAI) at longer ISIs of 200-1000 ms (Chen et al. 1999; Turco et al. 2018b). SAI is modulated by cholinergic activity (Di Lazzaro et al. 2000b), and both SAI and LAI are reduced by administration of gamma-aminobutyric acid type A (GABA_A) receptor allosteric modulators (Di Lazzaro et al. 2005b, 2005a, 2007a; Turco et al. 2018a). Both LAI and SAI are reduced in populations with disorders of the sensorimotor system including Parkinson's disease (Dubbioso et al. 2019; Sailer et al. 2003), while SAI is reduced in disorders of cognition (Cantone et al. 2014; Di Lazzaro et al. 2002; Nardone et al. 2006, 2008a).

Both SAI and LAI may be evoked by stimulation of cutaneous and mixed nerves when recorded from muscles innervated by those nerves or in close spatial proximity to those nerves (Classen et al. 2000; Tamburin et al. 2001). While stimulation of mixed versus

cutaneous nerves leads to activation of different cytoarchitectonic areas within the primary somatosensory cortex (S1) (Kaukoranta et al. 1986), the magnitude of afferent inhibition does not appear to be influenced by the type of nerve stimulated (Bailey et al. 2016; Chen et al. 1999; Tamburin et al. 2005; Turco et al. 2018b). However, the depth of inhibition varies as a function of nerve stimulation intensity. Both SAI and LAI reach maximal depth at intensities that evoke at least 50% of the maximum sensory nerve action potential (SNAP_{max}) in both the mixed median or cutaneous digital nerve (Turco et al. 2017). Further, a somatotopic effect of SAI (heterotopic vs homotopic stimulation) emerges when cutaneous nerve stimulation intensity is increased from sensory threshold to 3x sensory threshold (Dubbioso et al. 2017; Tamburin et al. 2001).

Information regarding the reliability of SAI and LAI is required if these measures are to achieve greater utility in basic and clinical neuroscience. First, TMS measures are prone to significant variability due to methodological and biological factors (van der Kamp et al. 1996; Kiers et al. 1993; Maeda et al. 2002; Orth et al. 2003; Wassermann 2002). Therefore, reliability testing is essential to validate whether or not, despite these sources of variability, TMS procedures can provide accurate measurements. Reliability can be classified into two types: relative and absolute (Beaulieu et al. 2017a). Relative reliability refers to the extent to which individuals or groups are distinguishable from one another with repeated testing (Bruton et al. 2000; Schambra et al. 2015). Relative reliability is best assessed via the intraclass correlation coefficient (ICC), which indicates the agreement or consistency among repeated measures by considering both random and systematic errors (Atkinson and

Nevill 1998; Koo and Li 2016; Weir 2005). High values of the ICCs indicate greater relative reliability, suggesting that the measurement has a better ability to detect differences between groups or individuals. High relative reliability would be needed for diagnostic purposes (e.g. the ability to differentiate between a healthy individual versus one with neurological injury/disease, or between groups of these individuals). One multi-site study examined SAI in a test-retest paradigm by stimulating the median nerve and recording inhibition in the abductor pollicis brevis (APB) muscle (Brown et al. 2017). SAI achieved an ICC of 0.67 (no confidence intervals reported), indicating moderate relative reliability (Brown et al. 2017). Relative reliability has yet to be assessed for SAI evoked by cutaneous nerve stimulation and has not been assessed for any measurement of LAI. Further, while SAI has been assessed at pre-determined ISIs ranging from 20-25 ms (Ni et al. 2011; Tamburin et al. 2001, 2002, 2005), an alternative method is to individualize the ISI according to the latency of the N20 component of the somatosensory-evoked potential (SEP) (Bailey et al. 2016; Fischer and Orth 2011; Guerra et al. 2016; Di Lazzaro et al. 2000b, 2005a, 2005b, 2007a; Tsang et al. 2014; Udupa et al. 2009, 2014). It is unknown whether the adjustment of the ISI to the N20 latency improves the reliability of SAI assessment.

Absolute reliability refers to the measurement error obtained with repeated measurements in stable individuals (Bruton et al. 2000; Hopkins 2000), and is typically assessed using the standard error of measurement (SEM_{eas}) (Weir 2005). The SEM_{eas} can be used to calculate the smallest detectable change ($SDC_{\text{individual}}$), which represents the minimum amount of

change in a variable that is above the measurement error in an individual (Beckerman et al. 2001; Weir 2005). An amount of change below the $SDC_{\text{individual}}$ is assumed to be due to measurement error (Beckerman et al. 2001; Weir 2005). SDC can also be expressed in terms of a group of participants (SDC_{group}), indicating the amount of change needed in the group-average to be considered above the error, providing a complementary method to hypothesis testing (Schambra et al. 2015). No studies have examined the absolute reliability of SAI and LAI, yet this information is important if these measures are to be used to monitor changes within an individual or group over time such as during the course of an intervention or treatment.

In the present study, we investigated the relative reliability, absolute reliability, and SDC of SAI and LAI evoked by stimulation of the median nerve and digital nerve across two separate sessions in thirty healthy, young individuals. These obtained results have important implications for the application of SAI and LAI in basic and clinical neuroscience.

5.2 Methods

Participants

Thirty healthy, right-hand dominant individuals participated (15 females; age = 20.9 ± 2.5 years) in two sessions separated by an average of 7 ± 4 days. Both sessions took place at the same time of day to account for circadian variations that may influence LAI (Bocquillon et al. 2017). Participants were screened for contraindications to TMS (Rossi et al. 2009),

and handedness was confirmed using a modified handedness questionnaire (Oldfield 1971) (<http://www.brainmapping.org/shared/Edinburgh.php>). All individuals provided informed written consent prior to participation. This research was approved by the McMaster Research Ethics Board and conformed to the declaration of Helsinki.

Electromyography

Electromyography (EMG) was recorded with surface disposable electrodes (9 mm Ag-AgCl) placed over the right first dorsal interosseous (FDI) muscle. A wet ground was placed around the forearm, distal to the elbow. EMG recordings were amplified 1000x (Intronix Technologies Corporation Model 2024F, Bolton, Canada) and band-pass filtered between 20 Hz and 2.5 kHz. Data was digitized using an analog-to-digital interface at 5 kHz (Power1401, Cambridge Electronics Design, Cambridge, UK) and stored on a secure computer for offline analysis (Signal v6.02, Cambridge Electronics Design, Cambridge, UK).

Electroencephalography

SEPs were acquired by positioning electroencephalography (EEG) electrodes over S1 at C3' (2 cm posterior to C3) and referenced to Fz (International 10-20 system). Electrical stimulation (Digitimer DS7AH, 200 μ s square wave pulses) was delivered over the median nerve at the wrist using a bar electrode, or over the digital nerve of the index finger using ring electrodes (cathode proximal). For median nerve (MN) stimulation, the minimum intensity to evoke a twitch in the APB muscle was used (Bailey et al. 2016; Turco et al.

2017). For digital nerve (DN) stimulation, the minimum intensity that elicited a perceived stimulus as reported by the participant was defined as sensory threshold. To assess sensory threshold, a suprathreshold stimulus was first applied and participants were queried to report the presence or absence of sensation. The stimulus intensity was subsequently reduced in increments of 1 mA until sensation was no longer perceived. The stimulus intensity was then increased and decreased in increments of 0.1 mA to determine the minimal stimulus intensity at which the stimulus was perceived. The intensity of DN stimulation was set to 2×sensory threshold (Bailey et al. 2016; Turco et al. 2017). The intensities of MN (motor threshold) and DN (2×sensory threshold) stimulation were chosen because they correspond to 50% SNAP_{max} in both nerves (Bailey et al. 2016; Turco et al. 2017). One study observed DN-evoked SAI at 3×sensory threshold only, however it is unclear whether the current (in mA) used in that study corresponds to the current used presently for 2×sensory threshold (Dubbioso et al. 2017). Five hundred stimuli were delivered at a rate of 2 Hz, and time-locked averaged to determine the latency of the N20 following both MN and DN stimulation.

Transcranial Magnetic Stimulation

Single-pulse TMS was delivered using a monophasic waveform to the left primary motor cortex (M1) using a figure-of-eight branding coil (50 mm diameter) connected to a Magstim 200² stimulator (Magstim, UK). The coil was oriented at a 45-degree angle to induce a posterior to anterior current and positioned over the motor hotspot that was digitally registered usingBrainsight Neuronavigation (Rogue Research, Canada). The motor hotspot

was defined as the location that elicited the largest MEP in the right FDI muscle (Rossini et al. 2015).

Afferent Inhibition

The intensity of TMS was adjusted to evoke a MEP of ~1 mV peak-to-peak amplitude. Both SAI and LAI were assessed following stimulation of the median (SAI_{MN}, LAI_{MN}) and digital (SAI_{DN}, LAI_{DN}) nerves. To assess SAI, the ISI between nerve stimulation and TMS was set to 24 ms (referred to as SAI₂₄) (Classen et al. 2000; Helmich et al. 2005; Ni et al. 2011; Tamburin et al. 2001, 2005; Tokimura et al. 2000; Tsutsumi et al. 2012b) or relative to the latency of the N20 component of the SEP (N20 + 4 ms, referred to as SAI_{N20}) (Helmich et al. 2005; Ni et al. 2011; Tamburin et al. 2005; Tokimura et al. 2000). To assess LAI, nerve stimulation preceded the TMS pulse by 200 ms (Chen et al. 1999). All measures of afferent inhibition included 12 conditioned MEPs (nerve stimulation and TMS) and 12 unconditioned MEPs (TMS alone), in line with previous studies investigating afferent inhibition (Helmich et al. 2005; Di Lazzaro et al. 2007a; Udupa et al. 2014). The order of nerve stimulation intensity was randomized across participants using a William's square design but held constant for the two sessions within individuals.

Statistical Analyses

EMG trials were discarded if the peak-to-peak amplitude of the signal 100 ms before the TMS artefact was greater than 100 μ V, similar to the analyses of previous work (Schambra et al. 2015). The average EMG area within this 100 ms window was compared across

sessions for each acquisition of afferent inhibition using paired t-tests to ensure that baseline noise was consistent. For SAI and LAI, inhibition was calculated as a ratio of the mean conditioned to mean unconditioned MEP for each individual: $SAI/LAI = (MEP_{conditioned}/MEP_{unconditioned}) \times 100\%$. Outliers were identified using Grubb's test and were removed from all analyses. Normality was assessed using the Shapiro-Wilks test and visual screening of box-and-whiskers and histogram plots, while heteroscedasticity was assessed using Bland-Altman plots in accordance with previous work (Damron et al. 2008; Schambra et al. 2015). Two-tailed paired t-tests were used to compare the means of each measure between sessions in order to determine whether systematic error was present between test and retest. However, SAI data was analyzed with a repeated measures ANOVA using the factors ISI (2 levels: 24ms and N20+4ms) and SESSION (2 levels: Session 1 and Session 2). The significance level was set to 5% so that a result is considered statistically significant when $p < 0.05$, while Bonferroni correction was used for multiple comparisons.

Reliability Assessment

Relative reliability was evaluated using estimates of the ICC (2, k). A two-way random effects model was used because all participants were tested by the same experimenter, assumed to be representative of a population of well-trained TMS experimenters (Weir 2005). There are no absolute guidelines for interpreting the ICC; however, previous sources have suggested that ICC values with 95% confidence intervals above 0.9 indicate excellent relative reliability, 0.75-0.9 is considered strong, 0.5 to 0.75 is considered moderate, and

values below 0.5 is considered poor (Koo and Li 2016; Portney and Watkins 2009). Interpretation of the ICC strictly based on these cutoffs is problematic as the magnitude of the ICC is dependent upon the heterogeneity of the sample tested. Therefore, to aid in the interpretation of the ICC, the coefficient of variation (CV) was obtained for each measure. The CV is defined with the following formula: $CV = SD/mean \times 100$, where SD is the standard deviation of the measure.

Absolute reliability describes the amount of variability within an individual as a result of repeated testing. This was quantified using the SEM_{eas} , which is expressed in the same units as the measure evaluated ($MEP_{conditioned}/MEP_{unconditioned} \times 100\%$). SEM_{eas} was calculated as: $SEM_{eas} = \sqrt{MSE}$, where MSE is mean square error term from a repeated measures ANOVA (Weir 2005). Measurement error was also expressed as a percentage of the mean using the following formula: $\%SEM_{eas} = SEM_{eas}/mean \times 100\%$ (Weir 2005). $\%SEM_{eas}$ was provided because it is independent of the units of the original measurement and so is more easily interpreted and comparable to other studies. A cutoff of $\%SEM_{eas} < 10\%$ was used as an indication of low measurement error, consistent with previous studies (Beaulieu et al. 2017b; Flansbjer et al. 2005; Schambra et al. 2015). The SEM_{eas} was also used to calculate the $SDC_{individual}$ with the following formula: $SDC_{individual} = SEM_{eas} \times \sqrt{2} \times 1.96$. The $SDC_{individual}$ provides the minimum amount of change in the dependent variable that is needed to be considered a real change with 95% confidence and that is not due to measurement error (Beckerman et al. 2001). Estimations of SDC for different group sizes

(from 1 to 100) were then calculated as $SDC_{group} = SDC/\sqrt{n}$ where n is the sample size. Similar to SEM_{cas} , the SDC is expressed in the same units of the original measurement.

5.3 Results

Procedures were well tolerated with no adverse events or attrition. Paired t-tests, with Bonferroni corrections, confirmed that EMG area prior to the stimulation artefacts was not significantly different across sessions for each permutation of SAI/LAI acquired (all $p > 0.01$, Bonferroni corrected for six comparisons). A DN-evoked N20 was not observed for one individual on both sessions due to artefacts in the EEG trace, suggesting that this participant could not relax during DN stimulation. Therefore, the data from this individual was removed from all DN analyses (LAI_{DN} , $SAI_{24,DN}$, $SAI_{N20+4,DN}$). Next, a DN-evoked N20 was not clearly observed for one individual in Session 2 due to electrical noise. Therefore, the data from this individual was removed from the $SAI_{N20+4,DN}$ condition. Following Grubb's test, one outlier was removed from LAI_{MN} , LAI_{DN} , $SAI_{24,MN}$, and $SAI_{N20+4,MN}$. Therefore, LAI_{MN} , $SAI_{24,MN}$, $SAI_{24,DN}$, and $SAI_{N20+4,MN}$ reflects $n = 29$ while LAI_{DN} and $SAI_{N20+4,DN}$ reflects $n = 28$. Importantly, all SAI and LAI data were homoscedastic and normally distributed. The intensity of nerve stimulation, the amplitude of the unconditioned MEP, and the latency of the N20 was not significantly different between sessions (Table 5.1). Importantly, the current (in mA) used to stimulate the MN and DN were similar across sessions and showed high relative reliability (ICC of 0.88 and 0.82, respectively) and high absolute reliability (SEM_{cas} of 0.10 and 0.13, respectively).

Table 5.1: Group-averaged data.

	Session 1 Mean ± SD (CV)	Session 2 Mean ± SD (CV)	% change	Statistics
MN stimulation (mA)	8.73 ± 2.16	8.76 ± 1.96	0.38%	p=0.91*
DN stimulation (mA)	3.74 ± 0.79	3.79 ± 0.85	1.43%	p=0.59*
MN N20 latency (ms)	18.35 ± 1.16	18.25 ± 1.01	-0.28%	p=0.64*
DN N20 latency (ms)	21.50 ± 1.89	21.26 ± 1.31	-0.74%	p=0.54*
Unconditioned MEP (mV)				
SAI _{24,MN}	1.12 ± 0.17	1.12 ± 0.27	0.49%	p=0.93*
SAI _{N20+4,MN}	1.14 ± 0.17	1.12 ± 0.27	-1.20%	p=0.82*
SAI _{24,DN}	1.09 ± 0.20	1.08 ± 0.21	-0.97%	p=0.89*
SAI _{N20+4,DN}	1.09 ± 0.21	1.08 ± 0.22	-1.48%	p=0.69*
LAI _{MN}	1.12 ± 0.17	1.12 ± 0.27	-0.08%	p=0.99*
LAI _{DN}	1.10 ± 0.21	1.09 ± 0.21	-0.74%	p=0.84*
% of unconditioned MEP				
SAI _{24,MN}	78.12 ± 22.97 (28.86%)	79.17 ± 24.72 (31.23%)	1.34%	ISI _(1,28) =18.30, p<0.001 Session _(1,28) =0.10, p=0.78 ISI*Session _(1,28) =0.85, p=0.37
SAI _{N20+4,MN}	63.73 ± 22.37 (35.11%)	60.27 ± 25.44 (42.20%)	-5.42%	
SAI _{24,DN}	73.27 ± 23.44 (32.60%)	85.07 ± 27.99 (32.90%)	16.10%	ISI _(1,27) =0.25, p=0.62 Session _(1,27) =2.93, p=0.10 ISI*Session _(1,27) =0.35, p=0.56
SAI _{N20+4,DN}	74.30 ± 22.98 (30.75%)	81.48 ± 24.42 (29.97%)	9.66%	
LAI _{MN}	60.29 ± 31.42 (52.11%)	61.20 ± 38.33 (66.54%)	1.50%	p=0.90*
LAI _{DN}	68.84 ± 34.11 (50.52%)	68.34 ± 34.86 (51.01%)	-0.73%	p=0.93*

*indicates that *P* values reflect two-tailed paired t-tests comparing Session 1 and Session 2.

CV: coefficient of variation, DN: digital nerve, LAI: long-latency afferent inhibition, MEP: motor-evoked potential; MN: median nerve, SAI₂₄: SAI acquired at an interstimulus interval of 24 ms, SAI_{N20+4}: SAI acquired at an interstimulus interval of N20 + 4 ms, SD: standard deviation

Short-latency Afferent Inhibition

Table 5.1 shows the group-averaged SAI data. A two-way repeated measure ANOVA on SAI evoked by MN stimulation showed a main effect of ISI ($F_{(1,28)}=18.299$, $p<0.001$), such that the magnitude of SAI_{N20+4,MN} was greater than SAI_{24,MN} (Figure 5.1). This ANOVA revealed no main effects or interaction on SAI evoked by DN stimulation (Figure 5.2). Therefore, we conclude that SAI was not different between sessions, regardless of ISI used or nerve stimulated.

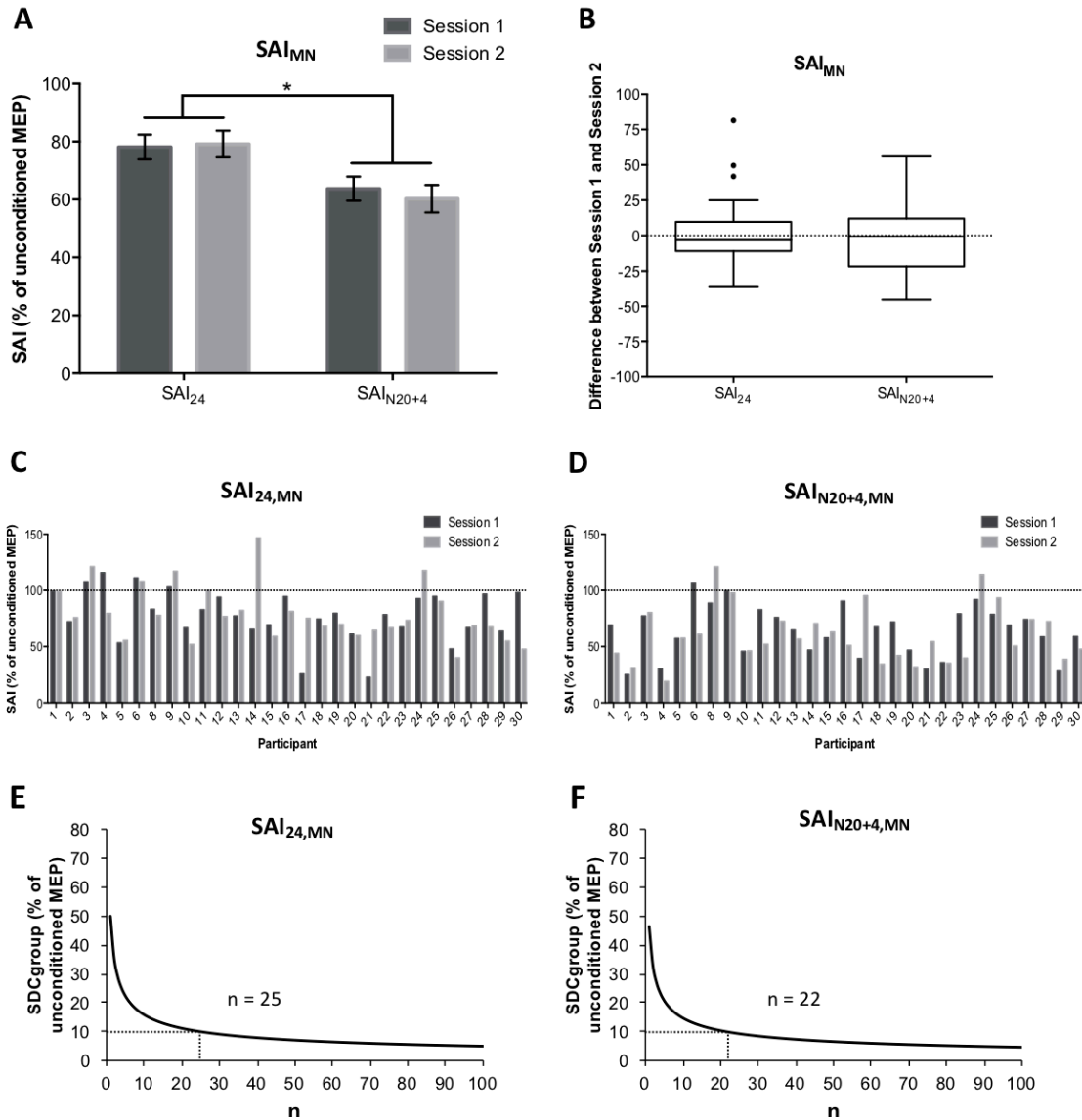


Figure 5.1: Group-averaged MN-evoked SAI data.

(A) SAI (expressed as a percentage of the unconditioned MEP), with standard error, evoked at the ISI of 24ms (SAI_{24}) or N20+4ms (SAI_{N20+4}) in Session 1 and Session 2. *indicates a significant difference between ISIs. (B) The distribution of the differences between Session 1 and Session 2 for SAI_{MN} evoked at the ISI of 24ms or N20+4ms. Shown is the median with whiskers spanning 1.5 x the interquartile range, and circles are values outside 1.5 x the interquartile range. (C) and (D) shows the individual magnitude of $SAI_{24,MN}$ and $SAI_{N20+4,MN}$, respectively. (E) and (F) shows the smallest detectable change for the group (SDC_{group}) as a function of sample size (n) (calculated as $SDC_{group} = SDC_{individual}/\sqrt{n}$). (E) For $SAI_{24,MN}$ stimulation, at least 25 participants are required to reduce SDC_{group} below 10% of the unconditioned MEP. (F) For $SAI_{N20+4,MN}$, at least 22 participants are required to reduced SDC_{group} below 10% of the unconditioned MEP.

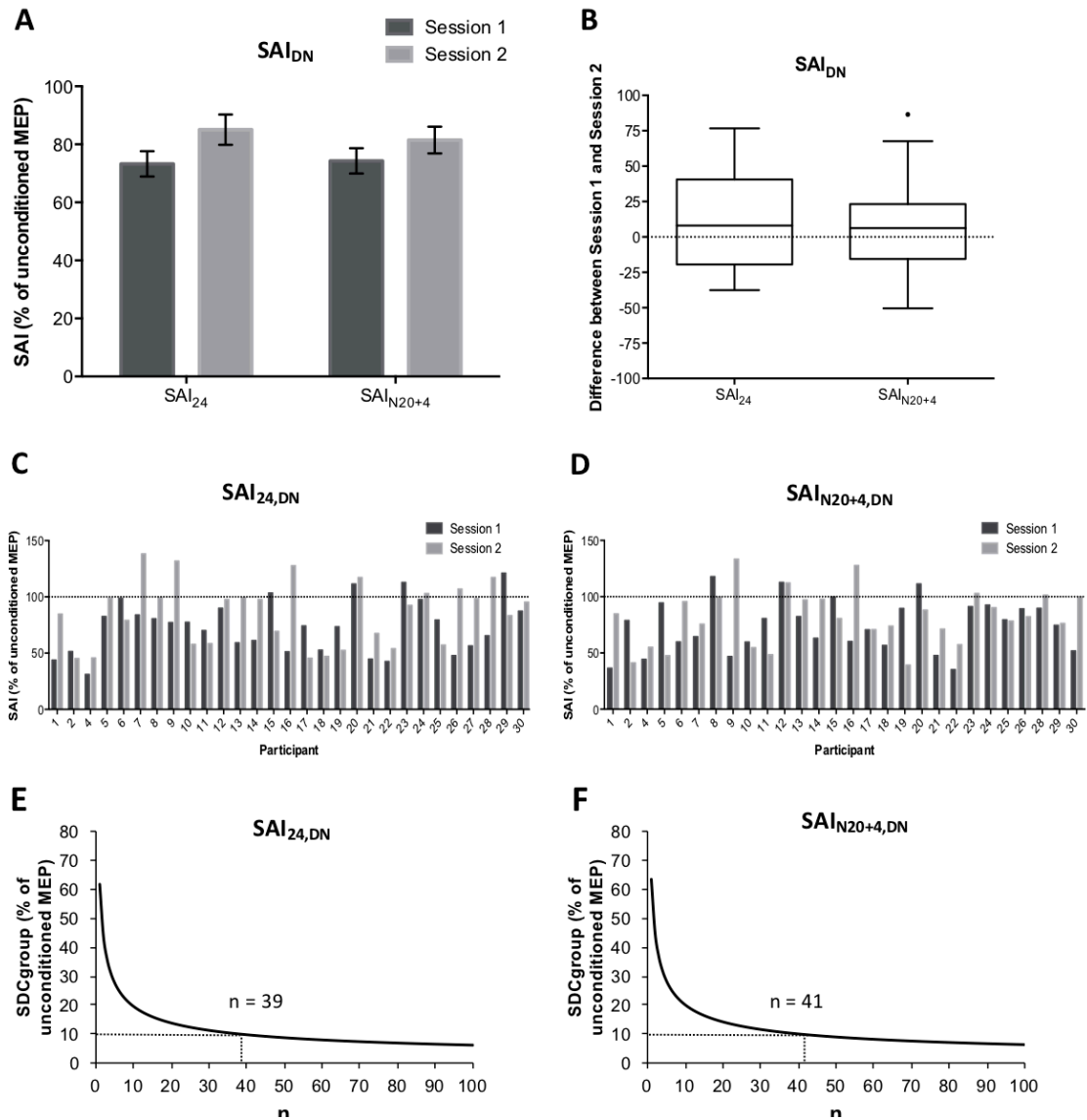


Figure 5.2: Group-averaged DN-evoked SAI data.

(A) SAI (expressed as a percentage of the unconditioned MEP), with standard error, evoked at the ISI of 24ms (SAI_{24}) or N20+4ms (SAI_{N20+4}) in Session 1 and Session 2. (B) The distribution of the differences between Session 1 and Session 2 for SAI_{DN} evoked at the ISI of 24ms or N20+4ms. Shown is the median with whiskers spanning 1.5 x the interquartile range, and circles are values outside 1.5 x the interquartile range. (C) and (D) shows the individual magnitude of $SAI_{24,DN}$ and $SAI_{N20+4,DN}$, respectively. (E) and (F) shows the smallest detectable change for the group (SDC_{group}) as a function of sample size (n) (calculated as $SDC_{group} = SDC_{individual}/\sqrt{n}$). (E) For $SAI_{24,DN}$ stimulation, at least 39 participants are required to reduce SDC_{group} below 10% of the unconditioned MEP. (F) For $SAI_{N20+4,DN}$, at least 41 participants are required to reduced SDC_{group} below 10% of the unconditioned MEP.

The reliability statistics for SAI data are shown in Table 5.2. SAI evoked by MN stimulation had moderate relative reliability (ICC = 0.61). In contrast, SAI evoked by DN stimulation had poor relative reliability (ICC < 0.5). SAI evoked by MN stimulation had an SEM_{cas} of ~18% of the mean unconditioned MEP, while SAI evoked by DN stimulation had an SEM_{cas} of ~22% of the mean unconditioned MEP. %SEM_{cas} was >10% for all measures of SAI, indicating large measurement error. SDC_{individual} was ~50% (of the mean unconditioned MEP) for SAI evoked by MN stimulation, and ~62% (of the mean unconditioned MEP) for SAI evoked DN stimulation. Our estimations of SDC_{group} based on our sample size is below 10% (of the mean unconditioned MEP) for SAI evoked by MN stimulation, indicating that our sample size was sufficient to obtain SAI_{N20+4,MN} (Figure 5.1E) and SAI_{24,MN} (Figure 5.2E) with an accuracy of <10% of mean unconditioned MEP. ~40 participants would be required to achieve an SDC_{group} below 10% for SAI_{N20+4, DN} (Figure 5.1F) and SAI_{24, DN} (Figure 5.2F).

Table 5.2: Reliability statistics.

	ICC (95% CI)	SEM _{cas}	SEM _{cas} %	SDC _{individual}	SDC _{group}
SAI _{24,MN}	0.61 (0.16 to 0.82)	18.00%	22.90%	49.91%	9.27%
SAI _{N20+4,MN}	0.68 (0.32, 0.85)	16.73%	26.99%	46.37%	8.61%
SAI _{24, DN}	0.38 (0 to 0.70)	22.26%	28.12%	61.71%	11.46%
SAI _{N20+4, DN}	0.13 (0, 0.59)	22.88%	29.38%	63.43%	11.99%
LAI _{MN}	0.59 (0.10 to 0.81)	27.00%	44.45%	74.84%	13.90%
LAI _{DN}	0.74 (0.44 to 0.88)	22.27%	32.47%	61.73%	11.67%

SEM_{cas}, SDC_{individual}, and SDC_{group} are expressed as a percentage of the unconditioned MEP, while %SEM_{cas} expresses the SEM_{cas} as a percentage of the mean.

CI: confidence interval, DN: digital nerve, ICC: intraclass correlation coefficient, LAI: long-latency afferent inhibition, MN: median nerve, SAI₂₄: SAI acquired at an interstimulus interval of 24 ms, SAI_{N20+4}: SAI acquired at an interstimulus interval of N20 + 4 ms, SD: standard deviation, SDC: smallest detectable change, SEM_{cas}: standard error of measurement, SEM_{cas} %: relative SEM_{cas}

Long-latency Afferent Inhibition

Table 5.1 shows the group-averaged LAI data with corresponding t-tests. LAI_{MN} and LAI_{DN} were not different across sessions (two-tailed paired t-tests, both $p > 0.05$). Figure 5.3A plots the magnitude of LAI evoked by median and digital nerve stimulation, while Figure 5.3B plots the distribution of differences between Session 1 and Session 2. Individual LAI data are shown in Figure 5.3C and 5.3D.

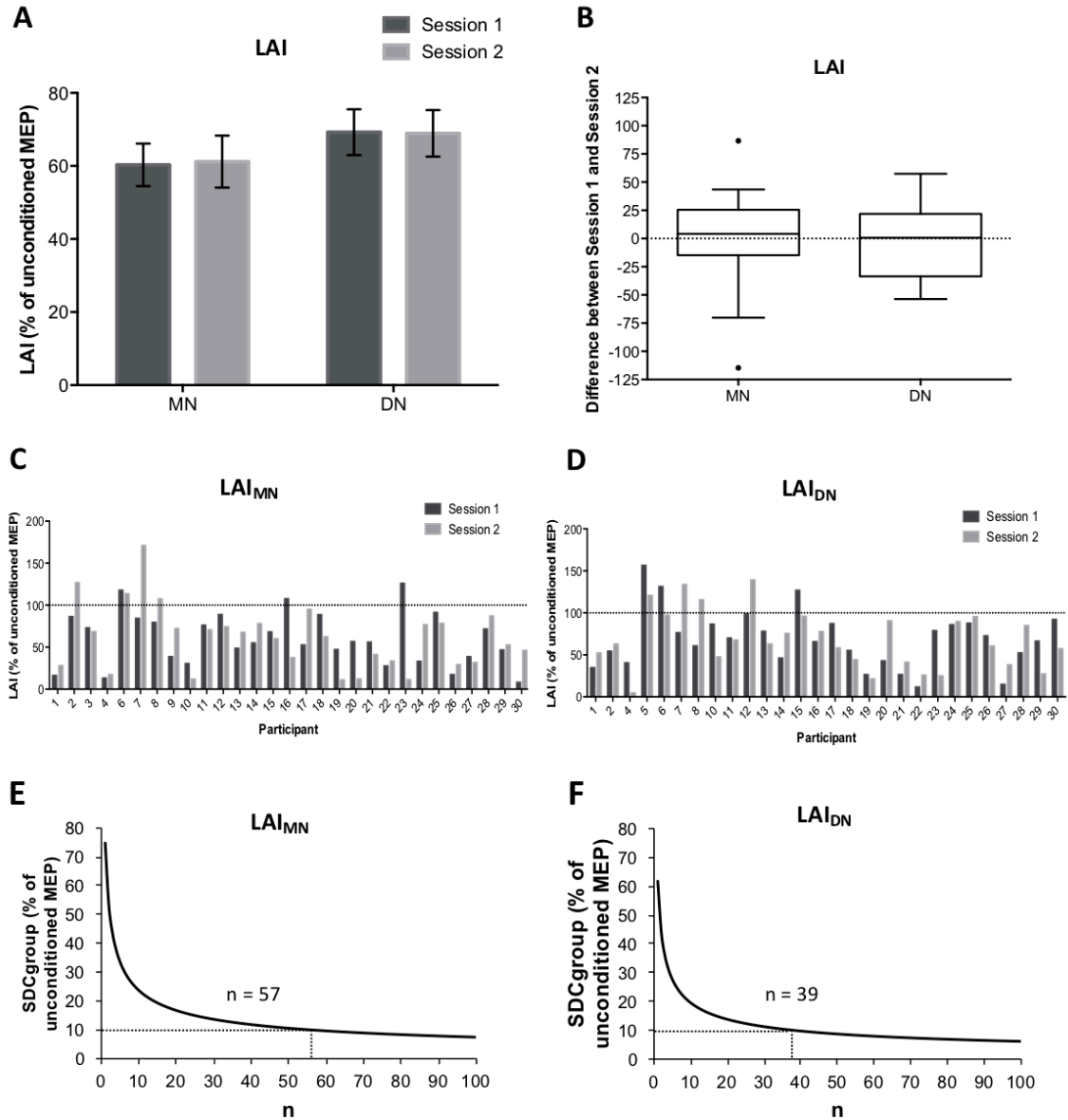


Figure 5.3: Group-averaged LAI data.

(A) LAI (expressed as a percentage of the unconditioned MEP), with standard error, evoked by MN or DN stimulation in Session 1 and Session 2. (B) The distribution of the differences between Session 1 and Session 2 for LAI evoked by MN or DN stimulation. (C) Individual LAI_{MN}, and (D) individual LAI_{DN} are shown. The smallest detectable change for the group (SDC_{group}) as a function of sample size (n) is shown for (E) LAI_{MN} and (F) LAI_{DN}. For LAI_{MN}, at least 57 participants are required to reduced SDC_{group} below 10% of the unconditioned MEP. For LAI_{DN}, at least 39 participants are required to reduced SDC_{group} below 10% of the unconditioned MEP.

Reliability statistics for LAI data are shown in Table 5.2. LAI_{MN} and LAI_{DN} had moderate reliability of an ICC of 0.59 and 0.74, respectively. SEM_{cas} for LAI_{MN} was 27.00% of the mean unconditioned MEP amplitude and for LAI_{DN} was 22.27% of mean unconditioned MEP amplitude. %SEM_{cas} was above 10% for both LAI_{MN} and LAI_{DN} (i.e., 44.45% and 32.46%, respectively). SDC_{individual} for LAI_{MN} was 74.84% of mean unconditioned MEP amplitude and for LAI_{DN} was 61.73% of mean unconditioned MEP amplitude, respectively. Therefore, individuals must show ~60-75% change in LAI_{MN}, for example, in order to attribute such change to a real neurophysiological event rather than measurement error. Our estimations show that to achieve an SDC_{group} below 10%, 57 participants would be required for LAI_{MN} (Figure 5.3E) and 39 participants would be needed for LAI_{DN} (Figure 5.3F).

Intersession interval

The interval between Sessions 1 and 2 was 7 ± 4 days to allow flexible scheduling and promote retention. We then questioned whether the individual's with longer intersession intervals showed greater changes in afferent inhibition between Sessions 1 and 2. To address this, we performed correlations between the percent change in SAI/LAI between Session 1 and Session 2 with the intersession interval (in days). None of these correlations were significant (all $p > 0.1$), indicating no relationship between the interval and the change in SAI/LAI.

5.4 Discussion

To our knowledge, this is the first study to provide a comprehensive reliability assessment of SAI and LAI. Reliability was evaluated through multiple approaches. *Relative* reliability was quantified using the ICC, providing an indication of the ability to discriminate between subjects or groups with repeated testing. The SEM_{cas} and SDC, indices of *absolute* reliability and responsiveness to change, respectively, were calculated to determine if SAI and LAI could be used as reliable neurophysiological biomarkers across multiple sessions within an individual and within a group.

Relative Reliability of SAI and LAI

A critical aspect of interpreting the ICC is an understanding of the confidence interval. The ICC and its corresponding 95% confidence interval should agree in the determination of the strength of reliability. ICC scores ranged between 0.13 and 0.74 for all measures of afferent inhibition but the 95% confidence intervals were quite large, hence precluding any valid qualitative interpretation. For example, our ICC data suggest that SAI_{DN} shows poor relative reliability while SAI_{MN} and LAI_{MN} show moderate relative reliability. However, the large confidence intervals do not support this conclusion. It is more appropriate to conclude that SAI_{MN} and LAI_{DN} have poor-to-moderate relative reliability. These results are comparable to the relative reliability of intracortical facilitation (ICF), a paired-pulse TMS paradigm that reports ICCs below 0.5 with large confidence interval ranges in 21 healthy, elderly individuals (Schambra et al. 2015). Interestingly, recent research shows that the reliability of conventional short-interval intracortical inhibition (SICI) (poor relative

reliability, ICC 0.37-0.51) was enhanced by the use of threshold-tracking (moderate-to-excellent relative reliability, ICC 0.61-0.88) (Samusyte et al. 2018). It is unknown if a similar technique would improve the reliability of SAI. One previous study assessed the test-retest reliability of SAI_{MN} and reported moderate reliability with an ICC of 0.67 (Brown et al. 2017). However, since the 95% confidence interval was not reported, it is unclear if the ICC agrees with the confidence interval in that study. Additionally, the sample distribution for SAI in that study was more variable (CV of ~49%) (Brown et al. 2017) compared to the present work (~30% for SAI) making comparisons between studies difficult. Notably, the between-subject variability in SAI obtained within this study is less than that obtained in previous work by Fischer & Orth (2011) (CV of ~50%) – this may be a consequence the smaller sample size (17 participants) used in that study.

Only LAI_{DN} showed a 95% confidence interval that was extended around the moderate reliability range. In this case, both the absolute ICC of 0.74 and the confidence interval of 0.44-0.88 allow us to conclude that LAI_{DN} is moderately reliable. From a quantitative point of view, these results underscore that between 44% and 88% of the total variance is likely due to inter-individual differences and the remaining result from intra-individual variations between sessions (Weir 2005). Therefore, based on our methods and sample, LAI_{DN} is better able to reliably differentiate between individuals, highlighting its potential diagnostic or prognostic value as suggested elsewhere (Beaulieu et al. 2017a).

Absolute Reliability and Smallest Detectable Change of SAI and LAI

The SEM_{cas} was obtained to provide an understanding of absolute reliability. $\%SEM_{\text{cas}}$ was $>10\%$ for all measures of afferent inhibition, indicating high measurement noise (Beaulieu et al. 2017b; Flansbjer et al. 2005; Schambra et al. 2015). Comparatively, measurement noise was greater for LAI ($\sim 38\%$) compared to SAI ($\sim 27\%$). Although the explanation for this difference is unclear, the differing pharmacological profile of SAI and LAI may be a contributing factor. Previous work has shown that both SAI and LAI are modulated by activity of the $GABA_A$ receptor (Di Lazzaro et al. 2005a, 2005b, 2007a; Turco et al. 2018a). However, while SAI is modulated by cholinergic activity (Di Lazzaro et al. 2000b), it is unknown if LAI is also cholinergic in nature. We also show that measurement noise is similar for afferent inhibition evoked by MN ($\sim 31\%$) and DN ($\sim 30\%$) stimulation, suggesting that the composition of the nerve stimulated is not an influencing factor of absolute reliability.

Notably, we tested two different approaches to achieve our SAI measures. SAI was assessed using a standard ISI of 24 ms and an ISI relative to the latency of the N20 component of the SEP (N20 + 4 ms). Both methods have been used in the literature to evoke SAI (Classen et al. 2000; Helmich et al. 2005; Di Lazzaro et al. 2005b, 2005a, 2007a; Ni et al. 2011; Tamburin et al. 2001, 2005; Tokimura et al. 2000). Our results show that measurement error is similar between these two approaches, indicating that absolute reliability is not influenced by the experimental approach used to quantify SAI. However, use of the N20 latency led to significantly stronger SAI_{MN} in both sessions. Therefore, if future studies are seeking to reliably evoke SAI, our results suggest that the use of the N20

latency is not necessary. However, if the goal of a future study is to evoke maximal SAI via median nerve stimulation, the ISI relative to the N20 latency should be used rather than a standard ISI.

Both SAI and LAI had high values for $SDC_{\text{individual}}$ ranging from 46-75% of the unconditioned MEP. LAI_{MN} had an $SDC_{\text{individual}}$ of $\sim 75\%$, indicating that an individual must display a change of more than 75% of the unconditioned MEP to exceed measurement error. This high level of measurement error leads us to conclude that both SAI and LAI are insensitive to changes within an individual. Similarly, large $SDC_{\text{individual}}$ values have been reported for other TMS measures including SICI ($\sim 40\%$) and ICF ($\sim 60\%$) (Schambra et al. 2015). Importantly, $SDC_{\text{individual}}$ is reduced exponentially when expressed relative to the sample size (e.g. see Figure 5.1E). For example, the SDC_{group} for SAI_{MN} is $\sim 9\%$ of the unconditioned MEP. Therefore, a change greater than $\sim 9\%$ of the unconditioned MEP in the group mean is needed to exceed measurement noise in the group. Collectively, our data suggests that SAI and LAI reliably detect changes within a group but not within an individual.

Although there is no gold standard for the preferred value of SDC_{group} , one study has recommended to achieve a value less than or equal to 10% for SICI (Schambra et al. 2015). Using our data, we calculated the sample required to achieve $SDC_{\text{group}} \leq 10\%$ of the unconditioned MEP and show that more participants are required for SAI_{DN} compared to SAI_{MN} . Further, LAI_{MN} required more participants than LAI_{DN} to achieve this threshold.

This analysis approach could be used in future research to determine the appropriate sample size to achieve an appropriately low SDC_{group} .

Sources of Variability That Contribute to Reliability

Potential sources of inter-subject variability that contribute to reliability may include but are not limited to biological sex, ovarian hormones, fitness level, wellness, diet, personality and intelligence quotient (IQ). While our sample included an equal number of males and females, we were underpowered to perform analyses comparing the reliability of afferent inhibition between sexes. Future studies with larger sample sizes may consider whether afferent inhibition is influenced by biological sex. Further, there are many potential sources of inter-session variability. These include the intensity of TMS or nerve stimulation and baseline cortical excitability, although we found no statistically significant difference in TMS intensity or nerve stimulation intensity between sessions. Importantly, we obtained SAI and LAI with 12 trials only, similar to previous work investigating afferent inhibition (Helmich et al. 2005; Di Lazzaro et al. 2007a; Udupa et al. 2014). Future studies will be needed to investigate if a larger number of trials ensures higher measurement reliability. Interestingly, recent evidence indicates that SAI is reduced during the retrieval of negative memories, with no modulation of LAI suggesting that thought processes impact the magnitude of SAI (Mineo et al. 2018). In our study, we did not control the focus of attention or thought processes through the use of a task intended to distract or maintain focus. Therefore, it is possible that shifting of attentional focus throughout the experiment

contributed to the variability in SAI. This consideration would be particularly important when assessing SAI in populations experiencing altered cognition.

Significance of Afferent Inhibition

Importantly, this study only examined young, healthy adults and, therefore, the results are limited to this population and do not extend to aging and clinical populations. The results of this study will be beneficial for future basic science studies acquiring SAI and LAI in a similar population to that studied herein. Future studies should examine the reliability of SAI and LAI in aging and clinical populations.

Previous work shows that SAI is reduced in those with spinal cord injury (Bailey et al. 2015) and Alzheimer's disease (Nardone et al. 2008a), whereas LAI is abolished in Parkinson's disease (Sailer et al. 2003). This indicates that SAI and LAI have potential diagnostic value. Future studies should investigate the diagnostic potential of SAI and LAI by assessing relative reliability in clinical populations and individuals presenting with different severity levels of a particular neurological pathology, particularly in Alzheimer's and Parkinson's disease. If the goal of future reliability studies is to establish a TMS measure for diagnostic purposes, an effort should be made to ensure that the sample dispersion of the recruited participants is approximately representative of the population it is intended to be used for. That is, the ICC should be tested in a sample of individuals that are sufficiently different from one another (e.g. different pathologies, ages, genders, etc.).

However, if the goal is to find and reduce potential factors affected the variability of TMS outcomes, the recruited sample should be stable and homogenous.

Limitations

First, we note that the intersession interval ranged was, on average, 7 ± 4 days. We allowed this flexibility to accommodate personal schedules, thereby promoting participant retention. However, there was no correlation between the intersession interval and the change in SAI/LAI across sessions. This suggests that any variance in the intersession interval did not contribute to variability in afferent inhibition across sessions. In addition, because the purpose of this study was to assess intra-rater test-retest reliability, the data were acquired by a single experimenter (i.e. CVT delivered TMS in all sessions). However, future studies may include multiple experimenters to assess inter-rater reliability, which is a useful metric for study of clinical populations. Next, we note that SAI was acquired only at the ISIs of 24ms and N20+4ms, while LAI was only acquired with an ISI of 200ms. Previous research has shown that SAI and LAI can be acquired at ISIs ranging from ~20-25ms (Tokimura et al. 2000) and 200-1000ms (Chen et al. 1999; Turco et al. 2018b), respectively. Future studies should investigate whether the reliability of SAI and LAI is influenced by the precise ISI used to evoke these circuits.

Conclusions & Future Considerations

This study investigated the reliability of SAI and LAI in a healthy, young population. The ICCs indicate that LAI_{DN} has moderate relative reliability, SAI_{MN} and LAI_{MN} has poor-to-

moderate relative reliability, while SAI_{DN} has poor relative reliability. Based on the SEM_{eas} and $SDC_{individual}$ values obtained, we advise against using SAI and LAI as biomarkers to detect individual neurophysiological change. However, as shown by SDC_{group} , SAI and LAI can be used to reliably detect change within the group given an appropriate sample size. Future TMS studies should consider using the SDC as a compliment analysis in intervention studies to determine (1) if the change in the TMS measurement within an individual is real using $SDC_{individual}$ and (2) if sample size is sufficient to reduce SDC_{group} to an acceptable value to detect real group-level changes. We recommend measures of absolute reliability for all future studies of afferent inhibition to more accurately interpret meaningful change versus experimental error.

5.5 Rationale for Study 4

Following Study #3, it was clear that there was a large amount of variability that was present within SAI and LAI data. Therefore, in Study #4 I considered factors that may contribute to this variability. Specifically, glucose is a precursor to GABA, and previous animal work has shown that glucose upregulates activity of the GABA_A receptor. This may suggest that glucose administration would reduce afferent inhibition. Therefore, the purpose of Study #4 was to determine whether administration of glucose would influence the magnitude of SAI and/or LAI.

Chapter 6: Study 4

The Effect of Glucose Levels on Afferent Inhibition

A version of this manuscript is published in: Toepp, S. L., Turco, C.V., Locke, M.B., Nicolini, C., Ravi, R., & Nelson, A.J. (2019). The Impact of Glucose on Corticospinal Excitability. *Brain Sciences*, 9, 339.

6.1 Introduction

Glucose is the main source of energy for the brain. It is required for the maintenance of membrane potentials and ionic gradients, generation of action potentials, neurotransmitter synthesis, and neurotransmission (Mergenthaler et al. 2013). Therefore, normal circulating blood glucose levels are essential for proper brain function. Currently, it is unknown how the sensorimotor system is influenced by glucose.

The sensorimotor system can be probed by pairing peripheral nerve stimulation with transcranial magnetic stimulation (TMS). This evokes a phenomenon known as afferent inhibition, which occurs at both short and long interstimulus intervals (ISIs), also known as short-latency afferent inhibition (SAI) and long-latency afferent inhibition (LAI). We have recently shown that there is considerably between- and within-subject variability associated with SAI and LAI in a healthy, young population (Turco et al. 2019a). It is unknown how factors of daily living such as diet, specifically levels of circulating glucose, modulate afferent inhibition and contribute to this variability. However, this is especially important to establish because SAI and LAI are impaired in multiple neurodegenerative conditions such as Alzheimer's disease (Nardone et al. 2008a) and Parkinson's disease (Dubbioso et al. 2019; Sailer et al. 2003) and could therefore potentially be used as

diagnostic tools or biomarkers of neurophysiological change. Further, there is evidence showing that those with Parkinson's disease demonstrate cortical hypometabolism and subcortical hypermetabolism of glucose while those with Alzheimer's disease show cerebral hypometabolism of glucose (Borghammer 2012; Kapogiannis and Mattson 2011). It is unknown if the weakening of SAI/LAI in these populations reflects the impairment in glucose metabolism.

The effect of acute elevations in blood glucose on SAI and LAI has yet to be investigated. Previous TMS research has shown that resting corticospinal excitability is increased 60 minutes following ingestion of 68 g glucose drink (Specterman et al. 2005). Further, both carbohydrate solution intake (Gant et al. 2010) and carbohydrate mouth rinse (Bailey et al. 2019) are capable of increasing motor-evoked potentials (MEPs) acquired from upper (Gant et al. 2010) and lower-limb muscles (Bailey et al. 2019) during active contraction. Finally, Badawy et al. (2013) has shown using paired-pulse TMS that long-interval intracortical inhibition (LICI) within the primary motor cortex (M1) is reduced following a postprandial increase in glucose. This also suggests that M1 excitability is increased acutely with elevated blood glucose levels.

Afferent inhibition is modulated by activity of the gamma-aminobutyric acid type A (GABA_A) receptor, such that administration of lorazepam (a positive allosteric modulator of the GABA_A receptor) reduces both SAI (Di Lazzaro et al. 2005a, 2005b, 2007a) and LAI (Turco et al. 2018a). GABA is a major inhibitory neurotransmitter that is responsible for

regulating excitation within the brain. Hyperglycemia is associated higher human cortical GABA levels (Van Bussel et al. 2016), and glucose administration in neonatal rats increases GABA_A receptor activity (Anju et al. 2010).

The present study investigated the effects of a glucose drink on afferent inhibition in a double-blinded, placebo-controlled, three-way crossover design. Based on the evidence of glucose-induced increases in M1 excitability and GABAergic neurotransmission, it was hypothesized that afferent inhibition was modulated by glucose levels. Based on this hypothesis, we predicted that an acute increase blood glucose would reduce the magnitude of SAI and LAI.

6.2 Methods

Participants

Eighteen recreationally active, right-handed, healthy male subjects (mean age = 22.8 ± 2.4 years) participated in this study. Right-hand dominance was confirmed using a modified handedness questionnaire (Oldfield 1971). Participants were eligible for the study if they scored ‘moderate’ or ‘high’ on the International Physical Activity Questionnaire (IPAQ) or complete a minimum of 600 metabolic equivalents (MET)-min/week of physical activity. Inactive individuals were excluded to reduce the risk of influence from prediabetic impairment of glucose metabolism which is inversely correlated with physical activity level (Hu and Gu 2019). All individuals were screened for contraindications to TMS and provided written, informed consent prior to participation. This research was approved by

the Hamilton Integrated Research Ethics Board (HIREB) and conformed to the Declaration of Helsinki.

Electromyography

Surface electrodes (9 mm Ag-AgCl) were used to record electromyography (EMG) from the right first dorsal interosseous (FDI) muscle. EMG signals were band-pass filtered (20-2.5 kHz) (Intronix Technologies Corporation Model 2024F, Bolton, Canada), amplified ($\times 1000$) and then digitized (5 kHz) using an analog-to-digital interface (Power1401; Cambridge Electronics Design, Cambridge, UK). Data was analyzed using commercial software (Signal v6.02, Cambridge Electronics Design, Cambridge, UK) and stored for offline analysis.

Electroencephalography

Electroencephalography (EEG) electrodes were positioned over C3' (located 2 cm posterior to C3) and referenced to Fz (International 10-20 system). A bar electrode was positioned over the median nerve at the wrist (cathode proximal) to deliver square wave electrical pulses (200 μ s pulse width) using a constant current stimulator (DS7AH; Digitimer, Welwyn Garden City, UK). Nerve stimulation was delivered at the minimum intensity that evoked a visible twitch in the abductor pollicis brevis (APB) muscle. Time-locked averaging of five hundred stimuli delivered at 3 Hz was used to determine the latency of the N20 peak of the somatosensory-evoked potential (SEP).

Transcranial Magnetic Stimulation

TMS was delivered using a customized figure-of-eight “branding iron” coil (50 mm diameter), connected to a Magstim 200² stimulator (Magstim, Whitland, UK). The TMS coil was positioned over the left M1 at the location that elicited the largest and consistent MEPs in the right FDI muscle. The coil was oriented 45 degrees to the midsagittal plane to induce a posterior to anterior current. The location and orientation of the TMS coil was digitally registered on a standard magnetic resonance imaging (MRI) image with Brainsight Neuronavigation (Rogue Research, Montreal, QC, Canada). Resting motor threshold (RMT) was determined using the maximum-likelihood parameter estimation by sequential testing (ML-PEST) method, a predictive algorithm that determines the TMS intensity that yields a 50% probability of evoking a MEP with a peak-to-peak amplitude of 50 μ V (TMS Motor Threshold Assessment Tool, MTAT 2.0, (<http://www.clinicalresearcher.org/software.html>)). *A priori* was selected and the starting TMS intensity was set to 37% of the maximum stimulator output (MSO). The ML-PEST algorithm was stopped after 20 stimuli (Ah Sen et al. 2017).

To acquire afferent inhibition, the TMS intensity was set to evoke a MEP of \sim 1 mV in the right FDI muscle. Electrical stimulation was delivered to the median nerve at the wrist (cathode proximal) at the minimum intensity that evoked a visible twitch in the APB muscle. To acquire SAI, the ISI between peripheral nerve stimulation and TMS was 4 ms longer than the N20 latency (i.e. N20 + 4 ms). An ISI of 200 ms was used to acquire LAI. Twelve unconditioned stimuli (TMS alone) were randomly presented among 36

conditioned stimuli (nerve stimulation following by TMS, twelve stimuli per ISI), with a 5 s inter-trial interval. Inhibition was expressed as the ratio of the conditioned MEP amplitude to the unconditioned MEP amplitude:

$$SAI/LAI = \frac{\text{average MEP}_{\text{conditioned}}}{\text{average MEP}_{\text{unconditioned}}}$$

Blood Glucose and Blood Pressure

Capillary blood glucose measurements were performed via the glucose oxidase method using a hand-held diabetes monitoring device (Abbott MediSense FreeStyle Precision Neo Blood Glucose and Ketone Monitoring System, Abbott). Mean arterial blood pressure was also measured throughout the experimental session using an automated blood pressure monitor (OMRON Blood Pressure Monitor, OMRON Healthcare) because previous research has indicated that blood pressure may be elevated by ingestion of a large glucose bolus (Rebello et al. 1983; Synowski et al. 2013), The mean arterial pressure (MAP) was calculated from the systolic (SBP) and diastolic blood pressure (DBP) as indicated below:

$$MAP = \frac{2DBP + SBP}{3}$$

Experimental Protocol

This experiment consisted of four visits in total. Participants fasted for 10 hours prior to each visit. Visit 1 was a preliminary testing session, used to assess a time-course for glucose metabolism. Participants ingested a 75 g glucose bolus in 300 mL of solution and finger-prick blood samples were collected and analyzed at 10-minute intervals as indicated in

Figure 6.1A. The latency at which peak blood glucose occurred was used to ensure that TMS tests are conducted during a period of high circulating glucose for each individual.

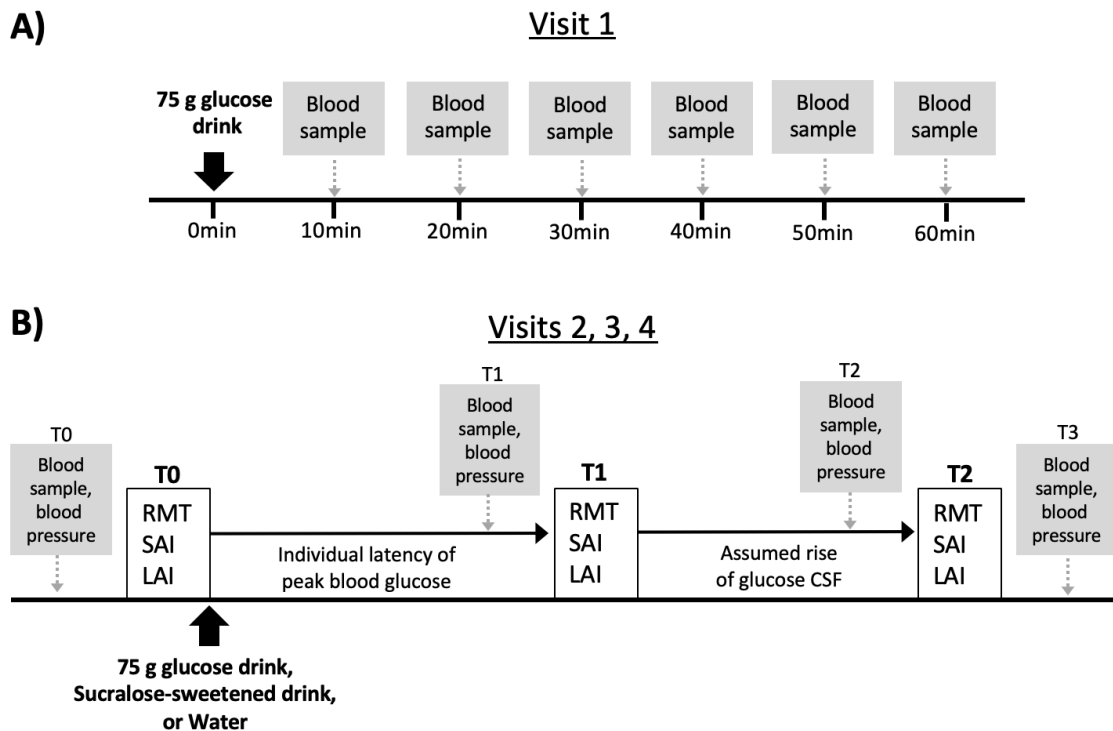


Figure 6.1: Experimental design.

The latency of peak blood glucose was obtained in Visit 1 by acquiring finger-prick blood samples every 10 min after ingestion of a 75 g glucose drink. Visits 2-4 involved the collection of dependent measures (RMT, SAI, LAI) at three time-points corresponding to baseline (T0), the participant's latency of peak blood glucose (T1), and the rise of glucose in the cerebrospinal fluid (T2, ~60 min after drink ingestion).

A minimum inter-session interval of 48 hours was imposed between Visits 2, 3, and 4. This study implemented a double-blinded, three-way crossover design in which TMS measurements were assessed before and after ingestion of water, a sucralose-flavored placebo (5 g Splenda®) or a 75 g glucose bolus (Figure 6.1B). All solutions were 300 mL. Sucralose-sweetened water was delivered to control for the sweet taste of glucose, and

water was delivered to control for drink ingestion. The order of delivery was randomized across the three sessions by the McMaster University Medical Center (MUMC) pharmacy. All treatment solutions were provided in uniform, shrouded bottles with a letter code corresponding to the order of delivery. The MUMC pharmacy held the drink randomization (i.e. drink identity) key until collection was complete to ensure that the experimenters were blind to the identity of the drink. Subjective ratings of perceived likeness and sweetness were obtained using a 10 cm Visual Analogue Scale (VAS). This scale that ranged from “dislike extremely” to “like extremely for the likeness rating and “not at all sweet” to “extremely sweet” for the sweetness rating. Blood glucose, blood pressure, perceived likeness and sweetness measurements were recorded by an unblinded researcher who did not otherwise take part in data collection or analysis. The sucralose-sweetened placebo was taste-matched with the 75 g glucose solution by MUMC pharmacy. Participants were explicitly asked not to comment on the taste of the drink to the researchers and it was made clear that this was very important to the integrity of the study. The participants were blind to the identity of the drink to the degree that they could not distinguish between the sucralose placebo and the glucose solutions.

TMS measures were acquired before (T0) and after the intervention at two time points (T1 and T2). The timing of T1 was based off of each individual’s latency of peak blood glucose determined in Visit 1. The timing of T2 was based off of the estimated latency of peak glucose levels in the cerebrospinal fluid (CSF), which occurs ~30 min after the peak of glucose in the blood plasma (Shestov et al. 2011). Blood samples via finger prick and blood

pressure were collected at baseline, 5 minutes prior to T1 and T2 measurements, and immediately following T2 measurements (termed T3).

Statistical Analyses

For all analyses, outliers were identified with SPSS and normality was assessed with the Shapiro-Wilks test. Trials were discarded if the EMG activity was $\geq 100 \mu\text{V}$ in the 100 ms preceding the stimulation artefacts (Turco et al. 2019a). First, to confirm that inhibition was observed for measures of SAI and LAI, two-way ANOVAs with the factors PATTERN (2 levels: unconditioned MEP and conditioned MEP) and TIME (3 levels: T0, T1, T2) were performed. The SAI and LAI ratios were subsequently analyzed using repeated-measure ANOVAs with factors TREATMENT (3 levels: glucose, sucralose, water) and TIME (3 levels: T0, T1, T2). Capillary blood glucose and MAP were assessed using two-way repeated measures ANOVA with four levels of TIME (T0, T1, T2, T3) and three levels of TREATMENT (glucose, sucralose, water). Degree of likeness and sweetness were assessed with a one-way ANOVA with three levels of TREATMENT (glucose, sucralose, water). Post-hoc testing of parametric ANOVAs was performed with Bonferroni-corrected two-tailed paired t-tests. A Conover's ANOVA (Conover and Iman 1982) was performed in lieu of a parametric ANOVA in cases where the data was not normally distributed (even after attempted transformations), with the Wilcoxon-signed rank test (WSRT) used for post-hoc testing.

Further analyses were performed to assess the influence of glucose on the variability and reliability of SAI and LAI. Correlation analyses were performed on data obtained within the glucose condition only, to assess the relationship between glucose levels and variability in SAI/LAI. First, the correlation between glucose levels and SAI/LAI at T0 was computed. Second, the change in SAI/LAI from T0 to T1 was correlated with the change in glucose levels from T0 to T1, and the change in SAI/LAI from T0 to T2 was correlated with the change in glucose levels from T0 to T2. This analysis explored the relationship between the variability in SAI/LAI across time with glucose levels at the approximate peak plasma (i.e. T1) and peak CSF (i.e. T2) concentrations of glucose. Next, the absolute reliability in SAI and LAI were assessed with the Standard Error of Measurement (SEM_{eas}). Absolute reliability refers to the variability of repeated measures within a stable individual and is quantified with the SEM_{eas} (Weir 2005). SEM_{eas} was calculated using the following formula:

$$SEM_{eas} = \sqrt{MSE}$$

where the MSE is the mean square error term obtained from a one-way repeated measure ANOVA with three levels of TIME (T0, T1, T2). For all statistical analyses, significance was set at $p < 0.05$ and effect sizes were calculated with Cohen's d .

6.3 Results

On Visit 1, fasting glucose concentration was 4.8 ± 0.4 mmol/L and peaked at 9.5 ± 1.0 mmol/L after ingestion of the glucose bolus. Ten participants had glucose peak latencies of 40 min ($n=10$), six had a peak latency of 30 min, one peaked at 20 min and one peaked at 50 min.

A Conover's ANOVA on glucose levels revealed a TIME*TREATMENT interaction [$F_{(6,17)} = 29.722$, $p < 0.001$] (Figure 6.2A). Glucose concentration was significantly higher following ingestion of glucose at T1, T2, and T3 (WSRT, all $p < 0.001$). Further, glucose concentration at T1 was slightly elevated following ingestion of the sucralose-sweetened placebo (WSRT, $p < 0.001$), but returned to fasting levels at T2 and T3. There was no significant change in glucose concentration following the ingestion of water. A two-way ANOVA on MAP revealed a main effect of TIME [$F_{(9,69)} = 26.602$, $p < 0.001$] (Figure 6.2B). MAP at T0 was lower than all other time points (paired t-tests, all $p < 0.001$). Further, MAP at T2 was lower than MAP at T3 (paired t-test, $p = 0.001$). A one-way Conover's ANOVA on perceived likeness revealed no effect of TREATMENT [$F_{(2,34)} = 0.357$, $p = 0.703$], suggesting that participants had a similar affinity for all three treatment solutions (glucose VAS score = 3.8 ± 2.6 cm; sucralose VAS score = 4.2 ± 2.7 cm; water VAS score = 3.6 ± 2.0 cm). A one-way Conover's ANOVA on perceived sweetness revealed a main effect of TREATMENT [$F_{(2,34)} = 79.936$, $p < 0.001$]. The glucose solution was rated as sweeter than water (glucose VAS score = 8.1 ± 1.8 cm; water VAS score = 0.7 ± 0.8 cm; WSRT, $p < 0.001$) or the sucralose solution (sucralose VAS score = 6.1 ± 2.2 cm; WSRT, $p < 0.001$). Further, the sucralose solution was rated as sweeter than water (WSRT, $p < 0.001$)

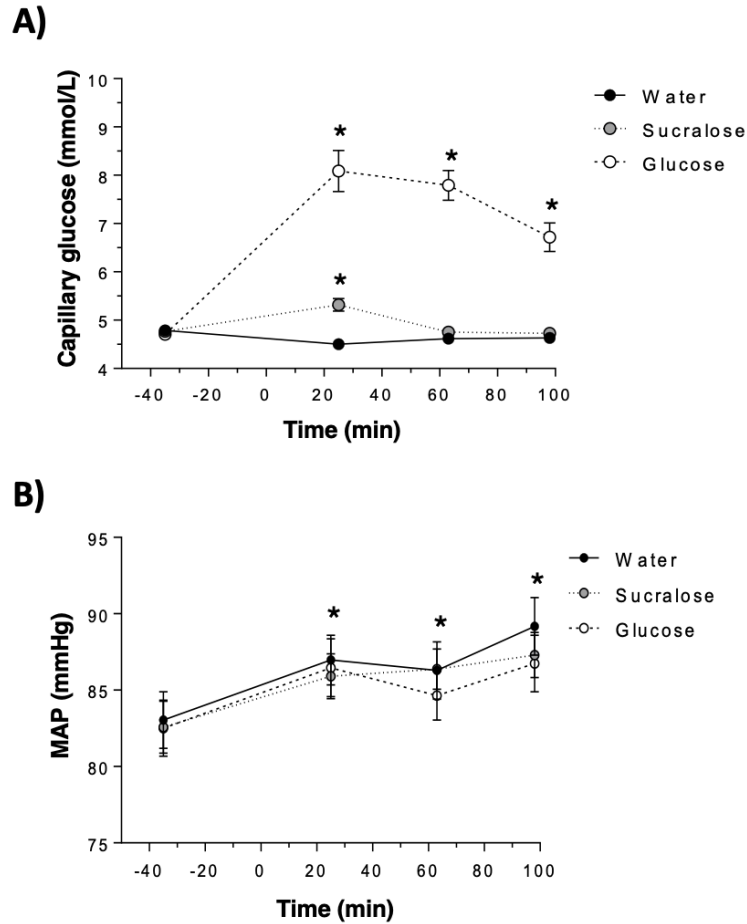


Figure 6.2: Glucose and blood pressure levels

Graphs show group-averaged means (\pm standard error). A) Blood glucose levels. *indicates a significant difference from T0 within a treatment condition. B) Mean arterial pressure (MAP). *indicates a significant difference from T0 when averaged across treatment conditions.

Results of statistical analyses on neurophysiology data are presented in Table 6.1. A two-way Conover's ANOVA on RMT revealed a main effect of TIME [$F_{(2,34)} = 8.098$, $p = 0.001$], whereby RMT was significantly higher at T0 compared to T1 (43.6% vs 42.2%, WSRT $p < 0.001$, $d = 0.235$) and T2 (43.6% vs 42.6%, WSRT $p = 0.014$, $d = 0.162$). Importantly, it is notable that the change in RMT across time, although significant, was very small ($\sim 1\%$ MSO change) with small effect sizes.

Table 6.1: Statistical Analyses

Measure	ANOVA	Post-hoc and Effect Size
RMT*	Treatment _(2,34) = 0.838, p = 0.441 Time _(2,34) = 8.098, p = 0.001 Treatment*Time _(4,68) = 1.844, p = 0.130	T0 vs T1: p = 0.001, d = 0.235 T0 vs T2: p = 0.014, d = 0.162 T1 vs T2: p = 0.446, d = 0.073
Testing for the presence of SAI		
Glucose	Time _(2,34) = 0.477, p = 0.625 Pattern _(1,17) = 24.709, p < 0.001 Time*Pattern _(2,34) = 0.100, p = 0.905	d = 1.683
Sucralose	Time _(2,34) = 0.778, p = 0.467 Pattern _(1,17) = 51.967, p < 0.001 Time*Pattern _(2,34) = 0.464, p = 0.632	d = 2.079
Water	Time _(2,32) = 0.002, p = 0.998 Pattern _(1,16) = 49.581, p < 0.001 Time*Pattern _(2,32) = 0.664, p = 0.522	d = 2.186
SAI ratio	Treatment _(2,30) = 0.059, p = 0.943 Time _(2,30) = 0.118, p = 0.889 Treatment*Time _(4,60) = 0.268, p = 0.897	
Testing for the presence of LAI		
Glucose	Time _(2,34) = 2.978, p = 0.064 Pattern _(1,17) = 8.101, p = 0.011 Time*Pattern _(2,34) = 1.024, p = 0.370	d = 1.033
Sucralose	Time _(2,34) = 1.763, p = 0.187 Pattern _(1,17) = 34.688, p < 0.001 Time*Pattern _(2,34) = 0.037, p = 0.964	d = 1.596
Water	Time _(2,32) = 0.214, p = 0.809 Pattern _(1,16) = 16.100, p = 0.001 Time*Pattern _(2,32) = 2.256, p = 0.121	d = 1.328
LAI ratio	Treatment _(2,32) = 2.663, p = 0.085 Time _(2,32) = 2.813, p = 0.075 Treatment*Time _(4,64) = 0.591, p = 0.679	

*indicates Conover's ANOVA and post-hoc testing with the Wilcoxon-Signed Rank Test. Effect sizes shown are Cohen's d.

A two-way ANOVA on the conditioned and unconditioned MEPs showed that significant SAI was present at all time points as seen by a main effect of PATTERN that was present for each condition. Further, a two-way ANOVA on the SAI ratio revealed no main effects or interaction, indicating that the magnitude of SAI was similar across all time points and treatments (Figure 6.3A). A two-way ANOVA on the conditioned and unconditioned MEPs showed that significant LAI was present at all time points as seen by a main effect of PATTERN that was present for each condition. Further, a two-way ANOVA revealed no main effects or interaction, indicating that the magnitude of LAI was similar across all time points and treatments (Figure 6.3B).

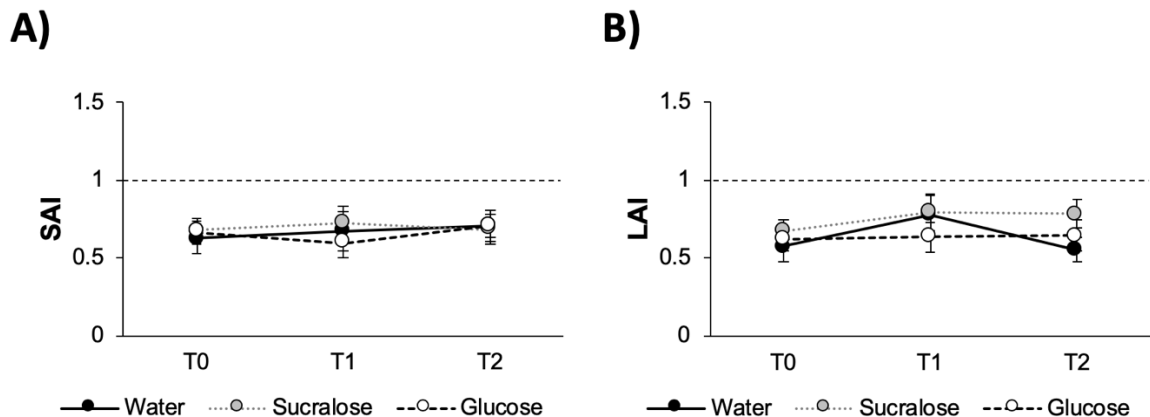


Figure 6.3: Afferent inhibition.

Mean (\pm standard error) SAI (A) and LAI (B) at baseline (T0) and following the ingestion of water, sucralose or glucose (T1, T2). Values below the dotted line indicate the presence of inhibition.

Correlations were performed on data obtained within the glucose condition. Glucose levels at T0 were not correlated with SAI at T0 ($r = -0.004$, $p > 0.05$) or with LAI at T0 ($r = -0.202$, $p > 0.05$). The change in glucose levels from T0 to T1 was not correlated with the change in SAI and LAI from T0 to T1 (SAI: $r = 0.092$, $p > 0.05$; LAI: $r = -0.168$, $p > 0.05$).

Further, the change in glucose levels from T0 to T2 was not correlated with the change in SAI and LAI from T0 to T2 (SAI: $r = -0.107$, $p > 0.05$; LAI: $r = -0.101$, $p > 0.05$).

The SEM_{eas} was computed for all conditions. The SEM_{eas} was similar for SAI across all conditions (Water: $SEM_{eas} = 0.29$, Sucralose: $SEM_{eas} = 0.28$, Glucose: $SEM_{eas} = 0.28$). Further, the SEM_{eas} was similar for LAI obtained within the glucose ($SEM_{eas} = 0.23$) and water ($SEM_{eas} = 0.24$) condition but was slightly higher ($SEM_{eas} = 0.32$) during the sucralose condition, suggesting slightly higher measurement error within this condition. These values for the SEM_{eas} are slightly higher than that reported previously for SAI and LAI evoked by median nerve stimulation (SEM_{eas} ranged from 0.18-0.22) (Turco et al. 2019b). However, this is not unexpected given that a smaller sample size was used here ($n = 18$) compared to previous work ($n = 30$ in (Turco et al. 2019b)).

6.4 Discussion

The present study is the first to examine the effect of glucose on afferent inhibition. Our novel findings indicate that acute elevations in blood glucose do not modulate the magnitude of SAI or LAI. These results and their implications are discussed below.

There was no change in SAI or LAI observed following intake of water, glucose or sucralose solutions. Further, baseline SAI/LAI and the change in SAI/LAI were not correlated with glucose levels. We also found that the absolute reliability in SAI was similar across all conditions, as assessed with the SEM_{eas} . Further, the absolute reliability in LAI

was similar between the water and glucose conditions. These results suggest that an elevation in glucose is not a significant contributor to the within-subject variability in afferent inhibition that has been previously reported (Turco et al. 2019a). Therefore, this suggests that the control of glucose levels do not need to be prioritized in TMS studies assessing afferent inhibition.

Importantly, these results are limited to healthy, recreationally active, young males. Future research is needed to determine if these results carry over to other populations. Females and inactive participants were excluded from the present study to reduce the influence of confounding variables on the results. Inactive participants are at a higher risk of showing prediabetic impairments in glucose metabolism (Hu and Gu 2019), and glucose metabolism is impaired during the luteal phase of the menstrual cycle compared to the follicular phase and menstruation (Bennal and Kerure 2013; Diamond et al. 1989; Jarrett and Graver 1968). Additionally, we only studied the effects of a 75 g glucose challenge, not in a dose-response fashion. It is unknown if this dose of glucose is an insufficient stimulus to change afferent inhibition and if higher doses of glucose would have yielded different results.

Previous studies have reported that glucose has a modulatory effect of corticospinal excitability (Bailey et al. 2019; Gant et al. 2010; Specterman et al. 2005). In the present study, we observed no real change in RMT, an indicator of baseline cortical excitability. Gant et al. (Gant et al. 2010) observed increases in MEPs obtained in the biceps brachii during maximum contraction following ingestion of glucose and other carbohydrate

solutions, and Bailey et al. (Bailey et al. 2019) observed increases in quadricep MEPs obtained during 50% maximum contraction following a carbohydrate mouth rinse. Corticospinal excitability in these studies was assessed during active conditions to determine the influence of carbohydrates on fatiguing muscle function. Prolonged fatiguing exercise leads to not only reduced neuronal output to the muscle (Taylor et al. 2006) but also hypoglycemia and depletion of muscle glycogen (Coggan and Coyle 1991). Previous research has demonstrated that SAI and LAI are reduced during finger movement (Asmussen et al. 2013, 2014; Bonassi et al. 2019; Ni et al. 2011; Richardson et al. 2008; Voller et al. 2005, 2006). Movement-related reductions in afferent inhibition are greatest in the contracted muscle compared to nearby, inactive muscles (Asmussen et al. 2014; Voller et al. 2005), suggesting that a release of afferent inhibition would allow for greater output to the contracted muscle (Turco et al. 2018b). It is unknown whether acute elevations in blood glucose would be more impactful on SAI/LAI if these measures were obtained during active muscle contraction.

Afferent inhibition is reduced in multiple neurodegenerative conditions including Alzheimer's and Parkinson's disease compared to healthy controls (Turco et al. 2018b), which also display altered glucose metabolism. There is evidence that those with Parkinson's disease exhibit cortical hypometabolism and subcortical hypermetabolism of glucose (Borghammer 2012) while those with Alzheimer's disease show cerebral hypometabolism of glucose (Kapogiannis and Mattson 2011). The results may suggest that the weakening of SAI/LAI in these neurodegenerative populations do not reflect the

impairment in glucose metabolism. However, the present study should be replicated in these populations to more firmly make this conclusion.

It has been repeatedly shown that SAI is reduced in populations with cognitive impairments (see (Turco et al. 2018b) for review). In addition, increases in SAI are related to improved performance on executive function and visuospatial tasks (Nardone et al. 2012b, 2013) and during the retrieval phase of memory tasks (Bonni et al. 2017), whereas SAI is reduced during working memory load (Suzuki and Meehan 2018). These results clearly highlight the relationship between SAI and cognition. This is in line with the findings that SAI reflects activity of the cholinergic system (Di Lazzaro et al. 2000b), which is thought to underlie proper cognitive function (Ballinger et al. 2016; Hampel et al. 2018). Interestingly, glucose levels impact several domains of cognitive functioning (see (Feldman and Barshi 2007) for review) and has been previously labeled as a “cognitive enhancer” (Riby 2004). Acute intake of glucose improves cognitive performance in elderly individuals (Kaplan et al. 2000) and, in healthy individuals, improves performance on working memory tasks (Riby 2004; Smith et al. 2011) but slows sensorimotor processing (Hope et al. 2013). Given the impact of glucose on cognitive function and the link between SAI and cognition, it is surprising that acute elevations in blood glucose did not lead to a change in SAI depth. Future research should investigate if SAI obtained in the context of cognitive tasks is modulated by glucose intake.

Although the present study did not show an impact of glucose on afferent inhibition, an important avenue of future research is to assess the relationship between dietary and lifestyle factors on TMS measures. This is especially important if these TMS measures are to be used as biological markers of function, as is the case with SAI as seen in recent literature (Benussi et al. 2019; Nardone et al. 2019; Snow et al. 2019). Recently, Yamazaki et al. (Yamazaki et al. 2019) showed that low-intensity cycling reduces SAI in exercised and non-exercised muscles. The impact of aerobic exercise on LAI is currently unknown. Future research should continue to investigate the influence of lifestyle factors on afferent inhibition.

6.5 Rationale for Study 5

There is a large body of research that reports manipulation of sensory afference leads to changes in motor cortex organization. However, the neural mechanisms underlying this effect are unknown. Evidence suggests that muscle representations within M1 are under GABAergic control. Given that I have shown that afferent inhibition is dependent on sensory afference (Study #1) and is reflective of GABA_A receptor activity (Study #2), I hypothesized that afferent inhibition may play a role in this neuroplastic effect. Therefore, in Study #5 it was proposed that afferent inhibition mediates the relationship between sensory afference and motor cortex organization. The findings from this study could also be used to determine whether sensory enrichment leads to a change in afferent inhibition, and whether motor cortex organization is under the control of afferent inhibition.

Chapter 7: Study 5

Cutaneous Modulation of Sensorimotor Function

7.1 Introduction

Understanding the interaction between sensory input and motor output is fundamental to the exploration of human movement. Evidence from animal literature suggests that sensory input continuously modulates the organization of the primary motor cortex (M1). M1 organization may be assessed by quantifying the location and spatial representation of muscles within the cortex. In rats, when sensory inputs are deprived via whisker trimming (Keller et al. 1996) or forelimb amputation (Donoghue and Sanes 1988), the representation of the denervated area in M1 is reduced while adjacent motor representations become enlarged. In primates, the representation of digit movements (i.e. the number of sites that evoked digit movement) are reduced following dorsal column transections (Kambi et al. 2011). In contrast, heightened afferent input through sensorimotor training in skilled reaching movements results in the enlargement of digit representations in the rat (Kleim et al. 1998) and monkey (Nudo et al. 1996) motor cortices, supporting the suggestion that motor cortical organization is influenced by sensory input.

In humans, transcranial magnetic stimulation (TMS) has been used to investigate the cortical changes that occur following the manipulation of sensory inputs. TMS studies have shown that limb amputation leads to the expansion of the representations of muscles proximal to the amputation (Cohen et al. 1991; Irlbacher et al. 2002; Rörich et al. 1999; Schwenkreis et al. 2001). Temporary deafferentation can also induce rapid and reversible

changes in M1 organization. For example, reversible nerve block with local anesthetic reduces motor output of distal muscles (Murphy et al. 2003) while ischaemic nerve block increases the excitability and area of representations of muscles proximal to the nerve block (Brasil-Neto et al. 1992, 1993; McNulty et al. 2002; Ridding and Rothwell 1995, 1997; Vallence et al. 2012b, 2012a; Werhahn et al. 2002; Ziemann et al. 1998a, 1998b). The increase in corticospinal excitability due to ischaemic nerve block may be mediated by the subsequent rapid increase in cortical gamma-aminobutyric acid (GABA) levels (Levy et al. 2002).

Neural changes in M1 have also been observed following *increased* sensory input. Hamdy et al. (1998) showed that prolonged electrical stimulation of a peripheral nerve is sufficient to drive M1 reorganization, such that 10 min of high-frequency pharyngeal nerve stimulation results in enlargement of the pharynx representation and reduction of the upper esophagus representation in M1. Two hours of mixed nerve stimulation enlarges the area of muscles innervated by the stimulated nerve (Ridding et al. 2000, 2001; Wu et al. 2005) and shifts the centre of gravity (CoG) of the motor maps (Ridding et al. 2001). Further, prolonged muscle vibration increases corticospinal excitability (Forner-Cordero et al. 2008; Rosenkranz et al. 2003; Rosenkranz and Rothwell 2003) and the aerial representation of the vibrated muscle in lesioned cortex following stroke (Marconi et al. 2011). Finally, heightened afferent input during sensorimotor learning also leads to enlargement of the trained muscle's representation in M1 (Kami et al. 1995; Karni et al. 1998; Pascual-Leone

et al. 1993; Tyč and Boyadjian 2006). Collectively, these data demonstrate that corticospinal excitability is increased following enhancement of afferent input.

Interestingly, if only cutaneous input is enhanced, as opposed to activation of proprioceptive afferents via mixed nerve stimulation or muscle vibration, there appears to be an opposite effect on M1 excitability. Kojima et al. (2018) demonstrated that 20 minutes of mechanical stimulation of the index fingertip reduces motor-evoked potentials (MEPs) in the first dorsal interosseous (FDI) muscle. The influence of prolonged electrical stimulation to the digits on corticospinal excitability is less clear. Corticospinal excitability was reportedly unchanged following 2 hours of digital nerve (DN) stimulation (Ridding et al. 2000) or 30 minutes of lateral antebrachial cutaneous nerve stimulation (Tinazzi et al. 2005). However, these results were obtained from very small sample sizes of four (Ridding et al. 2000) and five participants (Tinazzi et al. 2005), warranting further investigation to more clearly understand the effects of prolonged cutaneous input on M1 excitability.

Importantly, while afferent input is capable of driving changes in M1 organization and excitability, the mechanisms of such changes are unclear. In this study, it is proposed that a TMS-evoked phenomenon known as afferent inhibition may contribute to M1 organization. Afferent inhibition appears to contribute to the topography within M1, such that the greatest inhibition occurs for muscles in close spatial proximity to the nerve stimulated (Classen et al. 2000). The neural pathway underlying afferent inhibition is proposed to result from the activation of thalamocortical projections to M1 interneurons

that inhibit pyramidal output (Di Lazzaro et al. 2012b) and also disinhibition of excitatory pyramidal projections from the primary somatosensory cortex (S1) to M1 (Turco et al. 2018a, 2018b). The magnitude of afferent inhibition is directly related to nerve stimulation intensity, such that stronger inhibition is observed with greater recruitment of sensory afferent fibers (Bailey et al. 2016; Turco et al. 2017). Previous research has shown that neuromuscular electrical stimulation delivered to the ulnar nerve (UN) for 40 minutes abolishes short-latency afferent inhibition (SAI) (Mang et al. 2012). The effect of prolonged cutaneous nerve stimulation on afferent inhibition is unknown. However, the reduction in MEP amplitude following 20 min mechanical stimulation to the digit tip (Kojima et al. 2018) may suggest that afferent inhibition is increased, since corticospinal excitability is one component of afferent inhibition. However, further investigation is required to make this conclusion.

In the present study, sensory enrichment will be achieved with tactile coactivation protocols applied via electrical stimulation (termed *somatosensory electrical stimulation* or SES) (Godde et al. 2000; Höffken et al. 2007; Pleger et al. 2001). SES enhances tactile acuity of the digit (Godde et al. 2000), increases the size of the digit representation in S1 (Hodzic et al. 2004; Pleger et al. 2003), increases inhibition within M1 (Rocchi et al. 2017), and increases (Rocchi et al. 2017) or decreases (Höffken et al. 2007) inhibition in S1, depending on the stimulation frequency. Together, these findings demonstrate that this protocol is capable of driving cortical plasticity.

The purpose of this study is to investigate the effects of SES on motor maps within human M1 and afferent inhibition. This information is important for understanding the neural mechanisms by which sensory input influences motor cortical organization. The predictions are as follows:

1. SES of the UN will enlarge the area of the FDI motor map and reduce the magnitude of afferent inhibition.
2. SES of the index finger digital nerve will decrease the area of the FDI motor map and increase the magnitude of afferent inhibition.

7.2 Methods

Participants

Four right-handed healthy participants were recruited (age 20.5 ± 1.7 years, 3 males). Participants were screened for contraindications to TMS (Rossi et al. 2009) and right-handedness was confirmed using a modified handedness questionnaire (Oldfield 1971). All participants provided written informed consent prior to data collection on the dates of testing. This research was approved by the Hamilton Integrated Research Ethics Board (HiREB) and conformed to the declaration of Helsinki.

Experimental Design

Individuals participated in three sessions. A minimum inter-session interval of 48 hours was imposed to minimize carry-over effects. Figure 7.1 shows a timeline of an experimental session.

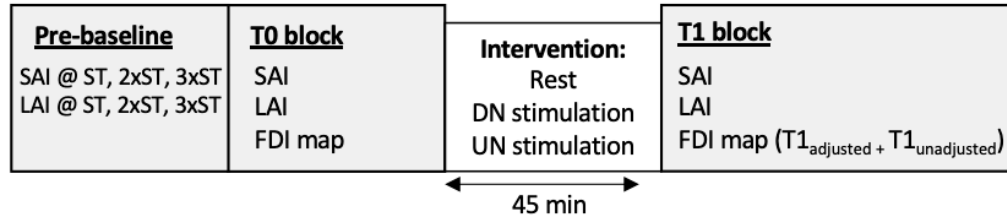


Figure 7.1: Experimental timeline.

Three 45 min interventions were delivered across three sessions where interventions include: rest, digital nerve stimulation, and ulnar nerve stimulation. Before the baseline T0 block (i.e. Pre-baseline), SAI and LAI were acquired at three nerve stimulation intensities: sensory threshold (ST), 2xST, and 3xST. At T0, short- (SAI) and long-latency afferent inhibition (LAI) and a map of the first dorsal interosseous (FDI) muscle in the left motor cortex was acquired. Immediately after the intervention at T1, SAI, LAI and the FDI map was acquired again. Further, the FDI map was acquired twice with two different TMS intensities, both adjusted and unadjusted for changes in resting motor threshold (RMT).

The following interventions were implemented on one of three sessions:

1. Rest condition: 45 min of rest (to control for the passage of time)
2. DN stimulation condition: 45 min of electrical stimulation to the index finger.
3. UN stimulation condition: 45 min of electrical stimulation to the UN at the wrist.

The order of sessions was counterbalanced using a Latin square design. The rest session involved a 45 min period where no stimulation was delivered. The SES protocol (DN stimulation and UN stimulation conditions) involved 20 Hz trains of electrical pulses (200 μ s pulse width) that were delivered for 1 s, with a 5 s rest in between trains (Digitimer DS7AH, Hertfordshire, UK) (Ragert et al. 2008; Rocchi et al. 2017). For the DN stimulation condition, electrical stimuli were delivered through surface adhesive electrodes (9 mm Ag-AgCl electrodes), with the anode placed on the distal phalanx of the index finger

and the cathode placed on the proximal phalanx of the index finger. For the UN stimulation condition, a bar electrode was placed over the UN on the volar surface of the wrist with the cathode directed proximally. The intensity of electrical stimulation ranged from 2 to 3 x sensory threshold (ST). Nerve stimulation intensity was initially set at 3 x ST. To ensure that high-frequency electrical stimulation was not perceived as painful, since pain reduces LAI (Burns et al. 2016), individuals were asked to rate the sensation of the electrical stimulus as mild, moderate, strong, or painful. If the sensation was deemed painful, they were asked to rate the pain on a scale of 0 to 10 according to the Numeric Rating Scale (NRS) (Hawker et al. 2011). If participants rated pain greater than 5, then the stimulation intensity was lowered until the sensation is no longer painful. The minimum stimulation intensity used during the DN and UN stimulation interventions was 2 x ST.

The dependent measures acquired with TMS included resting motor threshold (RMT), short-latency afferent inhibition (SAI), long-latency afferent inhibition (LAI) and a FDI map (details of procedures to acquire these measures are described in the Methods below). Dependent measures were acquired at baseline (T0) and immediately post-intervention (T1). At T1, the FDI map was acquired twice. Once with the same stimulation intensity used at T0 (termed T1_{unadjusted}, TMS intensity at 120% of RMT acquired at T0), and once with the stimulation intensity adjusted for changes in RMT (termed T1_{adjusted}, TMS intensity at 120% of RMT acquired at T1). Further, SAI and LAI were also acquired before T0, at “pre-baseline”, using three different nerve stimulation intensities: ST, 2xST, and 3xST. The purpose of the pre-baseline assessment was to confirm that the nerve stimulation intensity

used to acquire SAI/LAI at T0 and T1 was optimal.

Electromyography (EMG)

Surface EMG (9 mm Ag-AgCl electrodes) was recorded from the right FDI muscle. EMG recordings were band-pass filtered between 20 Hz and 2.5 kHz, amplified 1000x (Intronix Technologies Corporation Model 2024F, Bolton, Canada), and then digitized at 5 kHz using an analog-to-digital interface (Power1401, Cambridge Electronics Design, Cambridge, UK). EMG recordings were collected and analyzed in Signal software (Signal v6.02, Cambridge Electronics Design, Cambridge, UK).

Somatosensory Evoked Potentials (SEPs)

Somatosensory-evoked potentials (SEPs) were recorded using electroencephalography (EEG) from electrodes positioned at C3' and referenced to Fz (International 10-20 system) with a ground electrode placed over the clavicle. DN stimulation was delivered at the intensity of 2xST. One thousand epochs were averaged to determine the latency of the N20 component of the SEP. The N20 latency was used to determine the interstimulus interval (ISI) between nerve stimulation and TMS pulses in subsequent measures of SAI (described below).

Transcranial Magnetic Stimulation (TMS)

Single-pulse TMS was delivered to the left M1 using a custom figure-of-eight branding coil (50 mm diameter) connected to a Magstim Bistim stimulator (Magstim, Whitland,

UK). The coil was oriented at a 45° angle to the parasagittal plane to induce a posterior-to-anterior current in the cortex. The motor hotspot was identified as the optimal location whereby TMS elicited consistently large MEPs in the right FDI muscle. This site was digitally marked using Brainsight Neuronavigation (Rogue Research, Montreal, Canada).

Resting motor threshold (RMT) was obtained using ML-PEST, a systematic predictive algorithm that determines the TMS intensity predicted to yield a 50% probability of generating a MEP while the FDI muscle is at rest (TMS Motor Threshold Assessment Tool; MTAT, version 2.0 (<http://www.clinicalresearcher.org/software.html>). *A priori* information was selected, and the starting TMS intensity was set to 37%. Twenty stimuli were delivered to accurately determine the RMT (Ah Sen et al. 2017; Siebner and Rothwell 2003).

Afferent Inhibition

Two measures of afferent inhibition were acquired: SAI and LAI. DN stimulation was delivered prior to the TMS pulse at an interstimulus interval of N20 + 2 ms to acquire SAI and 200 ms to acquire LAI. At pre-baseline, SAI and LAI were acquired using DN stimulation intensities of ST, 2xST and 3xST. At T0 and T1, DN stimulation was delivered at an intensity of 2 x ST only. TMS was delivered at the intensity that evokes a 1 mV MEP in peak-peak amplitude. At pre-baseline, 20 unconditioned MEPs (i.e. TMS alone) were randomized among 60 conditioned MEPs (i.e. 20 nerve stimulation-TMS pairs per nerve stimulation intensity of ST, 2xST and 3xST). This was repeated for the acquisition of both

SAI and LAI. At T0 and T1, 20 unconditioned MEPs (i.e. TMS alone) were randomized among 40 conditioned MEPs (i.e. 20 nerve stimulation-TMS pairs for SAI, 20 for LAI). The magnitude of inhibition was calculated as a ratio of the averaged conditioned MEP over the averaged unconditioned MEP:

$$\text{Inhibition (SAI/LAI)} = \frac{\text{average conditioned MEP}}{\text{average unconditioned MEP}}$$

FDI Maps

A map of the FDI muscle representation within M1 was obtained using similar methods described by van de Ruit et al. (2015). 100 TMS pulses were delivered to pseudo-random locations within a 6x6 cm area centered over the FDI motor hotspot, at the intensity corresponding to 120% RMT with an inter-stimulus interval of 2 s. Brainsight Neuronavigation was used to identify the 6x6 cm area and provided feedback about stimuli and coil position throughout the measure. It was unknown whether the interventions delivered would change RMT. Therefore, at T1, maps were acquired with the same TMS intensity at T0 (120% of RMT obtained at T0, termed T1_{unadjusted}) and at the TMS intensity that corresponds to the change in RMT (120% of RMT obtained at T1, termed T1_{adjusted}).

Responses to individual stimuli were excluded according to established criteria (Van De Ruit et al. 2015): (1) if the stimulation was >10 mm outside of the pre-defined grid space, (2) if an MEP was greater than the mean MEP ± 3 SD, (3) if the root mean square of the EMG activity within a 45 ms window (from 50ms to 5ms before the TMS artefact) was not within the mean ± 2 SD of all stimuli, and (4) if angle and translation of the stimulus location

fell outside the 99% predication interval of all stimuli (Van De Ruit et al. 2015). A MATLAB script was used to construct a map of the FDI muscle representation from the peak-peak amplitude of the MEPs and the location of stimulation registered with Neuronavigation. The resultant map approximates the MEP size for 2500 partitions within the 6x6 cm space. Map area was calculated using the following formula (Van De Ruit et al. 2015):

$$area = \frac{N(aMEP_{10\%})}{N_{total}} \times area_{map}$$

Where $N(aMEP_{10\%})$ is the number of partitions where the approximated MEP is >10% of the maximum approximated MEP, N_{total} is the total number of partitions (i.e. 2500 partitions), and $area_{map}$ is the total mapped area (i.e. 36 cm²).

Statistical Analyses

SAI and LAI trials with peak-to-peak EMG activity greater than 100 μ V in a 100 ms window prior to the TMS artefact were discarded, similar to previous work (Schambra et al. 2015; Turco et al. 2019a). To increase clarity of the results, each variable was assigned a cut-off value. If the variable showed a change across time that was less than this cut-off value, then it was concluded that the variable did not change. For example, the cut-off for map area was set to 100 mm². If the group-averaged map area did not change by more than 100 mm², then it was concluded that map area did not change across time. The cut-off value for RMT was 1% maximum stimulator output (MSO), for CoG was set to 1 mm and for SAI and LAI was set to 0.1.

7.3 Results

FDI Maps

Rest Condition

The group averaged RMT decreased within the rest condition (56.8% at T0 vs 55.6% at T1). Individual FDI maps obtained within the rest condition can be seen in Figure 7.2.

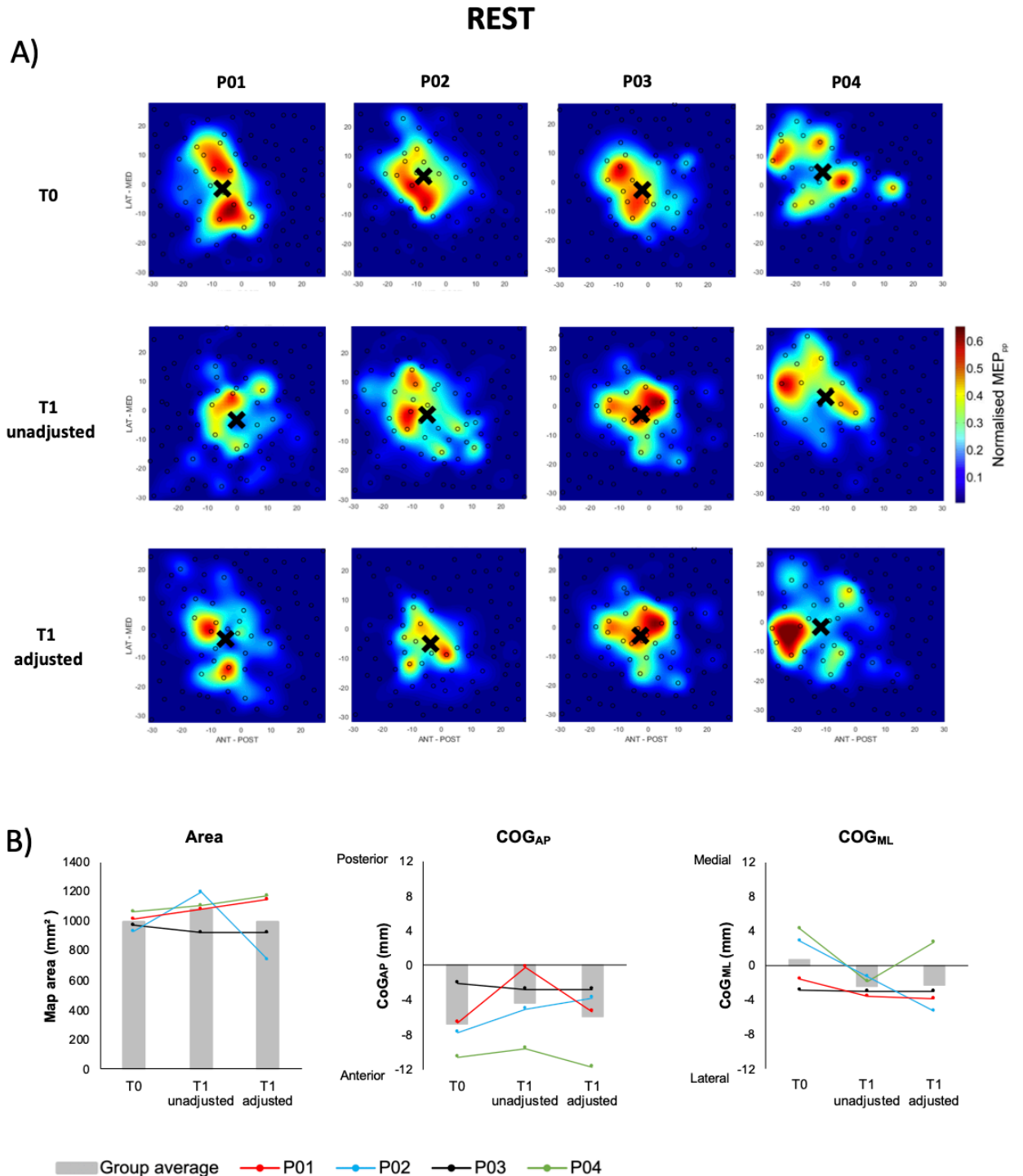


Figure 7.2: Maps obtained within the rest condition.

A) Individual FDI maps acquired at T0, T1_{unadjusted}, and T1_{adjusted}. The y-axis shows the medial-lateral plane (positive values are medial, negative values are lateral) and the x-axis shows the anterior-posterior plane (positive values are posterior, negative values are anterior). The colour-coded legend can be seen on the right. Red areas on a map correspond

to locations that elicited MEPs, whereas blue areas correspond to locations that did not elicit MEPs. B) Group-averaged map area, COG in the anterior-posterior plane (COG_{AP}) and COG in the medial-lateral plane (COG_{ML}).

As expected, the group-averaged map area showed no change across time, both at $T1_{unadjusted}$ ($T0 = 998.12 \text{ mm}^2$ vs $T1_{unadjusted} = 1079.13 \text{ mm}^2$) and $T1_{adjusted}$ ($T0 = 998.12 \text{ mm}^2$ vs $T1_{adjusted} = 998.51 \text{ mm}^2$). Specifically, three participants showed no change in map area at $T1_{unadjusted}$ (P01, P03, P04) while P02 showed an increase. At $T1_{adjusted}$, two participants showed an increase in map area (P01, P04), one showed a decrease (P02) and one showed no change (P03).

At $T1_{unadjusted}$, the group-averaged CoG shifted in the posterior direction ($T0 = -6.77 \text{ mm}$ vs $T1_{unadjusted} = -4.41 \text{ mm}$). Three participants showed this posterior shift (P01, P02, P04) while P03 showed no shift in the anterior-posterior plane. However, at $T1_{adjusted}$, the group-averaged CoG showed no shift in the anterior-posterior plane ($T0 = -6.77 \text{ mm}$ vs $T1_{adjusted} = -5.91 \text{ mm}$). Two participants showed a posterior shift (P01, P02), one showed an anterior shift (P04), while P03 again showed no shift in the anterior-posterior plane.

Finally, the group-averaged CoG shifted laterally at $T1_{unadjusted}$ ($T0 = 0.65$ vs $T1_{unadjusted} = -2.40$) and $T1_{adjusted}$ ($T0 = 0.65$ vs $T1_{adjusted} = -2.36$). Three participants showed this lateral shift at both $T1_{unadjusted}$ and $T1_{adjusted}$ (P01, P02, P04) while P03 showed no shift in the medial-lateral plane at both time-points.

DN Stimulation Condition

The group averaged RMT increased within the DN stimulation condition (60.0% at T0 vs 61.5% at T1). Individual motor maps obtained within this condition can be seen in Figure 7.3.

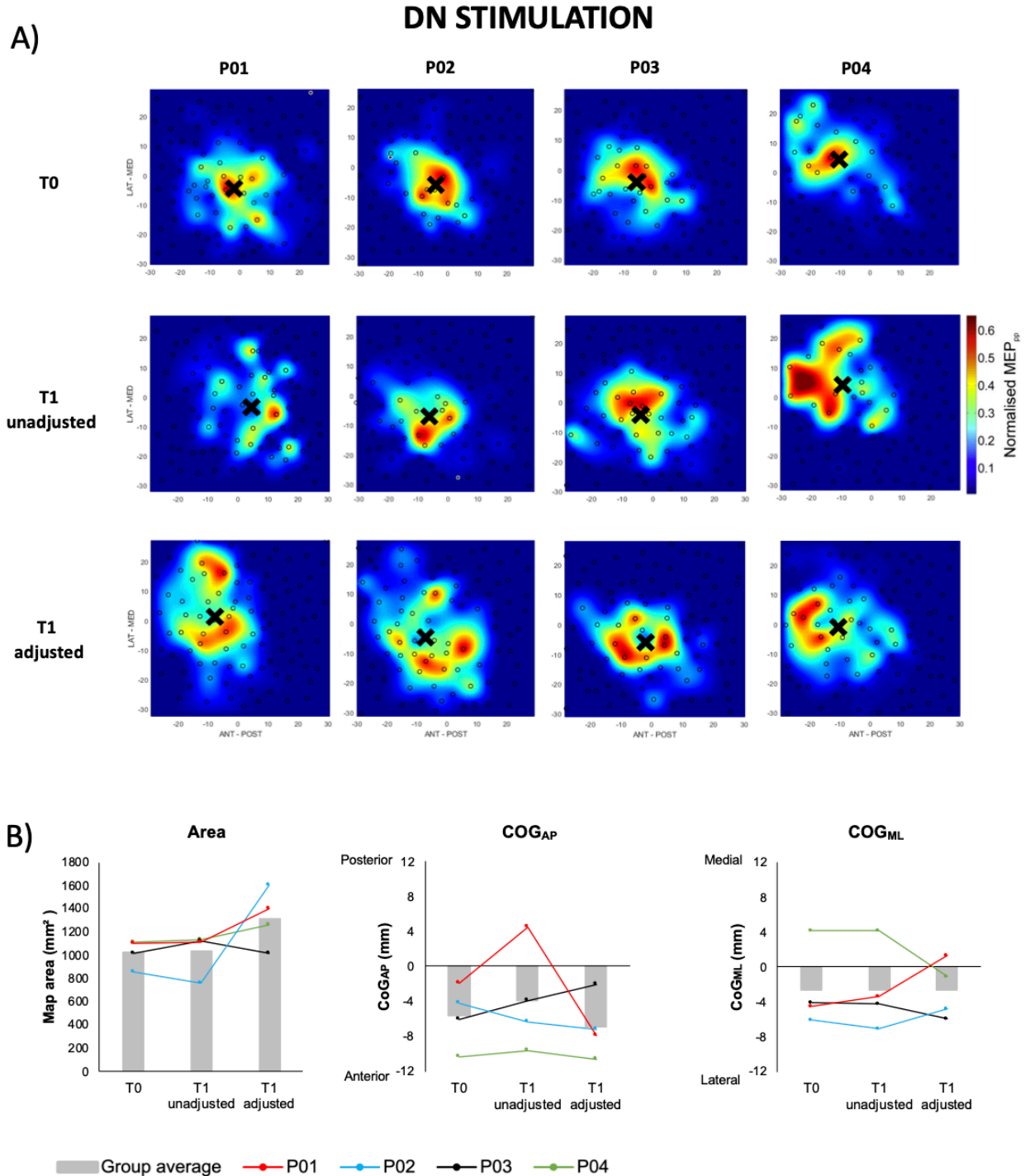


Figure 7.3: Maps obtained within the DN stimulation condition.

A) Individual FDI maps acquired at T0, T1_{unadjusted}, and T1_{adjusted}. The y-axis shows the medial-lateral plane (positive values are medial, negative values are lateral) and the x-axis shows the anterior-posterior plane (positive values are posterior, negative values are anterior). The colour-coded legend can be seen on the right. Red areas on a map correspond

to locations that elicited MEPs, whereas blue areas correspond to locations that did not elicit MEPs. B) Group-averaged map area, COG in the anterior-posterior plane (COG_{AP}) and COG in the medial-lateral plane (COG_{ML}).

The group-averaged map area showed no change at $T1_{unadjusted}$ ($T0 = 1023.69 \text{ mm}^2$ vs $T1_{unadjusted} = 1032.57 \text{ mm}^2$) but increased when stimulation intensity was adjusted at $T1_{adjusted}$ ($T0 = 1023.69 \text{ mm}^2$ vs $T1_{adjusted} = 1318.74 \text{ mm}^2$). At $T1_{unadjusted}$, P02 showed a decrease in map area, P03 showed an increase, while P01 and P04 showed no change. At $T1_{adjusted}$, P01, P02 and P04 showed an increase in map area while P03 showed no change.

The group-averaged CoG shifted posteriorly at $T1_{unadjusted}$ ($T0 = -5.62 \text{ mm}$ vs $T1_{unadjusted} = -3.85 \text{ mm}$) but shifted anteriorly when stimulation intensity was adjusted for changes in RMT at $T1_{adjusted}$ ($T0 = -5.62 \text{ mm}$ vs $T1_{adjusted} = -6.94 \text{ mm}$). At $T1_{unadjusted}$, P01 showed a very large posterior shift, P02 and P03 showed an anterior shift, while P04 showed no shift in the anterior-posterior plane. At $T1_{adjusted}$, P03 showed a posterior shift, P01 showed an anterior shift, while P02 and P04 showed no shift in the anterior-posterior plane.

Finally, the group-averaged CoG showed no shift in the medial-lateral plane at $T1_{unadjusted}$ ($T0 = -2.62 \text{ mm}$ vs $T1_{unadjusted} = -2.62 \text{ mm}$) or $T1_{adjusted}$ ($T0 = -2.62 \text{ mm}$ vs $T1_{adjusted} = -2.64 \text{ mm}$). At $T1_{unadjusted}$, P01 showed a medial shift, P02 showed a lateral shift, while P03 and P04 showed no shift in the medial-lateral plane. At $T1_{adjusted}$, P01 showed a medial shift, while P02, P03 and P04 showed a lateral shift.

UN Stimulation Condition

The group averaged RMT decreased within the UN (54.7% at T0 vs 53.0% at T1) stimulation conditions. Individual motor maps obtained within this condition can be seen in Figure 7.4.

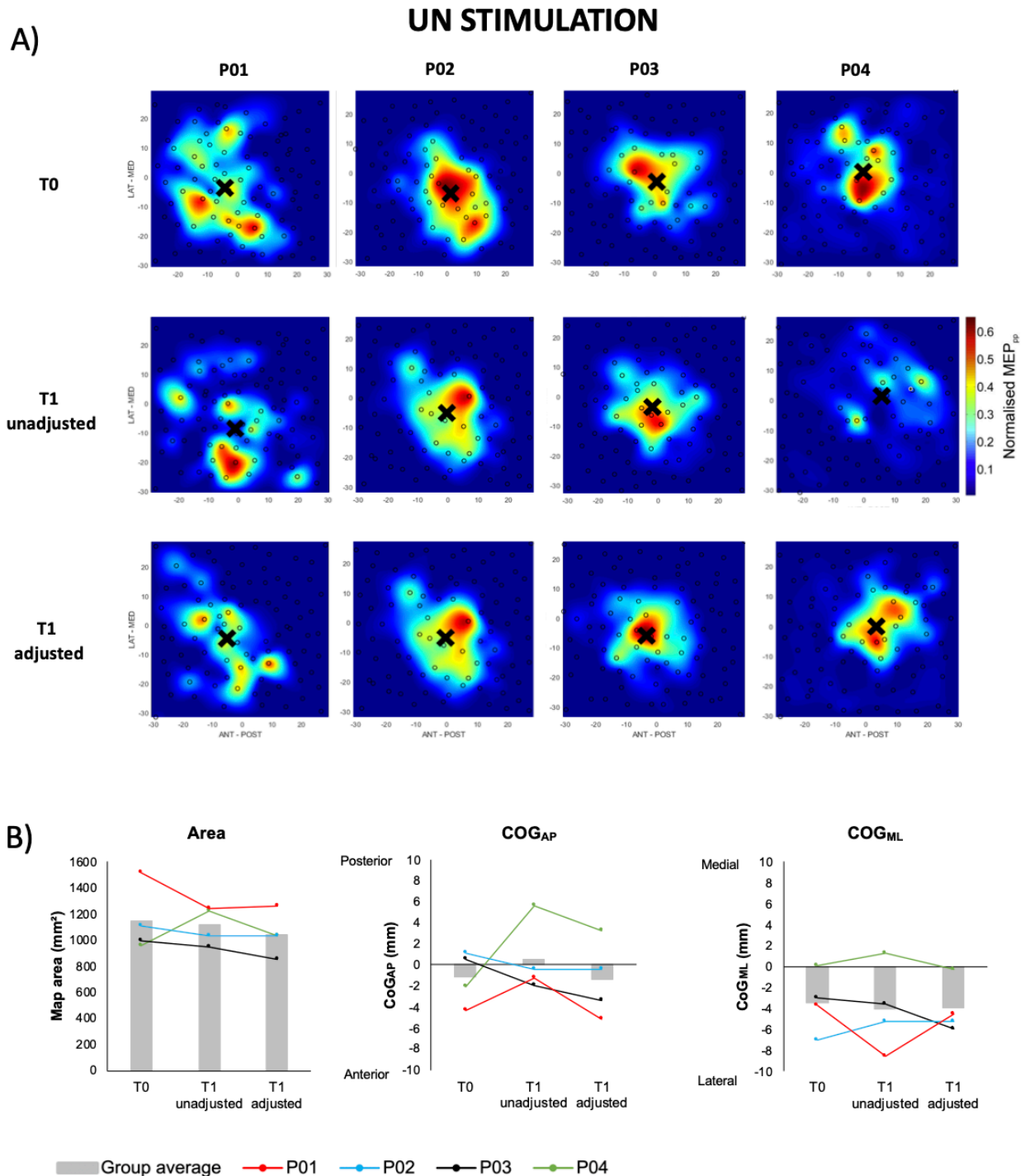


Figure 7.4: Maps obtained within the UN stimulation condition.

A) Individual FDI maps acquired at T0, T1_{unadjusted}, and T1_{adjusted}. The y-axis shows the medial-lateral plane (positive values are medial, negative values are lateral) and the x-axis shows the anterior-posterior plane (positive values are posterior, negative values are anterior). The colour-coded legend can be seen on the right. Red areas on a map correspond

to locations that elicited MEPs, whereas blue areas correspond to locations that did not elicit MEPs. B) Group-averaged map area, COG in the anterior-posterior plane (COG_{AP}) and COG in the medial-lateral plane (COG_{ML}).

The group-averaged map area showed no change at $T1_{unadjusted}$ ($T0 = 1147.88 \text{ mm}^2$ vs $T1_{unadjusted} = 1115.36 \text{ mm}^2$) but decreased at $T1_{adjusted}$ ($T0 = 1147.88 \text{ mm}^2$ vs $T1_{adjusted} = 1046.89 \text{ mm}^2$). At $T1_{unadjusted}$, P01 showed a decrease in map area, P04 showed an increase, while P02 and P03 showed no change. At $T1_{adjusted}$, P01 and P03 showed a decrease in map area while P02 and P04 showed no change.

The group-averaged CoG shifted posteriorly at $T1_{unadjusted}$ ($T0 = -1.17 \text{ mm}$ vs $T1_{unadjusted} = 0.52 \text{ mm}$) but did not shift in the anterior-posterior plane at $T1_{adjusted}$ ($T0 = -1.17 \text{ mm}$ vs $T1_{adjusted} = -1.52 \text{ mm}$). At $T1_{unadjusted}$, P01 and P04 showed a posterior shift, P03 showed an anterior shift, while P02 showed no shift in the anterior-posterior plane. At $T1_{adjusted}$, P04 showed a posterior shift, P03 showed an anterior shift, while P01 and P02 showed no shift in the anterior-posterior plane.

Finally, the group-averaged CoG showed no shift in the medial-lateral plane at $T1_{unadjusted}$ ($T0 = -3.40 \text{ mm}$ vs $T1_{unadjusted} = -4.03 \text{ mm}$) or $T1_{adjusted}$ ($T0 = -3.40 \text{ mm}$ vs $T1_{adjusted} = -3.99 \text{ mm}$). At $T1_{unadjusted}$, P02 and P04 showed a medial shift, P01 showed a lateral shift, while P03 showed no shift in the medial-lateral plane. At $T1_{adjusted}$, P02 showed a medial shift, P03 showed a lateral shift, while P01 and P04 showed no shift in the medial-lateral plane.

Afferent Inhibition

Figure 7.5 shows pre-baseline SAI and LAI acquired at three nerve stimulation intensities. In all conditions, pre-baseline SAI was strongest at stimulation intensities of 2xST and 3xST, whereas inhibition was not present (DN and UN stimulation conditions) or very weak (rest condition) using a stimulation intensity of ST. Pre-baseline LAI was weak (DN stimulation condition) or non-existent (UN stimulation and rest conditions) at a low stimulation intensity of ST. At a stimulation intensity of 3xST, LAI was present in the rest and UN stimulation conditions but was absent in the DN stimulation condition. However, LAI acquired with a stimulation intensity of 2xST present in all conditions. Overall, these results indicate that SAI and LAI are consistently present at a stimulation intensity of 2xST, justifying our decision to use this stimulation intensity to acquire SAI and LAI at T0 and T1.

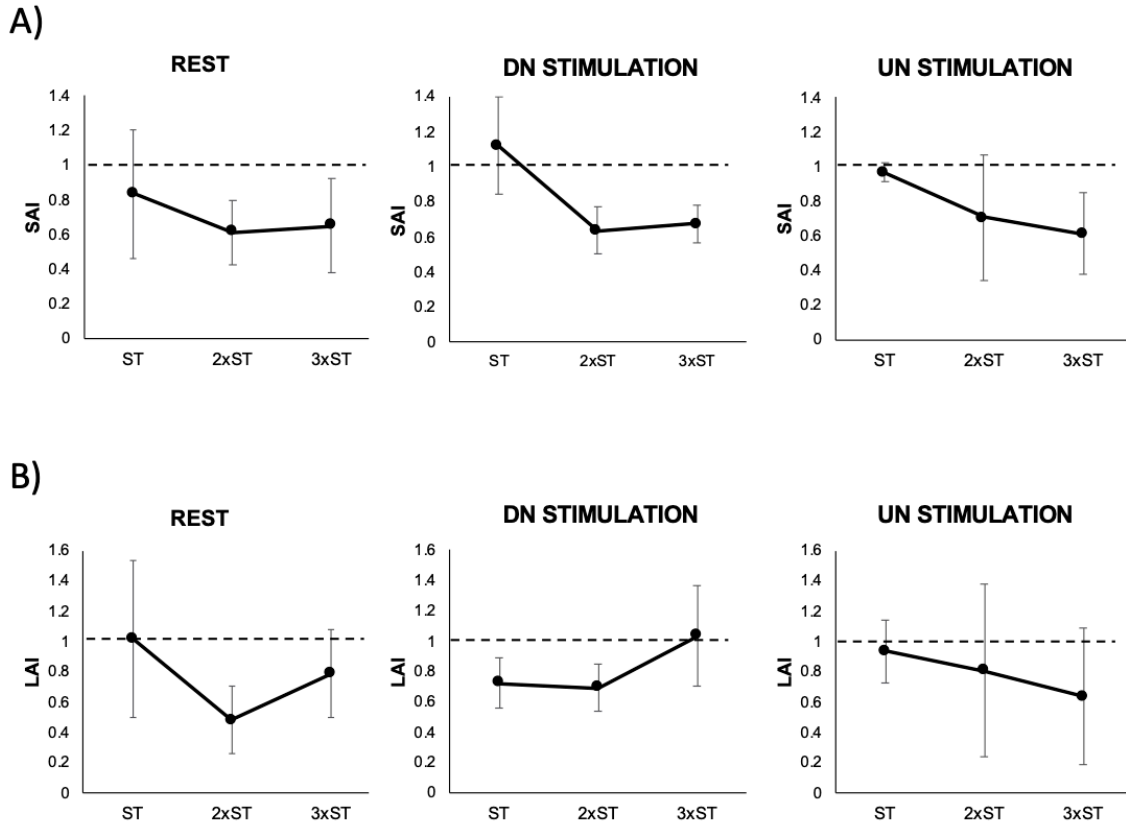


Figure 7.5: Pre-baseline SAI and LAI.

Graphs show group-averaged means \pm standard deviations. SAI (A) and LAI (B) were acquired at three intensities of DN stimulation corresponding to sensory threshold (ST), 2xST and 3xST. This was repeated in all three conditions (Rest, DN stimulation, and UN stimulation conditions). The y-axis shows the ratio between the amplitude of the averaged conditioned MEP versus the average unconditioned MEP. Values above the dotted line indicate no inhibition is present, while values below the dotted line indicate inhibition is present.

Figure 7.6 shows group-averaged and individual SAI and LAI data acquired at T0 and T1.

Within the rest condition, the group-averaged SAI showed no change from T0 to T1 (T0 = 0.83 vs T1 = 0.89). Individually, P01 and P02 showed an increase in SAI while P03 and P04 showed a decrease. Within the DN stimulation condition, the group-averaged SAI again showed no change from T0 to T1 (T0 = 0.80 vs T1 = 0.87). Individually, similar to the rest condition, P01 and P02 showed an increase in SAI while P03 and P04 showed a

decrease. Finally, within the UN stimulation condition, the group-averaged SAI decreased ($T0 = 0.71$ vs $T1 = 0.88$), driven by a decrease in SAI exhibited by P01, P02 and P03. Alternatively, P04 did not show SAI at T0 or T1 within this condition.

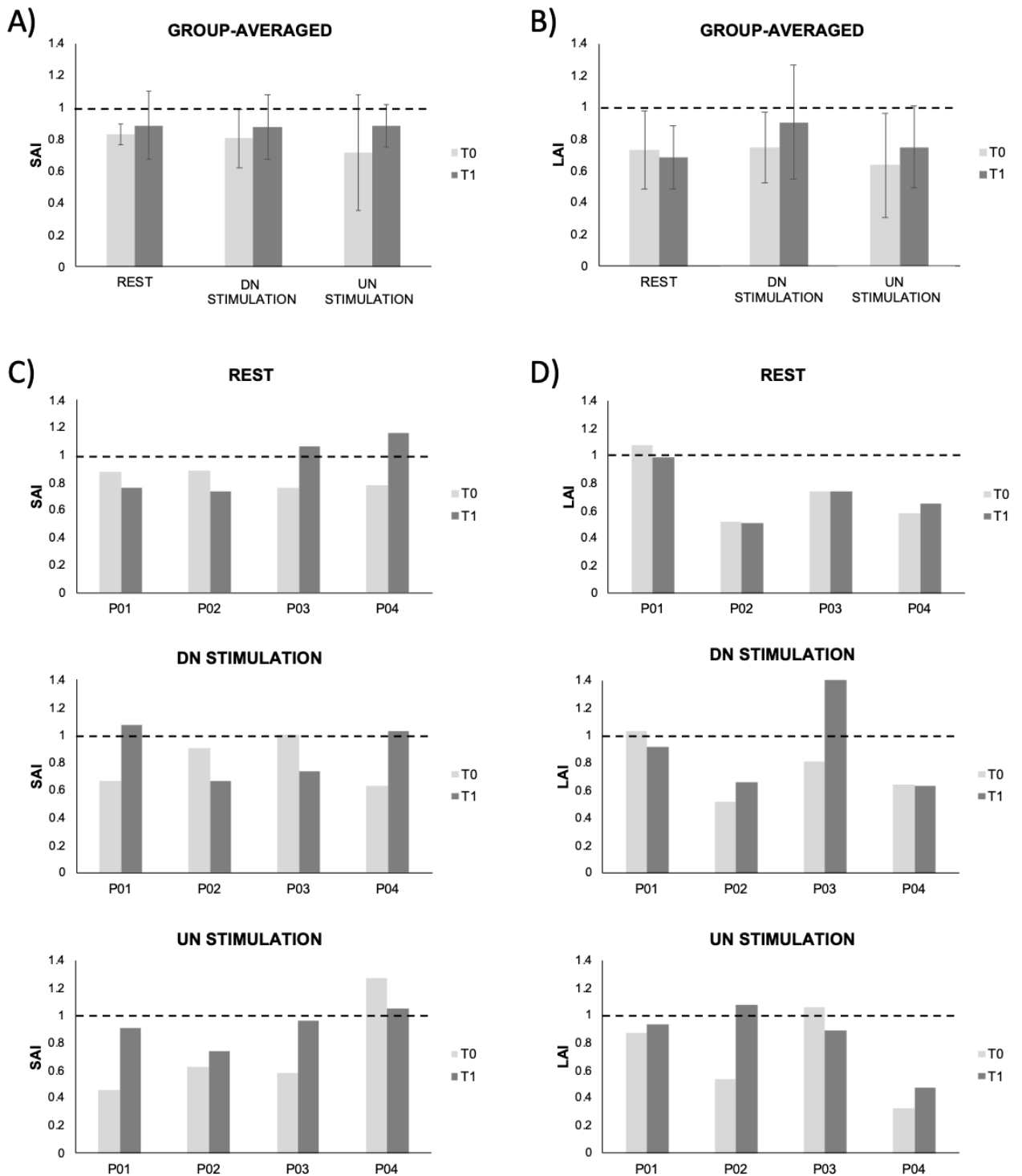


Figure 7.6: SAI and LAI acquired at T0 and T1.

Figures show group-averaged SAI (A) and LAI (B) \pm standard deviations, and individual SAI (C) and LAI (D). The y-axis shows the ratio between the amplitude of the averaged conditioned MEP versus the average unconditioned MEP. Values above the dotted line

indicate no inhibition is present, while values below the dotted line indicate inhibition is present.

Within the rest condition, all participants showed no change in LAI from T0 to T1 (group average: T0 = 0.73 vs T1 = 0.68). Within the DN stimulation condition, the group-averaged LAI decreased (T0 = 0.75 vs T1 = 0.90). This was shown by P01, P02 and P03, while P04 showed no change in LAI. Finally, within the UN stimulation condition, the group-averaged LAI also decreased (T0 = 0.63 vs T1 = 0.75). Individually, P02 and P04 showed a decrease in LAI, P03 showed an increase, while P01 showed no change in LAI.

7.4 Discussion

The results from this study indicate that 45 min of DN or UN stimulation does not modulate afferent inhibition or motor cortex organization in a predictable manner. We will discuss changes to the protocol that should be considered to improve the experimental design of the research for a future investigation.

Our results are in line with previous studies that have shown no effect of prolonged cutaneous nerve stimulation on corticospinal excitability (Ridding et al. 2000; Tinazzi et al. 2005). However, similar to the present study, these results were obtained from very small sample sizes of four (Ridding et al. 2000) and five participants (Tinazzi et al. 2005). With data acquired with from only four participants, it was not appropriate to statistically test our outlined predictions. Table 7.1 shows a sampling plan according to each prediction along with an accompanying statistical approach for a larger, future investigation. Power

analyses were based on results from Ridding et al. (2000), Ridding et al. (2001) and McKay et al. (2002) for prediction #1 and from Kojima et al. (2018) and Kojima et al. (2019) for prediction #2. Effect sizes were estimated as Cohen's d_z . With the exception of Ridding et al (2000) where the reported correlation among repeated measures was $r = 0.8$, the assumed correlation between repeated measures was $r = 0.5$. This is a conservative estimate given that van de Ruit et al. (2015) reported high test-retest reliability of motor map area obtained with the fast-mapping approach with an intraclass correlation coefficient (ICC) of 0.74 and Bastani et al. (2012) reported that averaged MEP amplitudes (over 10 trials) have ICCs ranging from 0.77 to 0.9. Power analyses were conducted in G*Power as two-tailed paired t-tests, with α of 0.02 and power of 0.90. The largest returned sample size was 16 participants. Thus, a sample size of 20 participants should be adequate to test the two stated predictions. Further, this sample size would allow for correlations between changes in map area and changes in afferent inhibition to be performed, which would uncover whether afferent inhibition is associated with motor cortex organization.

Table 7.1: Predictions with planned statistical approach and estimated sample sizes

Prediction	Statistical approach	Previous Study	Result	Estimated effect size (Cohen's dz)	Required sample size	
					Paired t-test	WSRT
#1	Paired t-test or WSRT comparing FDI map area between T0 and T1 for the UN stimulation intervention.	Ridding et al. (2000)*	↑ average MEP amplitude after 2h of UN stimulation	-1.06	15	16
		Ridding et al. (2001)	↑ FDI map area after 2h of UN stimulation	-3.38	8	8
		McKay et al. (2002)**	↑ average MEP amplitude after 45min of UN stimulation	-1.52	9	9
#2	Paired t-test or WSRT comparing FDI map area between T0 and T1 for the DN stimulation intervention.	Kojima et al. (2018)	↓ average MEP amplitude after 20min of mechanical digit stimulation	5.27	4	5
		Kojima et al. (2019)	↓ average MEP amplitude after 20min of mechanical digit stimulation	2.00	12	13

DN: digital nerve, FDI: first dorsal interosseous muscle, MEP: motor-evoked potential, UN: ulnar nerve, WSRT: Wilcoxon signed-rank test

*Means and standard deviations were visually estimated from data plotted in Figure 2 (top).

**Means and standard deviations were visually estimated from data plotted in Figure 1.

The purpose of the rest condition was to assess the reliability of the acquired data. However, given the limited sample size, these tests could not be implemented. A future investigation with an appropriate sample size should retain this rest condition so that the Smallest Detectable Change (SDC) can be calculated. The SDC is the minimum amount of change in a variable that is considered a “real” change (Weir 2005). This value should be estimated from data obtained before and after a period of rest, where the rest period is similar to the length of the intervention used. The SDC is then compared to the change in the dependent variable within the other conditions. For example, if the SDC of map area following a rest period is 100 mm², then the map area must increase or decrease by more than 100 mm² after an intervention (either DN or UN stimulation) in order for this to be considered a

“real” change that exceeds measurement error. This metric should be employed in addition to hypothesis testing to increase the validity of the results, especially given the variability in the data obtained in the present study within the rest condition.

There are several factors to consider that may explain why no predictable change in map area or afferent inhibition was observed in the present study. The first relates to the nerve stimulation protocol. The DN and UN were stimulated for 45 minutes in separate sessions. However, Ridding et al. (2001) stimulated the UN and radial nerves at the wrist simultaneously for a period of two hours to observe an increase in map area. McKay et al. (2002) used a similar protocol and observed an increase in MEP amplitude that lasted for approximately one hour. We opted to stimulate the DN and UN separately to specifically test whether cutaneous enrichment alone was sufficient to evoke changes in sensorimotor function (i.e. maps and/or afferent inhibition). Given that SES to the UN did not induce a predictable change in map area, this may suggest that the intervention was not potent enough to induce physiological change on an individual level. A larger investigation with an appropriate sample size is required to determine if stimulation of these targeted nerve types can change map area on a group-averaged level.

The pattern of stimulation is another important consideration. In the present study, we chose a “burst” stimulation pattern (1 s burst of 20 stimuli every 5 s). This pattern of stimulation has been previously shown to improve tactile discrimination performance in as little as 30 minutes (Ragert et al. 2008) and increase inhibitory processes within S1 and M1 (Rocchi

et al. 2017). However, this form of stimulation has not yet been shown to modulate M1 organization. Studies that have shown an enlargement of muscle representations within M1 used continuous patterns of stimulation (10 Hz train for 1 ms, delivered every 1 s) (Ridding et al. 2000, 2001). A future iteration of the present study may choose to compare different patterns of stimulation.

There are a number of limitations of the present study that should be addressed. First, attentional drift during the intervention period was not controlled for. It is unknown whether attentional focus on the intervention (i.e. focus on the stimulation delivered) must be maintained to maximize the neuroplastic effects. However, other protocols such as Paired Associative Stimulation (PAS), a neuroplasticity-induced protocol that involves prolonged paired delivery of nerve stimulation and TMS, does require participants to focus on the intervention to maximize the effects (Stefan et al. 2004). For example, these studies usually employ a counting task during the intervention, where participants are required to count the number of stimuli, to control for attentional drift (Sale et al. 2008). A future iteration of the present study should consider employing a similar task during the intervention to control for attentional drift.

A second limitation is the absence of additional data acquired on somatosensory function. While the specific burst stimulation protocol has been shown to improve tactile performance for up to 24 hours after delivery of the intervention (Ragert et al. 2008), other studies have shown that increased corticospinal excitability following 10-30 min of

stimulation persists only for 30-60 minutes (Hamdy et al. 1998; Khaslavskaja et al. 2002). Therefore, we limited the number of dependent variables to ensure that all post-intervention assessments could be acquired within 30 minutes. However, longer periods of stimulation have been shown to also have longer duration effects. For example, stimulation for 120 minutes has been shown to increase corticospinal excitability for 60-120 minutes (Charlton et al. 2003; McKay et al. 2002). Therefore, a future iteration of this study may consider using a longer intervention period to maximize the time allotted for acquisition of post-intervention data. This would allow measures such as the SNAP and SEP to be acquired after the intervention, which would provide valuable information on whether neuroplastic changes are occurring within the somatosensory pathways underlying SAI and LAI.

Finally, a future iteration of this study should consider implementing a second experiment investigating the effects of sensory *deprivation* rather than *enrichment*. As discussed earlier, sensory deprivation via denervation or ischemic nerve block induces changes in somatosensory (Nudo et al. 1996; Wang et al. 1995) and motor (Brasil-Neto et al. 1993; Sanes et al. 1990) representations within the cortex. One caveat of this research is that they include sensory deprivation protocols that affect both cutaneous and proprioceptive afferent fibers. Therefore, since both fiber types are altered it is difficult to reconcile the contribution from cutaneous inputs alone. The use of anesthetic creams applied to the skin circumvents this issue by targeting only cutaneous receptors and creating a cutaneous sensory deprivation (Kundu and Achar 2002). For example, cutaneous deprivation via application of EMLA to the forearm induces transient reorganization of the somatosensory cortex

(Björkman et al. 2009; Rossini et al. 1994; Sens et al. 2012) while simultaneously improving sensory and motor performance of the digits in healthy individuals (Petoe et al. 2013) and those with complex regional pain syndrome (Strauss et al. 2015). Similarly, EMLA applied to the skin alters motor cortical function as assessed via TMS (Petoe et al. 2013; Sehle et al. 2016; Strauss et al. 2015; Yildiz et al. 2004). Specifically, application of EMLA on the forearm increased short-interval intracortical inhibition (SICI) within the M1, as acquired with EMG from the FDI muscle (Petoe et al. 2013). Therefore, it is possible that application of EMLA on the forearm may result in stronger afferent inhibition.

Overall, the results obtained thus far do not show any obvious effect of SES on M1 organization or afferent inhibition. However, further participants will be recruited to test our predictions statistically before definitive conclusions can be made. The results of this study may be used to increase our understanding of interactions between the somatosensory and motor cortices, and the neural mechanisms underlying tactile-motor integration. Other research has shown that SES of peripheral nerves within the hand improves motor skill acquisition in both healthy individuals (Veldman et al. 2015, 2016) and individuals with stroke (Celnik et al. 2007; Conforto et al. 2007). Therefore, the results of the present study will be useful for gleaning the mechanisms underlying this effect.

Chapter 8: General Discussion

The main goal of this thesis was to further the understanding of afferent inhibition. To achieve this goal, I sought to answer two questions through a series of five experiments. First, what is the functional relevance of afferent inhibition? Second, how can the acquisition of afferent inhibition be optimized? Figure 8.1 illustrates the studies that directly address each of these questions. In the following sections I will provide a summary of how the results of these studies address the main questions of the thesis, while also discussing limitations of the thesis and directions for future research.

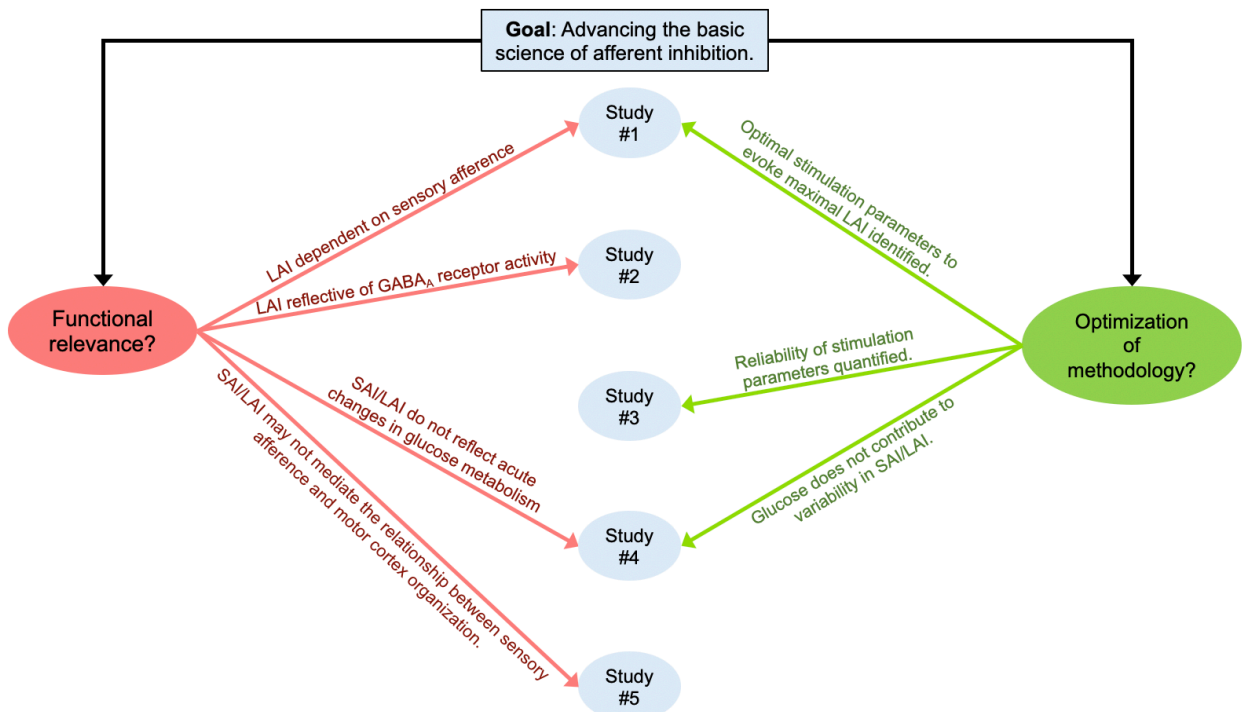


Figure 8.1: Schematic of studies that address goals of the thesis.

This figure depicts which studies address question #1 (red; What is the functional relevance of afferent inhibition?) and question #2 (green; How can the acquisition of afferent inhibition be optimized?) of the thesis. Further, blue arrows indicate how studies within the thesis are interconnected. Study #1: Modulation of long-latency afferent inhibition by the amplitude of the sensory afferent volley; Study #2: Effects of lorazepam and baclofen on short- and long-latency afferent inhibition; Study #3: Reliability of transcranial magnetic

stimulation measures of afferent inhibition; Study #4: The effects of glucose levels on afferent inhibition; Study #5: Cutaneous modulation of sensorimotor function.

8.1 Optimization of methodology

For the past two decades in the TMS literature, afferent inhibition has been interpreted as a marker of sensorimotor function. However, there is considerable variability in the methodological parameters that are used including stimulation targets, intensities, statistics, screening protocols, etc... (Chipchase et al. 2012; Guerra et al. 2020). As such, it is difficult to compare results across different studies. The results from Studies #1, #3 and #4 provided valuable information that can be used to inform the TMS methodology for future studies.

Previous research determined that maximal SAI is obtained at nerve stimulation intensities corresponding to 50% SNAP_{max} (Bailey et al. 2016), and I extended this knowledge to conclude that LAI is also maximal at this stimulation intensity. For the mixed median nerve (MN), this corresponds to motor threshold of the APB muscle. For the cutaneous digital nerve (DN), this corresponds to 2x sensory threshold. In order accurately acquire LAI and show true change in the magnitude of LAI (e.g., across an intervention), it is ideal to probe the maximal amount of inhibition possible within an individual. Therefore, these results will help guide future research when choosing the stimulation parameters to measure LAI.

After determining the stimulation parameters that evoked maximal LAI, the next step was to assess whether these parameters evoked LAI reliably. Rigorous reliability testing in the field of TMS is sparse and according to Schambra et al. (2015), there is a widespread

misunderstanding of the appropriate statistical assessments of reliability. For example, common approaches for evaluating test-retest reliability in TMS research included Pearson's correlation coefficient (Balslev et al. 2007; De Gennaro et al. 2003) and paired t-tests (Borojerdj et al. 2000; Maeda et al. 2002). However, these approaches are problematic because they do not directly assess the agreement between repeated measures and, therefore, fail to evaluate test-retest reliability accurately. Therefore, when addressing the reliability of SAI and LAI, it was important that appropriate reliability statistics were used such as the intraclass correlation coefficient (ICC), standard error of measurement (SEM_{eas}), and smallest detectable change (SDC). Prior to this dissertation, only one previous study had assessed the relative reliability of SAI, reporting a moderate ICC of 0.67 (Brown et al. 2017). However, the absolute reliability of SAI, quantified with the SEM_{eas} and SDC, was unknown and the reliability of LAI had yet to be investigated. This area of research is especially important if these measures are to be used in the future within a clinical setting as biomarkers of sensorimotor function or tools for diagnosis/prognosis as proposed previously (Benussi et al. 2017; Padovani et al. 2018; Snow et al. 2019).

In Study #3, I showed through metrics of the ICC, SEM_{eas} and SDC that afferent inhibition cannot reliably track individual neurophysiological change but can be used to detect changes at the group-level. Further, I investigated how determination of ISI influenced the reliability of SAI outcomes and showed that only SAI_{MN} was impacted by this parameter. If future studies are seeking to reliably evoke SAI, then normalization of the ISI to the N20

latency is not necessary. However, if the goal of a future study is to evoke *maximal* SAI, then this individualized ISI approach should be used.

Importantly, this reliability analysis applies only to research measuring afferent inhibition in a healthy, young population. Therefore, the results are not generalizable to the populations that display impaired afferent inhibition. This is because metrics such as the ICC are dependent upon heterogeneity of the sample tested. For example, the reliability metrics obtained from a sample of healthy individuals would not apply to a stroke population, as individuals within this sample would present with different pathologies, and therefore, greater between-subject variability. Thus, the results from Study #3 provide a control group comparison for future reliability research in clinical populations. Importantly, there is still much to be learned from future reliability studies in healthy individuals to improve the usefulness of afferent inhibition. Future research should consider investigating the inter-rater reliability of afferent inhibition (i.e., comparison between different experimenters delivering TMS), the influence of experimenter training, and the minimal number of TMS stimuli required for reliable assessments of afferent inhibition.

Having quantified the existing variance in afferent inhibition, it was important to identify factors that contribute to this variability in order to optimize the acquisition of this measure. The influence of diet is an area of TMS research that has been underexplored. Therefore, in Study #4 I sought to investigate the interaction between glucose levels and afferent inhibition. Ultimately, I found that acute elevations in blood glucose did not modulate SAI

or LAI. This suggests that glucose intake does not need to be controlled for prior to TMS testing. This study was an important first step for research investigating the physiological factors that influence afferent inhibition, which is important to minimize inter- and intra-individual variability in the data.

Although acute elevations in glucose did not change afferent inhibition, it is unknown if other dietary factors (e.g., proteins, fats) or lifestyles (e.g., Ketogenic diet, Vegan diet) are physiological confounds of afferent inhibition. Only one TMS study has investigated the influence of high-fat ketogenic diets on M1 function. Compared to baseline, participants undergoing two weeks of a ketogenic exhibited an increase in SICI (Cantello et al. 2007), a TMS measure reflective of GABA_A receptive activity (Di Lazzaro et al. 2005a). Given that SAI and LAI are also reflective of GABA_A receptor activity (refer to Study 2), this may suggest that ketogenic diets would also modulate afferent inhibition. Ultimately, furthering this line of research will help improve TMS screening protocols with the goal of minimizing variability in the data.

Besides glucose levels, other participant factors such as age (Opie et al. 2015; Shibuya et al. 2016), biological sex (Shibuya et al. 2016), hormonal changes (Smith et al. 1999), handedness (Hammond et al. 2004), and fitness (Lulic et al. 2017) have all been shown to modulate corticospinal and intracortical excitability. However, the influence of these factors on afferent inhibition are unknown. For example, there is strong evidence to suggest that afferent inhibition is influenced by sex differences and ovarian hormones. Compared

to males, females exhibit higher cortical GABA levels (Sanacora et al. 1999) and intracortical inhibition within M1 (Shibuya et al. 2016). Further, intracortical inhibition is greater in the luteal phase (Smith et al. 1999, 2002). In the somatosensory system, females exhibit greater SNAP (Bolton and Carter 1980; Fujimaki et al. 2009; Hasanzadeh et al. 2008) and N20 amplitudes compared to males (Ikuta and Furuta 1982; Kakigi and Shibasaki 1992). This suggests that females would exhibit greater afferent inhibition than males, particularly during the luteal phase of the menstrual cycle.

8.1 Functional relevance

The conditioning of MEPs with peripheral nerve stimulation provides a “snapshot” into the excitability of sensorimotor pathways. While measures of afferent inhibition may be used as markers of physiological change in these pathways, it is unknown if they are causally related to function or human behavior. Through the studies within the thesis, I investigated the relevance of afferent inhibition to various forms of function.

In Study #1, I characterized the relationship between LAI and sensory afferent fiber recruitment. Median nerve LAI showed a U-shaped relationship with SNAP amplitude, whereby maximal LAI was obtained at 50% SNAP_{max}. This corresponds to the recruitment of all sensory afferents within the median nerve bundle. Further, digital nerve LAI first appeared and was maximal at 50% SNAP_{max}. This corresponds to the recruitment of half the sensory afferents within the digital nerve bundle.

Further research is required to fully elucidate the relationship between LAI and somatosensory function. Previous work showed that SAI increases with the N20-P25 amplitude (Bailey et al. 2016), although the relationship between LAI and the SEP is still unknown. In extension, it is unknown if SAI or LAI are related to other cortical potentials such as the N30. The N30 potential is linked to activity within the thalamus, premotor areas, basal ganglia and M1 (Cebolla et al. 2011; Kaňovský et al. 2003), and is thought to reflect sensorimotor integration (Rossi et al. 2003). Finally, intensity-dependent modulation of SAI and LAI has only been demonstrated in healthy populations. It is unknown whether these relationships would exist in clinical populations that demonstrate impaired afferent inhibition. Absence of these relationships may be an indicator of impaired sensory afference and sensorimotor integration.

Investigating the intensity-dependent modulation of LAI prompted the question: how does sensory afference exert inhibition over M1? Administration of drugs with a clear mode of action within the CNS helps uncover the pharmacological properties of TMS measures, elucidates their relationship with neurotransmitter function, and provides insight into the neural pathways that TMS measures probe. Previous research showed SAI was reflective of GABA_A receptor activity (Di Lazzaro et al. 2005a), but it was unknown if LAI was also reflective of GABAergic neurotransmission. In Study #2, I discovered that both SAI and LAI were reduced following lorazepam administration while neither were modulated by baclofen. This indicates that LAI is also reflective of GABA_A receptor activity, while both SAI and LAI are not reflective of GABA_B receptor activity. Although this study was

conducted in healthy young adults, the results may indicate that instances of impaired afferent inhibition within clinical populations are reflective of abnormal GABAergic neurotransmission.

Importantly, it is unclear whether SAI and LAI are related to the function of other neuromodulators. One major candidate for future research is dopamine. In rodents, D2 receptor agonists increase the firing rate of M1 pyramidal neurons (Vitrac et al. 2014) whereas D2 receptor antagonists reduce the forelimb area in M1 (Hosp et al. 2009). This evidence shows that dopamine modulates M1 function. Next, both SAI and LAI are impaired in PD (Dubbioso et al. 2019; Sailer et al. 2003), who display a progressive loss of nigrostriatal dopaminergic neurons (Dubbioso et al. 2019). This may suggest that dopamine plays a major role in afferent inhibition. I had originally planned to conduct a study investigating the influence of dopaminergic medication on afferent inhibition and include the results within the thesis. The protocol was approved by the Hamilton Integrated Research Ethics Board (HiREB) and was registered as a clinical trial with Health Canada. However, the study was halted during participant recruitment due to the COVID-19 pandemic. Another major neuromodulator of M1 activity is acetylcholine. Muscarinic antagonists reduce SAI (Di Lazzaro et al. 2000b) and SAI is abnormally reduced in populations exhibiting cognitive impairments driven by cholinergic deficits (Mimura et al. 2020). However, it is unknown if LAI is similarly modulated by cholinergic activity. Further, it has yet to be tested whether LAI is also abnormal in cognitively impaired

populations such as Alzheimer's disease. Overall, further pharmaco-TMS studies are required to fully elucidate the pharmacophysiology of afferent inhibition.

After determining the relationship between LAI and GABA_A receptor function, I wanted to test whether modulators of GABA_A receptor activity impacted afferent inhibition. One such modulator is glucose, which is a precursor to GABA (Mergenthaler et al. 2013) and increases GABA_A receptor activity (Anju et al. 2010). Prior to this dissertation, the relationship between afferent inhibition and glucose function had yet to be investigated, despite the fact that glucose is an essential for normal brain function. Upon uptake across the blood brain barrier (BBB), glucose fuels neuronal function through the astrocyte-neuron lactate shuttle or direct uptake into neurons (Mergenthaler et al. 2013). In both pathways, glucose enters glycolysis and the citric acid (TCA) cycle to generate energy in the form of adenosine triphosphate (ATP) and provide carbon for neurotransmitter synthesis. Neurotransmitters including glutamate, GABA, acetylcholine are all derived from intermediates of the glycolytic and TCA cycle pathways (Mergenthaler et al. 2013).

In Study #4, I showed that acute elevations in blood glucose did not change SAI or LAI. It is possible that these measures are not sensitive enough to detect change in neuronal excitability as a result of acute fluctuations in glucose levels. However, it is unknown whether afferent inhibition reflects change in chronic impairments of glucose metabolism. For example, Type-1 diabetics exhibit reduced corticospinal excitability (Andersen et al.

1995). It is unknown if diabetic or pre-diabetic individuals also demonstrate altered excitability of sensorimotor pathways or afferent inhibition.

For Study #5, I returned back to the question: how does sensory afference exert inhibition over M1? Animal research suggests that the size of muscle representations are under GABAergic control (Jacobs and Donoghue 1991). Given that SAI and LAI are reflective of GABA_A receptor activity, I wanted to test whether afferent inhibition was important for controlling M1 organization. Therefore, I implemented a plasticity-inducing protocol known as somatosensory electrical stimulation (SES) that has been shown to enlarge digit representations within S1 (Pleger et al. 2003) and muscle representations in M1 (Ridding et al. 2001).

The original goal of Study #5 was to test whether SES induced a change in afferent inhibition, and if the change in afferent inhibition was related to the change in M1 organization. This study would have provided novel information regarding the relationship between afferent inhibition and M1 function. Further, the results would have elucidated the neural mechanisms underlying SES. Unfortunately, participant recruitment was halted prematurely due to the COVID-19 pandemic. I was unable to conduct the original statistical analysis that aimed to address the relationship between afferent inhibition and M1 organization. Using the data acquired from four participants, I qualitatively assessed the influence of SES on afferent inhibition and motor maps separately. Compared to the rest intervention, the results did not show any consistent changes in afferent inhibition or motor

maps following SES. Further participant recruitment will be required to fully understand the relationship between afferent inhibition and motor cortex function.

Future studies should continue to investigate the relationship between afferent inhibition and function. It is unknown if the magnitude of afferent inhibition is causally related to human behavior or task performance. I recently showed that both SAI and LAI are not related to tactile acuity as assessed by the Temporal Order Judgement (TOJ) task and Grating Orientation Task (GOT) or manual dexterity as assessed by the Purdue Pegboard Task (Turco et al. 2018c). However, SAI and LAI were acquired outside of task context, and it is unknown whether these measures were modulated during task performance. Further, the influence of motor training protocols on afferent inhibition remains unclear (for review, see (Turco et al. 2021)) and it is unknown whether SAI or LAI are differentially modulated in skilled individuals such as athletes or musicians. If there is a relationship between afferent inhibition and human behavior, then perhaps training protocols or interventions can be implemented to strengthen afferent inhibition and subsequently improve behavior.

8.3 Neural pathways underlying afferent inhibition

As shown in Study #2, lorazepam reduced both SAI and LAI, suggesting that GABAergic mechanisms contribute to the genesis of afferent inhibition. However, the path traversed by the afferent volley that leads to inhibition of M1 remains unclear. Possibilities include a relay through S1 prior to arriving in M1, or a direct thalamocortical projection to M1.

Figure 8.2 shows the proposed model of afferent inhibition, based on the I-wave generating microcircuitry proposed by Di Lazzaro et al. (2012b). To aid in the description of the model, number superscripts will be used in the following paragraphs to reference specific sections of Figure 8.1.

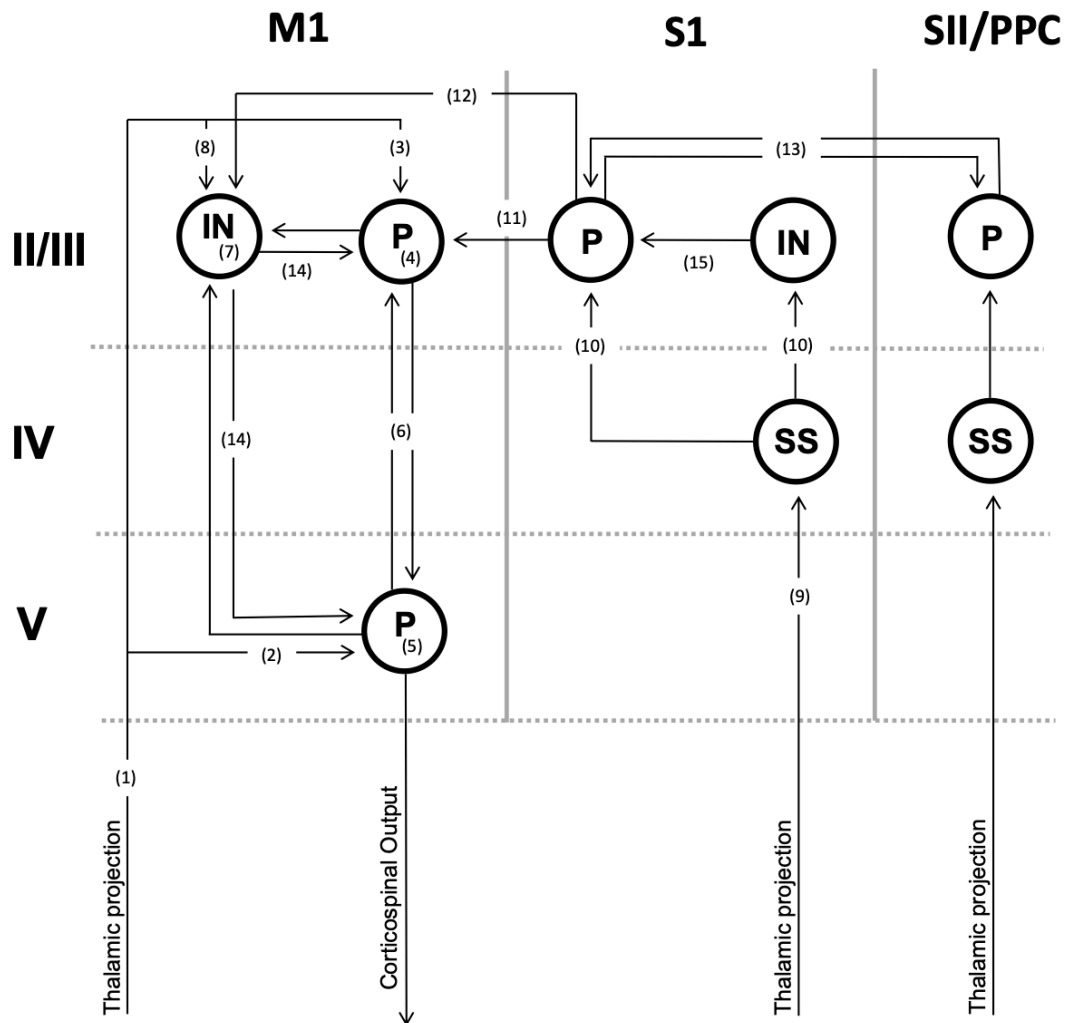


Figure 8.2: Proposed model of afferent inhibition.

This model is a simplified representation of the neural connections within the sensorimotor cortex necessary to understand afferent inhibition. IN: inhibitory interneuron, P: pyramidal cell; SS: spiny stellate cell.

8.3.1 Pathway underlying SAI

SAI is abolished in individuals with thalamic stroke (Bertolasi et al. 1998; Oliviero et al. 2005) while the N20 potential remains intact (Oliviero et al. 2005). This suggests that *SAI may involve direct thalamocortical projections to M1*¹. These projections to synapse on pyramidal neurons in layers II/III² and V³ (Hooks et al. 2013). Stimulation of M1 pyramidal neurons via TMS evokes descending corticospinal volleys known as I-waves that can be recorded epidurally. Early I1-waves are thought to be generated by activation of superficial pyramidal neurons in layers II/III⁴, which in turn depolarize large pyramidal tract neurons in layer V⁵ (Di Lazzaro et al. 2012b). Later I-waves are then generated by the reciprocal connection between pyramidal neurons in layers II/III and V⁶ (Di Lazzaro et al. 2012b). The connections between layers II/III and V are thought to be modulated by disynaptic connections with inhibitory GABAergic interneurons⁷ (Di Lazzaro et al. 2012b; Di Lazzaro and Ziemann 2013). Thalamocortical projections to M1 also innervate GABAergic interneurons⁸, and it is here where SAI is proposed to originate. SAI reduces late I2- and I3-waves (Tokimura et al. 2000), likely through activation of thalamic projections to the inhibitory GABAergic interneurons by the afferent volley, leading to suppression of corticospinal excitability (Di Lazzaro and Ziemann 2013).

SAI may also involve a relay through S1, given that SAI is modulated by neuroplasticity-inducing TMS protocols targeting S1 (Jacobs et al. 2014; Tsang et al. 2014). Afferent input is relayed through the thalamus and sent to the spiny stellate cells in layer IV of S1⁹ (Markram et al. 2004), which have excitatory synapses with layer II/III pyramidal neurons

(Feldmeyer et al. 2002) and inhibitory interneurons¹⁰ (Feldmeyer et al. 2018; Helmstaedter et al. 2008). Networks of inhibitory interneurons exist within S1 to provide in-field inhibition of pyramidal neurons for filtering afferent input to process specific stimulus properties (DiCarlo and Johnson 2000; Wood et al. 2017). Long-range excitatory projections extend from S1 to M1 through layers II/III (Kaneko et al. 1994). These projections innervate pyramidal neurons¹¹ and interneurons¹² in M1 (Caria et al. 1997; Rocco-Donovan et al. 2011; Rosén and Asanuma 1972). Arrival of the afferent volley in S1 would increase the inhibitory drive on sensory pyramidal neurons, thereby reducing the excitatory influence of the long-range connections to M1 and reducing the excitability of M1.

Therefore, SAI may result from a direct thalamocortical project to M1 or a relay through S1. Perhaps instead of two mutually exclusive pathways, one may be responsible for the genesis of SAI and the other is more of a modulatory pathway. In monkeys, peripheral nerve stimulation evokes cortical potentials in M1, and ablation of S1 does not abolish this short-latency response (Asanuma et al. 1980). Further, given that SAI is abolished following thalamic stroke (Bertolasi et al. 1998; Oliviero et al. 2005), it is likely that a thalamocortical projection to M1 is responsible for the genesis of SAI, and the S1 relay is the modulatory pathway.

8.3.2 Pathway underlying LAI

The neural pathway traversed by the afferent volley to evoke LAI remains unclear. LAI is thought to be cortical in origin because median nerve stimulation has no effect on spinal reflexes at the timing that corresponds to LAI (i.e. 200 ms) (Chen et al. 1999).

LAI may involve similar neural pathways as SAI. However, LAI occurs at longer ISIs, meaning that inhibition occurs following the opportunity for widespread activation of various cortical responsive to nerve stimulation. S1, S2 and the posterior parietal cortex are activated during the first 200 ms after median nerve stimulation (Allison et al. 1989; Boakye et al. 2000; Forss et al. 1994; Korvenoja et al. 1999; Stephen et al. 2006), and S2 is activated ~100 ms after digital nerve stimulation (Hari et al. 1984). There is dense reciprocal connectivity between all cytoarchitectural areas of S1 and S2, particularly in layers II/III¹³ (Aronoff et al. 2010; Krubitzer and Kaas 1990). Therefore, afferent input evoking LAI is may pass through cortico-cortical connections between higher-order sensory areas. Following arrival of afferent input to M1, LAI may then be under control of GABAergic neurons within M1, that then reduce the excitability of the corticospinal tract.

8.5 Limitations

Measures of spinal excitability (e.g., Hoffman reflex, F-wave) were not assessed within the thesis. Although previous work suggested that SAI and LAI are cortical in origin (Asmussen et al. 2013, 2014; Chen et al. 1999; Tokimura et al. 2000), the interventions used throughout the thesis have a global effect (i.e. lorazepam/baclofen, glucose tolerance

test, SES). Therefore, it cannot be ruled out that spinal mechanisms may underlie any changes in afferent inhibition that were observed.

The results of the thesis are limited by the parameters used to acquire afferent inhibition. Specifically, a restricted set of ISIs were used to evoke SAI and LAI, limiting the applicability of the results obtained to other ISIs. For example, Study #1 describes the relationship between LAI and the sensory afferent volley. However, LAI was only acquired at an ISI of 200 ms even though it exists at ISIs ranging from 200-1000 ms (Chen et al. 1999). It is unknown whether the neural pathways underlying LAI is similar across this large range of ISIs. Therefore, it is unknown whether the relationship between LAI and the sensory afferent volley extends to other ISIs.

LAI is stronger in muscles of the hand such as the APB and FDI compared to more proximal muscles such as the flexor carpi radialis (FCR) and extensor carpi radialis (ECR) (Abbruzzese et al. 2001; Chen et al. 1999). Afferent inhibition was only measured in distal hand muscles within the thesis experiments and it is unknown if similar results would be obtained if afferent inhibition was measured within more proximal muscles. For example, the relationship between LAI and the sensory afferent volley was only quantified for muscles of the hand in Study #1. It is unknown whether the magnitude of the afferent volley is also a mediator of LAI acquired from more proximal muscles of the upper limb or of muscles of the lower limb that do not require such fine motor control as hand muscles.

Only male participants were recruited for Study #2 and #4. Within females, the behavioral effects of GABAergic drugs are enhanced during the luteal phase of the menstrual cycle when progesterone levels are elevated (Babalonis et al. 2011). Further, glucose tolerance worsens during the luteal and menstruation phases of the menstrual cycle (Bennal and Kerure 2013; Diamond et al. 1989) and glucose concentrations tend to be higher during the luteal (Rani 2013). To avoid variability in lorazepam-induced effects and glucose metabolism, females were excluded from these studies and thus, the results are only applicable to males.

Finally, the data was obtained from healthy, young individuals only in all experiments of the thesis. Therefore, the results of the thesis do not extend to older or clinical populations. Despite this, my research offers a basis for subsequent clinical investigations by providing fundamental insight into the normal neural mechanisms of afferent inhibition.

8.6 Conclusions

In conclusion, this thesis furthers our understanding of the neurophysiology underlying afferent inhibition. I found that SAI and LAI are reflective of sensory afferent fibre recruitment and GABAergic neurotransmission, while also identifying optimal stimulation parameters to evoke these measures. Further, the research in this thesis provides an important step for understanding the reliability of afferent inhibition and exploring methods for improving such reliability. The knowledge from this thesis contributed to a model of afferent inhibition proposing the neural pathways that ultimately inhibit corticospinal

output from M1. Taken together, this thesis highlights the need to determine whether afferent inhibition is causally related to human function, which is essential to improve the future utility of these measures in a clinical setting where they could be used as markers function or diagnostic tools.

Chapter 9: References

- Abbruzzese G, Berardelli A.** Sensorimotor integration in movement disorders. *Mov Disord* 18: 231–240, 2003.
- Abbruzzese G, Marchese R, Buccolieri A, Gasparetto B, Trompetto C.** Abnormalities of sensorimotor integration in focal dystonia: a transcranial magnetic stimulation study. *Brain* 124: 537–45, 2001.
- Abi-Saab WM, Bubser M, Roth RH, Deutch a Y.** 5-HT₂ receptor regulation of extracellular GABA levels in the prefrontal cortex. *Neuropsychopharmacology* 20: 92–6, 1999.
- Ah Sen CB, Fassett HJ, El-Sayes J, Turco C V., Hameer MM, Nelson AJ.** Active and resting motor threshold are efficiently obtained with adaptive threshold hunting. *PLoS One* 12, 2017.
- Allison T, McCarthy G, Wood CC, Williamson PD, Spencer DD.** Human cortical potentials evoked by stimulation of the median nerve. II. Cytoarchitectonic areas generating long-latency activity. *J Neurophysiol* 62: 711–722, 1989.
- Amassian VE, Stewart M, Quirk GJ, Rosenthal JL.** Physiological basis of motor effects of a transient stimulus to cerebral cortex. *Neurosurgery* 20: 74–93, 1987.
- Andersen H, Nielsen JF, Poulsen PL, Mogensen CE, Jakobsen J.** Motor pathway function in normoalbuminuric IDDM patients. *Diabetologia* 38: 1191–1196, 1995.
- Anju TR, Kumar TP, Paulose CS.** Decreased GABA receptors functional regulation in the cerebral cortex and brainstem of hypoxic neonatal rats: Effect of glucose and oxygen supplementation. *Cell Mol Neurobiol* 30: 599–606, 2010.

Aronoff R, Matyas F, Mateo C, Ciron C, Schneider B, Petersen CCH. Long-range connectivity of mouse primary somatosensory barrel cortex. *Eur. J. Neurosci.* 31: 2221–2233, 2010.

Asanuma H, Larsen K, Yumiya H. Peripheral input pathways to the monkey motor cortex. *Exp Brain Res* 38: 349–355, 1980.

Asmussen MJ, Jacobs MF, Lee KGH, Zapallow CM, Nelson AJ. Short-Latency Afferent Inhibition Modulation during Finger Movement. *PLoS One* 8: e60496, 2013.

Asmussen MJ, Zapallow CM, Jacobs MF, Lee KGH, Tsang P, Nelson AJ. Modulation of short-latency afferent inhibition depends on digit and task-relevance. *PLoS One* 9: e104807, 2014.

Atkinson G, Nevill AM. Statistical methods for assessing measurement error (reliability) in variables relevant to sports medicine. *Sport Med* 26: 217–238, 1998.

Avanzino L, Martino D, van de Warrenburg BPC, Schneider SA, Abbruzzese G, Defazio G, Schrag A, Bhatia KP, Rothwell JC. Cortical excitability is abnormal in patients with the “fixed dystonia” syndrome. *Mov Disord* 23: 646–652, 2008.

Babalonis S, Lile JA, Martin CA, Kelly TH. Physiological doses of progesterone potentiate the effects of triazolam in healthy, premenopausal women. *Psychopharmacology (Berl)* 215: 429–439, 2011.

Badawy RAB, Vogrin SJ, Lai A, Cook MJ. Cortical excitability changes correlate with fluctuations in glucose levels in patients with epilepsy. *Epilepsy Behav* 27: 455–460, 2013.

Bailey AZ, Asmussen MJ, Nelson AJ. Short-latency afferent inhibition determined by

the sensory afferent volley. *J Neurophysiol* 116: 637–644, 2016.

Bailey AZ, Mi YP, Nelson AJ. Short-latency afferent inhibition in chronic spinal cord injury. *Transl Neurosci* 6: 235–243, 2015.

Bailey SP, Hibbard J, La Forge D, Mitchell M, Roelands B, Harris GK, Folger S.

Impact of a Carbohydrate Mouth Rinse on Quadriceps Muscle Function and Corticomotor Excitability. *Int J Sports Physiol Perform* 14: 927–933, 2019.

Ballinger EC, Ananth M, Talmage DA, Role LW. Basal Forebrain Cholinergic Circuits and Signaling in Cognition and Cognitive Decline. *Neuron* 91: 1199–1218, 2016.

Balslev D, Braet W, McAllister C, Miall RC. Inter-individual variability in optimal current direction for transcranial magnetic stimulation of the motor cortex. *J Neurosci Methods* 162: 309–313, 2007.

Barker AT, Jalinous R, Freeston IL. Non-Invasive Magnetic Stimulation of Human Motor Cortex. *Lancet* 325: 1106–1107, 1985.

Bastani A, Jaberzadeh S. A Higher Number of TMS-Elicited MEP from a Combined Hotspot Improves Intra- and Inter-Session Reliability of the Upper Limb Muscles in Healthy Individuals. *PLoS One* 7, 2012.

Beaulieu LD, Flamand VH, Massé-Alarie H, Schneider C. Reliability and minimal detectable change of transcranial magnetic stimulation outcomes in healthy adults: A systematic review. *Brain Stimul* 10: 196–213, 2017a.

Beaulieu LD, Massé-Alarie H, Ribot-Ciscar E, Schneider C. Reliability of lower limb transcranial magnetic stimulation outcomes in the ipsi- and contralesional hemispheres of adults with chronic stroke. *Clin Neurophysiol* 128: 1290–1298, 2017b.

Beckerman H, Roebroek ME, Lankhorst GJ, Becher JG, Bezemer PD, Verbeek

ALM. Smallest real difference, a link between reproducibility and responsiveness. *Qual Life Res* 10: 571–578, 2001.

Bennal A, Kerure S. Glucose handling during menstrual cycle. *Int J Reprod*

Contraception, Obstet Gynecol 284–287, 2013.

Benussi A, Cotelli MS, Cantoni V, Bertasi V, Turla M, Dardis A, Biasizzo J,

Manenti R, Cotelli M, Padovani A, Borroni B. Clinical and neurophysiological characteristics of heterozygous NPC1 carriers. *JIMD Rep* 49: 80–88, 2019.

Benussi A, Di Lorenzo F, Dell’Era V, Cosseddu M, Alberici A, Caratozzolo S, Cotelli

MS, Micheli A, Rozzini L, Depari A, Flammini A, Ponzio V, Martorana A,

Caltagirone C, Padovani A, Koch G, Borroni B. Transcranial magnetic stimulation

distinguishes Alzheimer disease from frontotemporal dementia. *Neurology* 89: 665–672, 2017.

Bertolasi L, Priori A, Tinazzi M, Bertasi V, Rothwell JC. Inhibitory action of forearm

flexor muscle afferents on corticospinal outputs to antagonist muscles in humans. *J*

Physiol 511: 947–956, 1998.

Bestmann S, Krakauer JW. The uses and interpretations of the motor-evoked potential

for understanding behaviour. *Exp Brain Res* 233: 679–689, 2015.

Bhandari A, Radhu N, Farzan F, Mulsant BH, Rajji TK, Daskalakis ZJ,

Blumberger DM. A meta-analysis of the effects of aging on motor cortex

neurophysiology assessed by transcranial magnetic stimulation. *Clin Neurophysiol* 127:

2834–2845, 2016.

Björkman A, Weibull A, Rosén B, Svensson J, Lundborg G. Rapid cortical reorganisation and improved sensitivity of the hand following cutaneous anaesthesia of the forearm. *Eur J Neurosci* 29: 837–844, 2009.

Boakye M, Huckins SC, Szeverenyi NM, Taskey BI, Hodge J. Functional magnetic resonance imaging of somatosensory cortex activity produced by electrical stimulation of the median nerve or tactile stimulation of the index finger. *J Neurosurg* 93: 774–783, 2000.

Bocquillon P, Charley-Monaca C, Houdayer E, Marques A, Kwiatkowski A, Derambure P, Devanne H. Reduced afferent-induced facilitation of primary motor cortex excitability in restless legs syndrome. *Sleep Med* 30: 31–35, 2017.

Bolton CF, Carter KM. Human sensory nerve compound action potential amplitude: Variation with sex and finger circumference. *J Neurol Neurosurg Psychiatry* 43: 925–928, 1980.

Bonassi G, Bisio A, Lagravinese G, Ruggeri P, Bove M, Avanzino L. Selective sensorimotor modulation operates during cognitive representation of movement. *Neuroscience* 409: 16–25, 2019.

Bonni S, Ponzo V, Di Lorenzo F, Caltagirone C, Koch G. Real-time activation of central cholinergic circuits during recognition memory. *Eur J Neurosci* 45: 1485–1489, 2017.

Borghammer P. Perfusion and metabolism imaging studies in Parkinson's disease. *Dan Med J* 59, 2012.

Borojerdi B, Battaglia F, Muellbacher W, Cohen LG. Mechanisms influencing

stimulus-response properties of the human corticospinal system. *Clin Neurophysiol* 112: 931–937, 2001.

Boroojerdi B, Kopylev L, Battaglia F, Facchini S, Ziemann U, Muellbacher W, Cohen LG. Reproducibility of intracortical inhibition and facilitation using the paired-pulse paradigm. *Muscle and Nerve* 23: 1594–1597, 2000.

Boyd IA, Kalu KU. Scaling factor relating conduction velocity and diameter for myelinated afferent nerve fibres in the cat hind limb. *J Physiol* 289: 277–297, 1979.

Brasil-Neto JP, Cohen LG, Pascual-Leone A, Jabir FK, Wall RT, Hallett M. Rapid reversible modulation of human motor outputs after transient deafferentation of the forearm: A study with transcranial magnetic stimulation. *Neurology* 42: 1302–1306, 1992.

Brasil-Neto JP, Valls-Sole J, Pascual-Leone A, Cammarota A, Amassian VE, Cracco R, Maccabee P, Cracco J, Hallett M, Cohen LG. Rapid modulation of human cortical motor outputs following ischaemic nerve block. *Brain* 116: 511–525, 1993.

Brinkman J, Colebatch JG, Porter R, York DH. Responses of precentral cells during cooling of post-central cortex in conscious monkeys. *J Physiol* 368: 611–625, 1985.

Brodie SM, Meehan S, Borich MR, Boyd LA. 5 Hz repetitive transcranial magnetic stimulation over the ipsilesional sensory cortex enhances motor learning after stroke. *Front Hum Neurosci* 8: 143, 2014.

Brown KE, Lohse KR, Mayer IMS, Strigaro G, Desikan M, Casula EP, Meunier S, Popa T, Lamy JC, Odish O, Leavitt BR, Durr A, Roos RAC, Tabrizi SJ, Rothwell JC, Boyd LA, Orth M. The reliability of commonly used electrophysiology measures.

Brain Stimul 10: 1102–1111, 2017.

Bruton A, Conway JH, Holgate ST. Reliability: What is it, and how is it measured?

Physiotherapy 86: 94–99, 2000.

Burns E, Chipchase LS, Schabrun SM. Reduced Short- and Long-Latency Afferent

Inhibition Following Acute Muscle Pain: A Potential Role in the Recovery of Motor

Output. *Pain Med* pnv104, 2016.

Van Bussel FCG, Backes WH, Hofman PAM, Puts NAJ, Edden RAE, Van Boxtel

MPJ, Schram MT, Stehouwer CDA, Wildberger JE, Jansen JFA. Increased GABA

concentrations in type 2 diabetes mellitus are related to lower cognitive functioning. *Med*

(United States) 95, 2016.

Cantello R, Varrasi C, Tarletti R, Cecchin M, D'Andrea F, Veggiotti P, Bellomo G,

Monaco F. Ketogenic diet: Electrophysiological effects on the normal human cortex.

Epilepsia 48: 1756–1763, 2007.

Cantone M, Di Pino G, Capone F, Piombo M, Chiarello D, Cheeran B, Pennisi G, Di

Lazzaro V. The contribution of transcranial magnetic stimulation in the diagnosis and in

the management of dementia. *Clin. Neurophysiol.* 125: 1509–1532, 2014.

Caria M, Kaneko T, Kimura A, Asanuma H. Functional organization of the projection

from area 2 to area 4gamma in the cat. *J. Neurophysiol.* 77: 3107–14, 1997.

Cebolla AM, Palmero-Soler E, Dan B, Cheron G. Frontal phasic and oscillatory

generators of the N30 somatosensory evoked potential. *Neuroimage* 54: 1297–1306,

2011.

Celebi O, Temuçin CM, Elibol B, Saka E. Short latency afferent inhibition in

Parkinson's disease patients with dementia. *Mov Disord* 27: 1052–1055, 2012.

Celnik P, Hummel F, Harris-Love M, Wolk R, Cohen LG. Somatosensory Stimulation Enhances the Effects of Training Functional Hand Tasks in Patients With Chronic Stroke. *Arch Phys Med Rehabil* 88: 1369–1376, 2007.

Charlton CS, Ridding MC, Thompson PD, Miles TS. Prolonged peripheral nerve stimulation induces persistent changes in excitability of human motor cortex. *J Neurol Sci* 208: 79–85, 2003.

Chen R. Interactions between inhibitory and excitatory circuits in the human motor cortex. *Exp Brain Res* 154: 1–10, 2004.

Chen R, Corwell B, Hallett M. Modulation of motor cortex excitability by median nerve and digit stimulation. *Exp Brain Res* 129: 77–86, 1999.

Chipchase L, Schabrun S, Cohen L, Hodges P, Ridding M, Rothwell J, Taylor J, Ziemann U. A checklist for assessing the methodological quality of studies using transcranial magnetic stimulation to study the motor system: An international consensus study. *Clin Neurophysiol* 123: 1698–1704, 2012.

Cho HJ, Panyakaew P, Thirugnanasambandam N, Wu T, Hallett M. Dynamic modulation of corticospinal excitability and short-latency afferent inhibition during onset and maintenance phase of selective finger movement. *Clin Neurophysiol* 127: 2343–2349, 2016.

Classen J, Steinfelder B, Liepert J, Stefan K, Celnik P, Cohen LG, Hess A, Kunesch E, Chen R, Benecke R, Hallett M. Cutaneomotor integration in humans is somatotopically organized at various levels of the nervous system and is task dependent.

Exp brain Res 130: 48–59, 2000.

Coggan AR, Coyle EF. Carbohydrate ingestion during prolonged exercise: Effects on metabolism and performance. *Exerc Sport Sci Rev* 19: 1–40, 1991.

Cohen LG, Bandinelli S, Findley TW, Hallett M. Motor reorganization after upper limb amputation in man: A study with focal magnetic stimulation. *Brain* 114: 615–627, 1991.

Conforto AB, Cohen LG, Santos RL Dos, Scaff M, Marie SKN. Effects of somatosensory stimulation on motor function in chronic cortico-subcortical strokes. *J Neurol* 254: 333–339, 2007.

Conover WJ, Iman RL. Analysis of Covariance Using the Rank Transformation. *Biometrics* 38: 715, 1982.

Damron LA, Dearth DJ, Hoffman RL, Clark BC. Quantification of the corticospinal silent period evoked via transcranial magnetic stimulation. *J Neurosci Methods* 173: 121–128, 2008.

DeFelipe J. Types of neurons, synaptic connections and chemical characteristics of cells immunoreactive for calbindin-D28K, parvalbumin and calretinin in the neocortex. *J Chem Neuroanat* 14: 1–19, 1997.

Devanne H, Degardin A, Tyvaert L, Bocquillon P, Houdayer E, Manceaux A,

Derambure P, Cassim F. Afferent-induced facilitation of primary motor cortex excitability in the region controlling hand muscles in humans. *Eur J Neurosci* 30: 439–448, 2009.

Devanne H, Lavoie BA, Capaday C. Input-output properties and gain changes in the

human corticospinal pathway. *Exp Brain Res* 114: 329–338, 1997.

Diamond MP, Simonson DC, DeFronzo RA. Menstrual cyclicality has a profound effect on glucose homeostasis. *Fertil Steril* 52: 204–208, 1989.

DiCarlo JJ, Johnson KO. Spatial and temporal structure of receptive fields in primate somatosensory area 3b: effects of stimulus scanning direction and orientation. *J Neurosci* 20: 495–510, 2000.

Domenech J, Barrios C, Tormos JM, Pascual-Leone Á. Somatosensory cortectomy induces motor cortical hyperexcitability and scoliosis: An experimental study in developing rats. *Spine J* 13: 938–946, 2013.

Donoghue JP, Sanes JN. Organization of adult motor cortex representation patterns following neonatal forelimb nerve injury in rats. *J Neurosci* 8: 3221–3232, 1988.

Douglas RJ, Martin KA. A functional microcircuit for cat visual cortex. *J Physiol* 440: 735–769, 1991.

Dubbioso R, Manganelli F, Siebner HR, Di Lazzaro V. Fast intracortical sensory-motor integration: A window into the pathophysiology of parkinson's disease. *Front Hum Neurosci* 13: 111, 2019.

Dubbioso R, Raffin E, Karabanov A, Thielscher A, Siebner HR. Centre-surround organization of fast sensorimotor integration in human motor hand area. *Neuroimage* 158: 37–47, 2017.

Erro R, Rocchi L, Antelmi E, Palladino R, Tinazzi M, Rothwell J, Bhatia KP. High frequency repetitive sensory stimulation improves temporal discrimination in healthy subjects. *Clin Neurophysiol* 127: 817–820, 2016.

Feldman J, Barshi I. The Effects of Blood Glucose Levels on Cognitive Performance: A Review of Literature [Online]. Moffett Field, California, NASA Ames Research Center <http://ntrs.nasa.gov/archive/nasa/casi.ntrs.nasa.gov/20070031714.pdf>.

Feldmeyer D, Lübke J, Silver RA, Sakmann B. Synaptic connections between layer 4 spiny neurone-layer 2/3 pyramidal cell pairs in juvenile rat barrel cortex: Physiology and anatomy of interlaminar signalling within a cortical column. *J Physiol* 538: 803–822, 2002.

Feldmeyer D, Qi G, Emmenegger V, Staiger JF. Inhibitory interneurons and their circuit motifs in the many layers of the barrel cortex. *Neuroscience* 368: 132–151, 2018.

Ferezou I, Haiss F, Gentet LJ, Aronoff R, Weber B, Petersen CCH. Spatiotemporal Dynamics of Cortical Sensorimotor Integration in Behaving Mice. *Neuron* 56: 907–923, 2007.

Filippi MM, Oliveri M, Pasqualetti P, Cicinelli P, Traversa R, Vernieri F, Palmieri MG, Rossini PM. Effects of motor imagery on motor cortical output topography in Parkinson's disease. *Neurology* 57: 55–61, 2001.

Fischer M, Orth M. Short-latency sensory afferent inhibition: Conditioning stimulus intensity, recording site, and effects of 1 Hz repetitive TMS. *Brain Stimul* 4: 202–209, 2011.

Fisher RJ, Galea MP, Brown P, Lemon RN. Digital nerve anaesthesia decreases EMG-EMG coherence in a human precision grip task. *Exp Brain Res* 145: 207–214, 2002.

Flanders M. What is the biological basis of sensorimotor integration? *Biol Cybern* 104: 1–8, 2011.

Flansbjer UB, Holmbäck AM, Downham D, Patten C, Lexell J. Reliability of gait performance tests in men and women with hemiparesis after stroke. *J Rehabil Med* 37: 75–82, 2005.

Forner-Cordero A, Steyvers M, Levin O, Alaerts K, Swinnen SP. Changes in corticomotor excitability following prolonged muscle tendon vibration. *Behav Brain Res* 190: 41–49, 2008.

Forss N, Hari R, Salmelin R, Ahonen A, Hämäläinen M, Kajola M, Knuutila J, Simola J. Activation of the human posterior parietal cortex by median nerve stimulation. *Exp Brain Res* 99: 309–315, 1994.

Fujimaki Y, Kuwabara S, Sato Y, Iose S, Shibuya K, Sekiguchi Y, Nasu S, Noto Y, Taniguchi J, Misawa S. The effects of age, gender, and body mass index on amplitude of sensory nerve action potentials: multivariate analyses. *Clin Neurophysiol* 120: 1683–6, 2009.

Gandevia SC, Burke D. Saturation in human somatosensory pathways. *Exp Brain Res* 54: 582–585, 1984.

Gant N, Stinear CM, Byblow WD. Carbohydrate in the mouth immediately facilitates motor output. *Brain Res* 1350: 151–158, 2010.

De Gennaro L, Ferrara M, Bertini M, Pauri F, Cristiani R, Curcio G, Romei V, Fratello F, Rossini PM. Reproducibility of callosal effects of transcranial magnetic stimulation (TMS) with interhemispheric paired pulses. *Neurosci Res* 46: 219–227, 2003.

Gentilucci M, Toni I, Daprati E, Gangitano M. Tactile input of the hand and the control of reaching to grasp movements. *Exp Brain Res* 114: 130–137, 1997.

Gerlai R, Thibodeaux H, Palmer JT, Van Lookeren Campagne M, Van Bruggen N.

Transient focal cerebral ischemia induces sensorimotor deficits in mice. *Behav Brain Res* 108: 63–71, 2000.

Godde B, Stauffenberg B, Spengler F, Dinse HR. Tactile coactivation-induced changes in spatial discrimination performance. *J Neurosci* 20: 1597–1604, 2000.

Grundey J, Freznosa S, Klinker F, Lang N, Paulus W, Nitsche MA. Cortical excitability in smoking and not smoking individuals with and without nicotine.

Psychopharmacology (Berl) 229: 653–664, 2013.

Guerra A, López-Alonso V, Cheeran B, Suppa A. Solutions for managing variability in non-invasive brain stimulation studies. *Neurosci Lett* 719: 133332, 2020.

Guerra A, Pogosyan A, Nowak M, Tan H, Ferreri F, Di Lazzaro V, Brown P. Phase Dependency of the Human Primary Motor Cortex and Cholinergic Inhibition Cancellation during Beta tACS. *Cereb Cortex* 26: 3977–3990, 2016.

Hallett M. Transcranial Magnetic Stimulation: A Primer. *Neuron* 55: 187–199, 2007.

Hamdy S, Rothwell JC, Aziz Q, Singh KD, Thompson DG. Long-term reorganization of human motor cortex driven by short-term sensory stimulation. *Nat Neurosci* 1: 64–68, 1998.

Hammond G, Faulkner D, Byrnes M, Mastaglia F, Thickbroom G. Transcranial magnetic stimulation reveals asymmetrical efficacy of intracortical circuits in primary motor cortex. *Exp Brain Res* 155: 19–23, 2004.

Hampel H, Mesulam MM, Cuello AC, Farlow MR, Giacobini E, Grossberg GT, Khachaturian AS, Vergallo A, Cavedo E, Snyder PJ, Khachaturian ZS. The

cholinergic system in the pathophysiology and treatment of Alzheimer's disease. *Brain* 141: 1917–1933, 2018.

Hari R, Reinikainen K, Kaukoranta E, Hämäläinen M, Ilmoniemi R, Penttinen A, Salminen J, Teszner D. Somatosensory evoked cerebral magnetic fields from SI and SII in man. *Electroencephalogr Clin Neurophysiol* 57: 254–263, 1984.

Harrison TC, Silasi G, Boyd JD, Murphy TH. Displacement of sensory maps and disorganization of motor cortex after targeted stroke in mice. *Stroke* 44: 2300–2306, 2013.

Hasanzadeh P, Oveisgharan S, Sedighi N, Nafissi S. Effect of skin thickness on sensory nerve action potential amplitude. *Clin Neurophysiol* 119: 1824–1828, 2008.

Hawker GA, Mian S, Kendzerska T, French M. Measures of adult pain: Visual Analog Scale for Pain (VAS Pain), Numeric Rating Scale for Pain (NRS Pain), McGill Pain Questionnaire (MPQ), Short-Form McGill Pain Questionnaire (SF-MPQ), Chronic Pain Grade Scale (CPGS), Short Form-36 Bodily Pain Scale (SF. *Arthritis Care Res* 63, 2011.

Hayashi R, Ogata K, Nakazono H, Tobimatsu S. Modified ischaemic nerve block of the forearm: use for the induction of cortical plasticity in distal hand muscles. *J Physiol* 597: 3457–3471, 2019.

He H, Luo C, Chang X, Shan Y, Cao W, Gong J, Klugah-Brown B, Bobes MA, Biswal B, Yao D. The functional integration in the sensory-motor system predicts aging in healthy older adults. *Front Aging Neurosci* 8, 2017.

Helmich RCG, Bäumer T, Siebner HR, Bloem BR, Münchau A. Hemispheric asymmetry and somatotopy of afferent inhibition in healthy humans. *Exp Brain Res* 167:

211–219, 2005.

Helmstaedter M, Staiger JF, Sakmann B, Feldmeyer D. Efficient recruitment of layer 2/3 interneurons by layer 4 input in single columns of rat somatosensory cortex. *J Neurosci* 28: 8273–8284, 2008.

Hennings K, Arendt-Nielsen L, Christensen SS, Andersen OK. Selective activation of small-diameter motor fibres using exponentially rising waveforms: A theoretical study. *Med Biol Eng Comput* 43: 493–500, 2005.

Hikosaka O, Tanaka M, Sakamoto M, Iwamura Y. Deficits in manipulative behaviors induced by local injections of muscimol in the first somatosensory cortex of the conscious monkey. *Brain Res* 325: 375–380, 1985.

Hodzic A, Veit R, Karim AA, Erb M, Godde B. Improvement and Decline in Tactile Discrimination Behavior after Cortical Plasticity Induced by Passive Tactile Coactivation. *J Neurosci* 24: 442–446, 2004.

Höffken O, Veit M, Knossalla F, Lissek S, Bliem B, Ragert P, Dinse HR, Tegenthoff M. Sustained increase of somatosensory cortex excitability by tactile coactivation studied by paired median nerve stimulation in humans correlates with perceptual gain. *J Physiol* 584: 463–71, 2007.

Hooks BM, Mao T, Gutnisky DA, Yamawaki N, Svoboda K, Shepherd GMG. Organization of cortical and thalamic input to pyramidal neurons in mouse motor cortex. *J Neurosci* 33: 748–760, 2013.

Hope C, Seiss E, Dean PJA, Williams KEM, Sterr A. Consumption of glucose drinks slows sensorimotor processing: Double-blind placebo-controlled studies with the Eriksen

flanker task. *Front Hum Neurosci* 7: 651, 2013.

Hopkins WG. Measures of reliability in sports medicine and science. *Sport. Med.* 30: 1–15, 2000.

Hosp JA, Molina-Luna K, Hertler B, Atiemo CO, Luft AR. Dopaminergic Modulation of Motor Maps in Rat Motor Cortex: An In Vivo Study. *Neuroscience* 159: 692–700, 2009.

Hu X, Gu X. Inverse Association between Physical Activity and Blood Glucose Is Independent of Sex, Menopause, and Family History of Diabetes. *Diabetes* 68: 730-P, 2019.

Huffman KJ, Krubitzer L. Thalamo-cortical connections of areas 3a and M1 in marmoset monkeys. *J Comp Neurol* 435: 291–310, 2001.

Huttunen J, Pekkonen E, Kivisaari R, Autti T, Kähkönen S. Modulation of somatosensory evoked fields from SI and SII by acute GABAA-agonism and paired-pulse stimulation. *Neuroimage* 40: 427–434, 2008.

Ikuta T, Furuta N. Sex differences in the human group mean SEP. *Electroencephalogr Clin Neurophysiol* 54: 449–457, 1982.

Ilić T V., Korchounov A, Ziemann U. Methylphenidate facilitates and disinhibits the motor cortex in intact humans. *Neuroreport* 14: 773–776, 2003.

Irlbacher K, Meyer BU, Voss M, Brandt SA, Rörich S. Spatial reorganization of cortical motor output maps of stump muscles in human upper-limb amputees. *Neurosci Lett* 321: 129–132, 2002.

Izraeli R, Porter LL. Vibrissal motor cortex in the rat: connections with the barrel field.

Exp Brain Res 104: 41–54, 1995.

Jacobs K, Donoghue J. Reshaping the cortical motor map by unmasking latent intracortical connections. *Science (80-)* 251: 944–7, 1991.

Jacobs MF, Tsang P, Lee KGH, Asmussen MJ, Zapallow CM, Nelson AJ. 30 Hz theta-burst stimulation over primary somatosensory cortex modulates corticospinal output to the hand. *Brain Stimul* 7: 269–274, 2014.

Jarrett RJ, Graver HJ. Changes in Oral Glucose Tolerance During the Menstrual Cycle. *Br Med J* 2: 528–529, 1968.

Johnson KO. The roles and functions of cutaneous mechanoreceptors. *Curr Opin Neurobiol* 11: 455–461, 2001.

Jones EG. Gabaergic neurons and their role in cortical plasticity in primates. *Cereb Cortex* 3: 361–372, 1993.

Jones EG, Powell TPS. Connexions of the somatic sensory cortex of the rhesus monkey: I. Ipsilateral cortical connexions. *Brain* 92: 477–502, 1969.

Kaas JH. The organization of somatosensory cortex in primates and other mammals. London: Macmillan Press, 1984.

Kakigi R, Shibasaki H. Effects of age, gender, and stimulus side on the scalp topography of somatosensory evoked potentials following posterior tibial nerve stimulation. *J Clin Neurophysiol* 9: 431–40, 1992.

Kambi N, Tandon S, Mohammed H, Lazar L, Jain N. Reorganization of the primary motor cortex of adult macaque monkeys after sensory loss resulting from partial spinal cord injuries. *J Neurosci* 31: 3696–3707, 2011.

Kami A, Meyer G, Jezzard P, Adams MM, Turner R, Ungerleider LG. Functional MRI evidence for adult motor cortex plasticity during motor skill learning. *Nature* 377: 155–158, 1995.

van der Kamp W, Zwinderman a H, Ferrari MD, van Dijk JG. Cortical excitability and response variability of transcranial magnetic stimulation. *J Clin Neurophysiol* 13: 164–171, 1996.

Kandel ER, Schwartz JH, Jessell TM, Siegelbaum SA, Hudspeth AJ. *Principles of Neural Science (5th ed.)*. New York: 2007.

Kaneko T, Caria MA, Asanuma H. Information processing within the motor cortex. II. Intracortical connections between neurons receiving somatosensory cortical input and motor output neurons of the cortex. *J Comp Neurol* 345: 172–184, 1994.

Kaňovský P, Bareš M, Rektor I. The selective gating of the N30 cortical component of the somatosensory evoked potentials of median nerve is different in the mesial and dorsolateral frontal cortex: Evidence from intracerebral recordings. *Clin Neurophysiol* 114: 981–991, 2003.

Kaplan RJ, Greenwood CE, Winocur G, Wolever TMS. Cognitive performance is associated with glucose regulation in healthy elderly persons and can be enhanced with glucose and dietary carbohydrates. *Am J Clin Nutr* 72: 825–836, 2000.

Kapogiannis D, Mattson MP. Disrupted energy metabolism and neuronal circuit dysfunction in cognitive impairment and Alzheimer’s disease. *Lancet Neurol.* 10: 187–198, 2011.

Karni A, Meyer G, Rey-Hipolito C, Jezzard P, Adams MM, Turner R, Ungerleider

LG. The acquisition of skilled motor performance: Fast and slow experience-driven changes in primary motor cortex. *Proc Natl Acad Sci U S A* 95: 861–868, 1998.

Kaukoranta E, Hämäläinen M, Sarvas J, Hari R. Mixed and sensory nerve stimulations activate different cytoarchitectonic areas in the human primary somatosensory cortex SI - Neuromagnetic recordings and statistical considerations. *Exp Brain Res* 63: 60–66, 1986.

Keller A, Iriki A, Asanuma H. Identification of neurons producing long-term potentiation in the cat motor cortex: Intracellular recordings and labeling. *J Comp Neurol* 300: 47–60, 1990.

Keller A, Weintraub ND, Miyashita E. Tactile experience determines the organization of movement representations in rat motor cortex. *Neuroreport* 7: 2373–2378, 1996.

Khaslavskaja S, Ladouceur M, Sinkjaer T. Increase in tibialis anterior motor cortex excitability following repetitive electrical stimulation of the common peroneal nerve. *Exp Brain Res* 145: 309–315, 2002.

Kiers L, Cros D, Chiappa KH, Fang J. Variability of motor potentials evoked by transcranial magnetic stimulation. *Electroencephalogr Clin Neurophysiol Evoked Potentials* 89: 415–423, 1993.

Kleim JA, Barbay S, Nudo RJ. Functional reorganization of the rat motor cortex following motor skill learning. *J Neurophysiol* 80: 3321–3325, 1998.

Kleim JA, Boychuk JA, Adkins DAL. Rat models of upper extremity impairment in stroke. *ILAR J* 48: 374–384, 2007.

Kojima S, Miyaguchi S, Sasaki R, Tsuiki S, Saito K, Inukai Y, Otsuru N, Onishi H.

The effects of mechanical tactile stimulation on corticospinal excitability and motor function depend on pin protrusion patterns. *Sci Rep* 9, 2019.

Kojima S, Onishi H, Miyaguchi S, Kotan S, Sasaki R, Nakagawa M, Kirimoto H, Tamaki H. Modulation of corticospinal excitability depends on the pattern of mechanical tactile stimulation. *Neural Plast* 2018, 2018.

Koo TK, Li MY. A Guideline of Selecting and Reporting Intraclass Correlation Coefficients for Reliability Research. *J Chiropr Med* 15: 155–163, 2016.

Korvenoja A, Huttunen J, Salli E, Pohjonen H, Martinkauppi S, Palva JM, Lauronen L, Virtanen J, Ilmoniemi RJ, Aronen HJ. Activation of multiple cortical areas in response to somatosensory stimulation: Combined magnetoencephalographic and functional magnetic resonance imaging. *Hum Brain Mapp* 8: 13–27, 1999.

Krubitzer LA, Kaas JH. The organization and connections of somatosensory cortex in marmosets. *J Neurosci* 10: 952–74, 1990.

Kukaswadia S, Wagle-Shukla A, Morgante F, Gunraj C, Chen R. Interactions between long latency afferent inhibition and interhemispheric inhibitions in the human motor cortex. *J Physiol* 563: 915–924, 2005.

Kundu S, Achar S. Principles of office anesthesia: Part II. Topical anesthesia. *Am Fam Physician* 66: 99–102, 2002.

Kuo H-I, Paulus W, Batsikadze G, Jamil A, Kuo M-F, Nitsche MA. Acute and chronic noradrenergic effects on cortical excitability in healthy humans. *Int J Neuropsychopharmacol* , 2017. doi:10.1093/ijnp/pyx026.

Kyriakopoulos AA, Greenblatt DJ, Shader RI. Clinical pharmacokinetics of

lorazepam: A review. *J Clin Psychiatry* 39: 16–23, 1978.

Lang N, Hasan A, Sueske E, Paulus W, Nitsche MA. Cortical Hypoexcitability in Chronic Smokers? A Transcranial Magnetic Stimulation Study.

Neuropsychopharmacology 33: 2517–2523, 2008.

Lapole T, Tindel J. Acute effects of muscle vibration on sensorimotor integration.

Neurosci Lett 587: 46–50, 2015.

Di Lazzaro V, Oliviero A, Meglio M, Cioni B, Tamburrini G, Tonali P, Rothwell J.

Direct demonstration of the effect of lorazepam on the excitability of the human motor cortex. *Clin Neurophysiol* 111: 794–799, 2000a.

Di Lazzaro V, Oliviero A, Pilato F, Saturno E, Dileone M, Marra C, Daniele A,

Ghirlanda S, Gainotti G, Tonali PA. Motor cortex hyperexcitability to transcranial magnetic stimulation in Alzheimer's disease. *J Neurol Neurosurg Psychiatry* 75: 555–9, 2004.

Di Lazzaro V, Oliviero A, Profice P, Pennisi M, Di Giovanni S, Zito G, Tonali P,

Rothwell J. Muscarinic receptor blockade has differential effects on the excitability of intracortical circuits in the human motor cortex. *Exp Brain Res* 135: 455–461, 2000b.

Di Lazzaro V, Oliviero A, Profice P, Pennisi MA, Pilato F, Zito G, Dileone M,

Nicoletti R, Pasqualetti P, Tonali PA. Ketamine increases human motor cortex excitability to transcranial magnetic stimulation. *J Physiol* 547: 485–496, 2003.

Di Lazzaro V, Oliviero A, Saturno E, Dileone M, Pilato F, Nardone R, Ranieri F,

Musumeci G, Fiorilla T, Tonali P. Effects of lorazepam on short latency afferent inhibition and short latency intracortical inhibition in humans. *J Physiol* 564: 661–668,

2005a.

Di Lazzaro V, Oliviero A, Tonali P, Marra C, Daniele A, Profice P, Saturno E, Pilato F, Masullo C, Rothwell JC. Noninvasive in vivo assessment of cholinergic cortical circuits in AD using transcranial magnetic stimulation. *Neurology* 59: 392–7, 2002.

Di Lazzaro V, Pilato F, Dileone M, Profice P, Marra C, Ranieri F, Quaranta D, Gainotti G, Tonali PA. In vivo functional evaluation of central cholinergic circuits in vascular dementia. *Clin Neurophysiol* 119: 2494–2500, 2008.

Di Lazzaro V, Pilato F, Dileone M, Profice P, Ranieri F, Ricci V, Bria P, Tonali P, Ziemann U. Segregating two inhibitory circuits in human motor cortex at the level of GABAA receptor subtypes: A TMS study. *Clin Neurophysiol* 118: 2207–2214, 2007a.

Di Lazzaro V, Pilato F, Dileone M, Saturno E, Oliviero A, Marra C, Daniele A, Ranieri F, Gainotti G, Tonali P. In vivo cholinergic circuit evaluation in frontotemporal and Alzheimer dementias. *Neurology* 66: 1111–1113, 2006.

Di Lazzaro V, Pilato F, Dileone M, Saturno E, Profice P, Marra C, Daniele A, Ranieri F, Quaranta D, Gainotti G, Tonali P. Functional evaluation of cerebral cortex in dementia with Lewy bodies. *Neuroimage* 37: 422–429, 2007b.

Di Lazzaro V, Pilato F, Dileone M, Tonali P, Ziemann U. Dissociated effects of diazepam and lorazepam on short-latency afferent inhibition. *J Physiol* 569: 315–323, 2005b.

Di Lazzaro V, Pilato F, Saturno E, Oliviero A, Dileone M, Mazzone P, Insola A, Tonali P a, Ranieri F, Huang Y-Z, Rothwell JC. Theta-burst repetitive transcranial magnetic stimulation suppresses specific excitatory circuits in the human motor cortex. *J*

Physiol 565: 945–50, 2005c.

Di Lazzaro V, Profice P, Pilato F, Capone F, Ranieri F, Florio L, Colosimo C, Pravatà E, Pasqualetti P, Dileone M. The level of cortical afferent inhibition in acute stroke correlates with long-term functional recovery in humans. *Stroke* 43: 250–252, 2012a.

Di Lazzaro V, Profice P, Ranieri F, Capone F, Dileone M, Oliviero A, Pilato F. I-wave origin and modulation. *Brain Stimul* 5: 512–525, 2012b.

Di Lazzaro V, Ziemann U. The contribution of transcranial magnetic stimulation in the functional evaluation of microcircuits in human motor cortex. *Front Neural Circuits* 7: 18, 2013.

Lesemann FHP, Reuter EM, Godde B. Tactile stimulation interventions: Influence of stimulation parameters on sensorimotor behavior and neurophysiological correlates in healthy and clinical samples. *Neurosci. Biobehav. Rev.* 51: 126–137, 2015.

Levy LM, Ziemann U, Chen R, Cohen LG. Rapid modulation of GABA in sensorimotor cortex induced by acute deafferentation. *Ann Neurol* 52: 755–761, 2002.

Lim Y, Ham J, Lee AS, Oh E. Gait Disturbance Associated with Cholinergic Dysfunction in Early Parkinson's Disease. *J Alzheimer's Dis Park* 7: 363, 2017.

Di Lorenzo F, Martorana A, Ponzio V, Bonni S, D'Angelo E, Caltagirone C, Koch G. Cerebellar theta burst stimulation modulates short latency afferent inhibition in Alzheimer's disease patients. *Front Aging Neurosci* 5, 2013.

Lulic T, El-Sayes J, Fassett HJ, Nelson AJ. Physical activity levels determine exercise-induced changes in brain excitability. *PLoS One* 12: e0173672, 2017.

Maeda F, Gangitano M, Thall M, Pascual-Leone A. Inter-and intra-individual variability of paired-pulse curves with transcranial magnetic stimulation (TMS). *Clin Neurophysiol* 113: 376–382, 2002.

Mang CS, Bergquist AJ, Roshko SM, Collins DF. Loss of short-latency afferent inhibition and emergence of afferent facilitation following neuromuscular electrical stimulation. *Neurosci Lett* 529: 80–85, 2012.

Mao T, Kusefoglou D, Hooks BM, Huber D, Petreanu L, Svoboda K. Long-Range Neuronal Circuits Underlying the Interaction between Sensory and Motor Cortex. *Neuron* 72: 111–123, 2011.

Marconi B, Filippi GM, Koch G, Giacobbe V, Pecchioli C, Versace V, Camerota F, Saraceni VM, Caltagirone C. Long-term effects on cortical excitability and motor recovery induced by repeated muscle vibration in chronic stroke patients. *Neurorehabil Neural Repair* 25: 48–60, 2011.

Markram H, Toledo-Rodriguez M, Wang Y, Gupta A, Silberberg G, Wu C. Interneurons of the neocortical inhibitory system. *Nat Rev Neurosci* 5: 793–807, 2004.

Marra C, Quaranta D, Profice P, Pilato F, Capone F, Iodice F, Di Lazzaro V, Gainotti G. Central cholinergic dysfunction measured “in vivo” correlates with different behavioral disorders in Alzheimer’s disease and dementia with Lewy body. *Brain Stimul* 5: 533–538, 2012.

Martorana A, Mori F, Esposito Z, Kusayanagi H, Monteleone F, Codecà C, Sancesario G, Bernardi G, Koch G. Dopamine Modulates Cholinergic Cortical Excitability in Alzheimer’s Disease Patients. *Neuropsychopharmacology* 34: 2323–2328,

2009.

McCormick DA. GABA as an inhibitory neurotransmitter in human cerebral cortex. *J Neurophysiol* 62: 1018–1027, 1989.

McDonnell MN, Orekhov Y, Ziemann U. The role of GABAB receptors in intracortical inhibition in the human motor cortex. *Exp Brain Res* 173: 86–93, 2006.

McDonnell MN, Orekhov Y, Ziemann U. Suppression of LTP-like plasticity in human motor cortex by the GABA B receptor agonist baclofen. *Exp Brain Res* 180: 181–186, 2007.

McKay D, Brooker R, Giacomini P, Ridding M, Miles T. Time course of induction of increased human motor cortex excitability by nerve stimulation. *Neuroreport* 13: 1271–1273, 2002.

McNulty PA, Macefield VG, Taylor JL, Hallett M. Cortically evoked neural volleys to the human hand are increased during ischaemic block of the forearm. *J Physiol* 538: 279–288, 2002.

Mercier C, Dubois JD, Poitras I, Voisin JIA. Effect of pain on deafferentation-induced modulation of somatosensory evoked potentials. *PLoS One* 13, 2018.

Mergenthaler P, Lindauer U, Dienel GA, Meisel A. Sugar for the brain: The role of glucose in physiological and pathological brain function. *Trends Neurosci* 36: 587–597, 2013.

Metherate R, Ashe JH. Synaptic interactions involving acetylcholine, glutamate, and GABA in rat auditory cortex. *Exp Brain Res* 107: 59–72, 1995.

Mimura Y, Nishida H, Nakajima S, Tsugawa S, Morita S, Yoshida K, Tarumi R,

Ogyu KO, Wada M, Kurose S, Myazaki T, Blumberger DM, Daskalakis ZJ, Chen R, Mimura M, Noda Y. Neurophysiological biomarkers using transcranial magnetic stimulation in Alzheimer's disease and mild cognitive impairment: A systematic review and meta-analysis. *Neurosci Biobehav Rev* S0149-7634, 2020.

Mineo L, Concerto C, Patel D, Mayorga T, Chusid E, Infortuna C, Aguglia E, Sarraf Y, Battaglia F. Modulation of sensorimotor circuits during retrieval of negative Autobiographical Memories: Exploring the impact of personality dimensions. *Neuropsychologia* 110: 190–196, 2018.

Möhler H. A New Benzodiazepine Pharmacology. *J Pharmacol Exp Ther* 300: 2–8, 2002.

Möhler H, Fritschy J-M, Crestani F, Hensch T, Rudolph U. Specific GABA(A) circuits in brain development and therapy. *Biochem Pharmacol* 68: 1685–90, 2004.

Molnár Z, Cheung AFP. Towards the classification of subpopulations of layer V pyramidal projection neurons. *Neurosci Res* 55: 105–115, 2006.

Morgante F, Naro A, Terranova C, Russo M, Rizzo V, Risitano G, Girlanda P, Quartarone A. Normal sensorimotor plasticity in complex regional pain syndrome with fixed posture of the hand. *Mov Disord* 32: 149–157, 2017.

Mountcastle VB. Modality and topographic properties of single neurons of cat's somatic sensory cortex. *J Neurophysiol* 20: 408–434, 1957.

Mountcastle VB. The columnar organization of the neocortex. *Brain* 120: 701–722, 1997.

Müller-Dahlhaus JFM, Liu Y, Ziemann U. Inhibitory circuits and the nature of their

interactions in the human motor cortex a pharmacological TMS study. *J Physiol* 586: 495–514, 2008.

Murphy BA, Taylor HH, Wilson SA, Knight JA, Mathers KM, Schug S. Changes in median nerve somatosensory transmission and motor output following transient deafferentation of the radial nerve in humans. *Clin Neurophysiol* 114: 1477–1488, 2003.

Nardone R, Bergmann J, Brigo F, Christova M, Kunz A, Seidl M, Tezzon F, Trinkka E, Golaszewski S. Functional evaluation of central cholinergic circuits in patients with Parkinson's disease and REM sleep behavior disorder: A TMS study. *J Neural Transm* 120: 413–422, 2013.

Nardone R, Bergmann J, Christova M, Caleri F, Tezzon F, Ladurner G, Trinkka E, Golaszewski S. Short latency afferent inhibition differs among the subtypes of mild cognitive impairment. *J Neural Transm* 119: 463–471, 2012a.

Nardone R, Bergmann J, Kronbichler M, Kunz A, Klein S, Caleri F, Tezzon F, Ladurner G, Golaszewski S. Abnormal short latency afferent inhibition in early Alzheimer's disease: A transcranial magnetic demonstration. *J Neural Transm* 115: 1557–1562, 2008a.

Nardone R, Bergmann J, Kunz A, Christova M, Brigo F, Tezzon F, Trinkka E, Golaszewski S. Cortical afferent inhibition is reduced in patients with idiopathic REM sleep behavior disorder and cognitive impairment: A TMS study. *Sleep Med* 13: 919–925, 2012b.

Nardone R, Bergmann J, Tezzon F, Ladurner G, Golaszewski S. Cholinergic dysfunction in subcortical ischaemic vascular dementia: A transcranial magnetic

stimulation study. *J Neural Transm* 115: 737–743, 2008b.

Nardone R, De Blasi P, Seidl M, Höller Y, Caleri F, Tezzon F, Ladurner G, Golaszewski S, Trinka E. Cognitive function and cholinergic transmission in patients with subcortical vascular dementia and microbleeds: A TMS study. *J Neural Transm* 118: 1349–1358, 2011.

Nardone R, Bratti A, Tezzon F. Motor cortex inhibitory circuits in dementia with Lewy bodies and in Alzheimer's disease. *J Neural Transm* 113: 1679–1684, 2006.

Nardone R, Golaszewski S, Schwenker K, Brigo F, Maccarrone M, Versace V, Sebastianelli L, Saltuari L, Höller Y. Cholinergic transmission is impaired in patients with idiopathic normal-pressure hydrocephalus: a TMS study. *J Neural Transm* 126: 1073–1080, 2019.

Ni Z, Charab S, Gunraj C, Nelson AJ, Udupa K, Yeh I-J, Chen R. Transcranial magnetic stimulation in different current directions activates separate cortical circuits. *J Neurophysiol* 105: 749–756, 2011.

Nudo RJ, Milliken GW, Jenkins WM, Merzenich MM. Use-dependent alterations of movement representations in primary motor cortex of adult squirrel monkeys. *J Neurosci* 16: 785–807, 1996.

Oldfield RC. The assessment and analysis of handedness: The Edinburgh inventory. *Neuropsychologia* 9: 97–113, 1971.

Oliviero A, Molina León A, Holler I, Florensa Vila J, Siebner HR, Della Marca G, Di Lazzaro V, Tejeira Álvarez J. Reduced sensorimotor inhibition in the ipsilesional motor cortex in a patient with chronic stroke of the paramedian thalamus. *Clin*

Neurophysiol 116: 2592–2598, 2005.

Opie GM, Ridding MC, Semmler JG. Age-related differences in pre- and post-synaptic motor cortex inhibition are task dependent. *Brain Stimul* 8: 926–936, 2015.

Orth M, Snijders AH, Rothwell JC. The variability of intracortical inhibition and facilitation. *Clin Neurophysiol* 114: 2362–2369, 2003.

Otsuka T, Kawaguchi Y. Firing-pattern-dependent specificity of cortical excitatory feed-forward subnetworks. *J Neurosci* 28: 11186–11195, 2008.

Otsuka T, Kawaguchi Y. Cortical inhibitory cell types differentially form intralaminar and interlaminar subnetworks with excitatory neurons. *J Neurosci* 29: 10533–10540, 2009.

Padovani A, Benussi A, Cantoni V, Dell’Era V, Cotelli MS, Caratozzolo S, Turrone R, Rozzini L, Alberici A, Altomare D, Depari A, Flammini A, Frisoni GB, Borroni B. Diagnosis of mild cognitive impairment due to Alzheimer’s disease with transcranial magnetic stimulation. *J Alzheimer’s Dis* 65: 221–230, 2018.

Pascual-Leone A, Cammarota A, Wassermann EM, Brasil NJ, Cohen LG, Hallett M, Pascual LA, Cammarota A, Wassermann EM, Brasil NJ, Cohen LG, Hallett M. Modulation of motor cortical outputs to the reading hand of braille readers. *Ann Neurol* 34: 33–37, 1993.

Pavlidis C, Miyashita E, Asanuma H. Projection from the sensory to the motor cortex is important in learning motor skills in the monkey. *J Neurophysiol* 70: 733–741, 1993.

Pelosin E, Ogliastro C, Lagravinese G, Bonassi G, Mirelman A, Hausdorff JM, Abbruzzese G, Avanzino L. Attentional control of gait and falls: Is cholinergic

dysfunction a common substrate in the elderly and Parkinson's disease? *Front Aging Neurosci* 8: 104, 2016.

Penfield W, Boldrey E. Somatic motor and sensory representation in the cerebral cortex of man as studied by electrical stimulation. *Brain* 60: 389–443, 1937.

Petoe MA, Molina Jaque FA, Byblow WD, Stinear CM. Cutaneous anesthesia of the forearm enhances sensorimotor function of the hand. *J Neurophysiol* 109: 1091–1096, 2013.

Pleger B, Dinse HR, Ragert P, Schwenkreis P, Malin JP, Tegenthoff M. Shifts in cortical representations predict human discrimination improvement. *Proc Natl Acad Sci U S A* 98: 12255–60, 2001.

Pleger B, Foerster AF, Ragert P, Dinse HR, Schwenkreis P, Malin JP, Nicolas V, Tegenthoff M. Functional imaging of perceptual learning in human primary and secondary somatosensory cortex. *Neuron* 40: 643–653, 2003.

Portney LG, Watkins MP. Foundations of Clinical Research: Applications to Practice. 2009.

Rabin E, Gordon AM. Tactile feedback contributes to consistency of finger movements during typing. *Exp Brain Res* 155: 362–369, 2004.

Ragert P, Kalisch T, Bliem B, Franzkowiak S, Dinse HR. Differential effects of tactile high- and low-frequency stimulation on tactile discrimination in human subjects. *BMC Neurosci* 9, 2008.

Rani YS. Comparative Study of Variations in Blood Glucose Concentration in Different Phases of Menstrual Cycle in Young Healthy Women Aged 18-22 Years. *IOSR J Dent*

Med Sci 9: 09–11, 2013.

Rathelot JA, Strick PL. Muscle representation in the macaque motor cortex: An anatomical perspective. *Proc Natl Acad Sci U S A* 103: 8257–8262, 2006.

Rebello T, Hodges RE, Smith JL. Short-term effects of various sugars on antinatriuresis and blood pressure changes in normotensive young men. *Am J Clin Nutr* 38: 84–94, 1983.

Riby LM. The impact of age and task domain on cognitive performance: A meta-analytic review of the glucose facilitation effect. *Brain Impair* 5: 145–165, 2004.

Richardson SP, Bliem B, Lomarev M, Shamim E, Dang N, Hallett M. Changes in short afferent inhibition during phasic movement in focal dystonia. *Muscle and Nerve* 37: 358–363, 2008.

Richardson SP, Bliem B, Voller B, Dang N, Hallett M. Long-latency afferent inhibition during phasic finger movement in focal hand dystonia. *Exp Brain Res* 193: 173–179, 2009.

Ridding MC, Brouwer B, Miles TS, Pitcher JB, Thompson PD. Changes in muscle responses to stimulation of the motor cortex induced by peripheral nerve stimulation in human subjects. *Exp Brain Res* 131: 135–143, 2000.

Ridding MC, McKay DR, Thompson PD, Miles TS. Changes in corticomotor representations induced by prolonged peripheral nerve stimulation in humans. *Clin Neurophysiol* 112: 1461–1469, 2001.

Ridding MC, Rothwell JC. Reorganisation in human motor cortex. *Can J Physiol Pharmacol* 73: 218–222, 1995.

Ridding MC, Rothwell JC. Stimulus/response curves as a method of measuring motor

cortical excitability in man. *Electroencephalogr Clin Neurophysiol - Electromyogr Mot Control* 105: 340–344, 1997.

Rocchi L, Erro R, Antelmi E, Berardelli A, Tinazzi M, Liguori R, Bhatia K, Rothwell J. High frequency somatosensory stimulation increases sensori-motor inhibition and leads to perceptual improvement in healthy subjects. *Clin Neurophysiol* 128: 1015–1025, 2017.

Rocco-Donovan M, Ramos RL, Giraldo S, Brumberg JC. Characteristics of synaptic connections between rodent primary somatosensory and motor cortices. *Somatosens Mot Res* 28: 63–72, 2011.

Rochester L, Yarnall AJ, Baker MR, David R V., Lord S, Galna B, Burn DJ. Cholinergic dysfunction contributes to gait disturbance in early Parkinson's disease. *Brain* 135: 2779–2788, 2012.

Röricht S, Meyer BU, Niehaus L, Brandt SA. Long-term reorganization of motor cortex outputs after arm amputation. *Neurology* 53: 106–111, 1999.

Rosén I, Asanuma H. Peripheral afferent inputs to the forelimb area of the monkey motor cortex: Input-output relations. *Exp Brain Res* 14: 257–273, 1972.

Rosenkranz K, Pesenti A, Paulus W, Tergau F. Focal reduction of intracortical inhibition in the motor cortex by selective proprioceptive stimulation. *Exp Brain Res* 149: 9–16, 2003.

Rosenkranz K, Rothwell JC. Differential effect of muscle vibration on intracortical inhibitory circuits in humans. *J Physiol* 551: 649–660, 2003.

Rossi S, Hallett M, Rossini PM, Pascual-Leone A*, Group TS of TMS. Safety,

ethical considerations, and application guidelines for the use of transcranial magnetic stimulation in clinical practice and research. *Clinical Neurophysiol* 120: 2008–2039, 2009.

Rossi S, Della Volpe R, Ginanneschi F, Olivelli M, Bartalini S, Spidalieri R, Rossi A. Early somatosensory processing during tonic muscle pain in humans: Relation to loss of proprioception and motor “defensive” strategies. *Clin Neurophysiol* 114: 1351–1358, 2003.

Rossini PM, Burke D, Chen R, Cohen LG, Daskalakis Z, Di Iorio R, Di Lazzaro V, Ferreri F, Fitzgerald PB, George MS, Hallett M, Lefaucheur JP, Langguth B, Matsumoto H, Miniussi C, Nitsche MA, Pascual-Leone A, Paulus W, Rossi S, Rothwell JC, Siebner HR, Ugawa Y, Walsh V, Ziemann U. Non-invasive electrical and magnetic stimulation of the brain, spinal cord, roots and peripheral nerves: Basic principles and procedures for routine clinical and research application: An updated report from an I.F.C.N. Committee. *Clin Neurophysiol* 126: 1071–1107, 2015.

Rossini PM, Martino G, Narici L, Pasquarelli A, Peresson M, Pizzella V, Tecchio F, Torrioli G, Romani GL. Short-term brain “plasticity” in humans: transient finger representation changes in sensory cortex somatotopy following ischemic anesthesia. *Brain Res* 642: 169–177, 1994.

Rudy B, Fishell G, Lee SH, Hjerling-Leffler J. Three groups of interneurons account for nearly 100% of neocortical GABAergic neurons. *Dev Neurobiol* 71: 45–61, 2011.

Van De Ruit M, Perenboom MJL, Grey MJ. TMS brain mapping in less than two minutes. *Brain Stimul* 8: 231–239, 2015.

Sailer A, Cunic D, Paradiso G, Gunraj C, Wagle-Shukla A, Moro E, Lozano A,

Lang A, Chen R. Subthalamic nucleus stimulation modulates afferent inhibition in Parkinson disease. *Neurology* 68: 356–363, 2007.

Sailer A, Molnar GF, Cunic DI, Chen R. Effects of peripheral sensory input on cortical inhibition in humans. *J Physiol* 544: 617–629, 2002.

Sailer A, Molnar GF, Paradiso G, Gunraj CA, Lang AE, Chen R. Short and long latency afferent inhibition in Parkinson's disease. *Brain* 126: 1883–94, 2003.

Sakuma K, Murakami T, Nakashima K. Short latency afferent inhibition is not impaired in mild cognitive impairment. *Clin Neurophysiol* 118: 1460–1463, 2007.

Sale M V., Ridding MC, Nordstrom MA. Cortisol inhibits neuroplasticity induction in human motor cortex. *J Neurosci* 28: 8285–8293, 2008.

Samusyte G, Bostock H, Rothwell J, Koltzenburg M. Short-interval intracortical inhibition: Comparison between conventional and threshold-tracking techniques. *Brain Stimul* , 2018. doi:10.1016/j.brs.2018.03.002.

Sanacora G, Mason GF, Rothman DL, Behar KL, Hyder F, Petroff OA, Berman RM, Charney DS, Krystal JH. Reduced cortical gamma-aminobutyric acid levels in depressed patients determined by proton magnetic resonance spectroscopy. *Arch Gen Psychiatry* 56: 1043–1047, 1999.

Sanes JN, Suner S, Donoghue JP. Dynamic organization of primary motor cortex output to target muscles in adult rats I. Long-term patterns of reorganization following motor or mixed peripheral nerve lesions. *Exp Brain Res* 79: 479–491, 1990.

Schambra HM, Ogden RT, Martínez-Hernández IE, Lin X, Chang YB, Rahman A, Edwards DJ, Krakauer JW. The reliability of repeated TMS measures in older adults

and in patients with subacute and chronic stroke. *Front Cell Neurosci* 9: 335, 2015.

Schwenkreis P, Witscher K, Janssen F, Pleger B, Dertwinkel R, Zenz M, Malin JP, Tegenthoff M. Assessment of reorganization in the sensorimotor cortex after upper limb amputation. *Clin Neurophysiol* 112: 627–635, 2001.

Sehle A, Büsching I, Vogt E, Liepert J. Temporary deafferentation evoked by cutaneous anesthesia: behavioral and electrophysiological findings in healthy subjects. *J Neural Transm* 123: 473–480, 2016.

Sens E, Teschner U, Meissner W, Preul C, Huonker R, Witte OW, Miltner WHR, Weiss Prof. T. Effects of temporary functional deafferentation on the brain, sensation, and behavior of stroke patients. *J Neurosci* 32: 11773–11779, 2012.

Shestov AA, Emir UE, Kumar A, Henry PG, Seaquist ER, Öz G. Simultaneous measurement of glucose transport and utilization in the human brain. *Am J Physiol - Endocrinol Metab* 301, 2011.

Shibuya K, Park SB, Geevasinga N, Huynh W, Simon NG, Menon P, Howells J, Vucic S, Kiernan MC. Threshold tracking transcranial magnetic stimulation: Effects of age and gender on motor cortical function. *Clin Neurophysiol* 127: 2355–2361, 2016.

Shipp S. The importance of being agranular: A comparative account of visual and motor cortex. *Philos Trans R Soc B Biol Sci* 360: 797–814, 2005.

Siebner HR, Rothwell J. Transcranial magnetic stimulation: New insights into representational cortical plasticity. *Exp Brain Res* 148: 1–16, 2003.

Sieghart W. Structure and pharmacology of gamma-aminobutyric acidA receptor subtypes. *Pharmacol Rev* 47: 181–234, 1995.

Smith MA, Riby LM, Eekelen JAM van, Foster JK. Glucose enhancement of human memory: A comprehensive research review of the glucose memory facilitation effect. *Neurosci Biobehav Rev* 35: 770–783, 2011.

Smith MJ, Adams LF, Schmidt PJ, Rubinow DR, Wassermann EM. Effects of ovarian hormones on human cortical excitability. *Ann Neurol* 51: 599–603, 2002.

Smith MJ, Keel JC, Greenberg BD, Adams LF, Schmidt PJ, Rubinow DA, Wassermann EM. Menstrual cycle effects on cortical excitability. *Neurology* 53: 2069–2072, 1999.

Snow N, Wadden K, Chaves A, Ploughman M. Transcranial Magnetic Stimulation as a Potential Biomarker in Multiple Sclerosis: A Systematic Review with Recommendations for Future Research. *Neural Plast* 2019, 2019.

Specterman M, Bhuiya A, Kuppuswamy A, Strutton PH, Catley M, Davey NJ. The effect of an energy drink containing glucose and caffeine on human corticospinal excitability. *Physiol Behav* 83: 723–728, 2005.

Stefan K, Wycislo M, Classen J. Modulation of associative human motor cortical plasticity by attention. *J Neurophysiol* 92: 66–72, 2004.

Stephen JM, Ranken D, Best E, Adair J, Knoefel J, Kovacevic S, Padilla D, Hart B, Aine CJ. Aging changes and gender differences in response to median nerve stimulation measured with MEG. *Clin Neurophysiol* 117: 131–143, 2006.

Strauss S, Grothe M, Usichenko T, Neumann N, Byblow WD, Lotze M. Inhibition of the primary sensorimotor cortex by topical anesthesia of the forearm in patients with complex regional pain syndrome. *Pain* 156: 2556–2561, 2015.

Stude P, Lenz M, Höffken O, Tegenthoff M, Dinse H. A single dose of lorazepam reduces paired-pulse suppression of median nerve evoked somatosensory evoked potentials. *Eur J Neurosci* 43: 1156–1160, 2016.

Suzuki LY, Meehan SK. Verbal working memory modulates afferent circuits in motor cortex. *Eur J Neurosci* 48: 3117–3125, 2018.

Synowski SJ, Kop WJ, Warwick ZS, Waldstein SR. Effects of glucose ingestion on autonomic and cardiovascular measures during rest and mental challenge. *J Psychosom Res* 74: 149–154, 2013.

Tamburin S, Fiaschi A, Andreoli A, Marani S, Zanette G. Sensorimotor integration to cutaneous afferents in humans: the effect of the size of the receptive field. *Exp Brain Res* 167: 362–9, 2005.

Tamburin S, Manganotti P, Marzi CA, Fiaschi A, Zanette G. Abnormal somatotopic arrangement of sensorimotor interactions in dystonic patients. *Brain* 125: 2719–2730, 2002.

Tamburin S, Manganotti P, Zanette G, Fiaschi A. Cutaneomotor integration in human hand motor areas: Somatotopic effect and interaction of afferents. *Exp Brain Res* 141: 232–241, 2001.

Taylor JL, Todd G, Gandevia SC. Evidence for a supraspinal contribution to human muscle fatigue. *Clin Exp Pharmacol Physiol* 33: 400–405, 2006.

Teo JTH, Terranova C, Swayne O, Greenwood RJ, Rothwell JC. Differing effects of intracortical circuits on plasticity. *Exp Brain Res* 193: 555–563, 2009.

Terranova C, Sant'Angelo A, Morgante F, Rizzo V, Allegra R, Arena Maria G,

Ricciardi L, Ghilardi Maria F, Girlanda P, Quartarone A. Impairment of sensory-motor plasticity in mild Alzheimer's disease. *Brain Stimul* 6: 62–66, 2013.

Thickbroom GW, Byrnes ML, Walters S, Stell R, Mastaglia FL. Motor cortex reorganisation in Parkinson's disease. *J Clin Neurosci* 13: 639–642, 2006.

Thobois S, Dominey P, Decety J, Pollak P, Gregoire MC, Broussolle E. Overactivation of primary motor cortex is asymmetrical in hemiparkinsonian patients. *Neuroreport* 11: 785–789, 2000.

Tinazzi M, Zarattini S, Valeriani M, Romito S, Farina S, Moretto G, Smania N, Fiaschi A, Abbruzzese G. Long-lasting modulation of human motor cortex following prolonged transcutaneous electrical nerve stimulation (TENS) of forearm muscles: Evidence of reciprocal inhibition and facilitation. *Exp Brain Res* 161: 457–464, 2005.

Tokimura H, Di Lazzaro V, Tokimura Y, Oliviero A, Profice P, Insola A, Mazzone P, Tonali P, Rothwell JC. Short latency inhibition of human hand motor cortex by somatosensory input from the hand. *J Physiol* 523 Pt 2: 503–513, 2000.

Tsang P, Jacobs MF, Lee KGH, Asmussen MJ, Zapallow CM, Nelson AJ. Continuous theta-burst stimulation over primary somatosensory cortex modulates short-latency afferent inhibition. *Clin Neurophysiol* 125: 2253–2259, 2014.

Tsutsumi R, Hanajima R, Hamada M, Shirota Y, Matsumoto H, Terao Y, Ohminami S, Yamakawa Y, Shimada H, Tsuji S, Ugawa Y. Reduced interhemispheric inhibition in mild cognitive impairment. *Exp Brain Res* 218: 21–26, 2012a.

Tsutsumi R, Shirota Y, Ohminami S, Terao Y, Ugawa Y, Hanajima R. Conditioning intensity-dependent interaction between short-latency interhemispheric inhibition and

short-latency afferent inhibition. *J Neurophysiol* 108: 1130–1137, 2012b.

Tubbs RS, Rogers JM, Loukas M, Cömert A, Shoja MM, Cohen-Gadol AA.

Anatomy of the palmar branch of the ulnar nerve: Application to ulnar and median nerve decompressive surgery - Laboratory investigation. *J Neurosurg* 114: 263–267, 2011.

Turco C V., El-Sayes J, Fassett HJ, Nelson AJ. Modulation of long-latency afferent inhibition by the amplitude of sensory afferent volley. *J Neurophysiol* 118: 610–618, 2017.

Turco C V., El-Sayes J, Locke MB, Chen R, Baker S, Nelson AJ. Effects of lorazepam and baclofen on short- and long-latency afferent inhibition. *J Physiol* 596: 5267–5280, 2018a.

Turco C V., El-Sayes J, Savoie MJ, Fassett HJ, Locke MB, Nelson AJ. Short- and long-latency afferent inhibition; uses, mechanisms and influencing factors. *Brain Stimul* 11: 59–74, 2018b.

Turco C V., Locke MB, El-Sayes J, Tommerdahl M, Nelson AJ. Exploring Behavioral Correlates of Afferent Inhibition. *Brain Sci* 8: 1–8, 2018c.

Turco C V., Pesevski A, McNicholas PD, Beaulieu L-D, Nelson AJ. Reliability of transcranial magnetic stimulation measures of afferent inhibition. *Brain Res* 1723: 146394, 2019a.

Turco C V., Toepp SL, Foglia SD, Dans PW, Nelson AJ. Association of short- and long-latency afferent inhibition with human behavior. *Clin Neurophysiol* In Press, 2021.

Turco CV, Pesevski A, McNicholas PD, Beaulieu L-D, Nelson AJ. Reliability of transcranial magnetic stimulation measures of afferent inhibition. *Brain Res* 1723, 2019b.

- Tyč F, Boyadjian A.** Cortical plasticity and motor activity studied with transcranial magnetic stimulation. *Rev. Neurosci.* 17: 469–495, 2006.
- Udupa K, Ni Z, Gunraj C, Chen R.** Interactions between short latency afferent inhibition and long interval intracortical inhibition. *Exp Brain Res* 199: 177–183, 2009.
- Udupa K, Ni Z, Gunraj C, Chen R.** Effects of short-latency afferent inhibition on short-interval intracortical inhibition. *J Neurophysiol* 111: 1350–61, 2014.
- Vallence AM, Hammond GR, Reilly KT.** Increase in flexor but not extensor corticospinal motor outputs following ischemic nerve block. *J Neurophysiol* 107: 3417–3427, 2012a.
- Vallence AM, Reilly K, Hammond G.** Excitability of intracortical inhibitory and facilitatory circuits during ischemic nerve block. *Restor Neurol Neurosci* 30: 345–354, 2012b.
- Valls-Solé J, Pascual-Leone A, Brasil-Neto JP, Cammarota A, McShane A, Hallett M.** Abnormal facilitation of the response to transcranial magnetic stimulation in patients with parkinson's disease. *Neurology* 44: 735–741, 1994.
- Valls-Solé J, Pascual-Leone A, Wassermann EM, Hallett M.** Human motor evoked responses to paired transcranial magnetic stimuli. *Electroencephalogr Clin Neurophysiol Evoked Potentials* 85: 355–364, 1992.
- Veinante P, Deschênes M.** Single-cell study of motor cortex projections to the barrel field in rats. *J Comp Neurol* 464: 98–103, 2003.
- Veldman MP, Zijdwind I, Maffiuletti NA, Hortobágyi T.** Motor skill acquisition and retention after somatosensory electrical stimulation in healthy humans. *Front Hum*

Neurosci 10: 115, 2016.

Veldman MP, Zijdwind I, Solnik S, Maffiuletti NA, Berghuis KMM, Javet M, Négyesi J, Hortobágyi T. Direct and crossed effects of somatosensory electrical stimulation on motor learning and neuronal plasticity in humans. *Eur J Appl Physiol* 115: 2505–2519, 2015.

Vidoni ED, Acerra NE, Dao E, Meehan SK, Boyd LA. Role of the primary somatosensory cortex in motor learning: An rTMS study. *Neurobiol Learn Mem* 93: 532–539, 2010.

Vitrac C, Péron S, Frappé I, Fernagut PO, Jaber M, Gaillard A, Benoit-Marand M. Dopamine control of pyramidal neuron activity in the primary motor cortex via D2 receptors. *Front Neural Circuits* 8: 13, 2014.

Vizi ES, Pasztor E. Release of Acetylcholine from Isolated Human Cortical Slices: Inhibitory Effect of Norepinephrine and Phenytoin. *Exp Neurol* 73: 144–153, 1981.

Voller B, St Clair Gibson A, Dambrosia J, Pirio Richardson S, Lomarev M, Dang N, Hallett M. Long-latency afferent inhibition during selective finger movement. *J Neurophysiol* 94: 1115–1119, 2005.

Voller B, St Clair Gibson A, Dambrosia J, Pirio Richardson S, Lomarev M, Dang N, Hallett M. Short-latency afferent inhibition during selective finger movement. *Exp Brain Res* 169: 226–231, 2006.

Wagle Shukla A, Moro E, Gunraj C, Lozano A, Hodaie M, Lang A, Chen R. Long-term subthalamic nucleus stimulation improves sensorimotor integration and proprioception. *J Neurol Neurosurg Psychiatry* 84: 1020–8, 2013.

Wang X, Merzenich MM, Sameshima K, Jenkins WM. Remodelling of hand representation in adult cortex determined by timing of tactile stimulation. *Nature* 378: 71–75, 1995.

Wassermann EM. Variation in the response to transcranial magnetic brain stimulation in the general population. *Clin Neurophysiol* 113: 1165–1171, 2002.

Waterhouse BD, Moises HC, Woodward DJ. Interaction of serotonin with somatosensory cortical neuronal responses to afferent synaptic inputs and putative neurotransmitters. *Brain Res Bull* 17: 507–518, 1986.

Weir J. Quantifying test-retest reliability using the intraclass correlation coefficient. *J Strength Cond Res* 19: 231–240, 2005.

Werhahn KJ, Behrang-Nia M, Bott MC, Klimpe S. Does the recruitment of excitation and inhibition in the motor cortex differ? *J Clin Neurophysiol* 24: 419–423, 2007.

Werhahn KJ, Mortensen J, Kaelin-Lang A, Boroojerdi B, Cohen LG. Cortical excitability changes induced by deafferentation of the contralateral hemisphere. *Brain* 125: 1402–1413, 2002.

Wood KC, Blackwell JM, Geffen MN. Cortical inhibitory interneurons control sensory processing. *Curr. Opin. Neurobiol.* 46: 200–207, 2017.

Wu CW, Seo HJ, Cohen LG. Influence of electric somatosensory stimulation on paretic-hand function in chronic stroke. *Arch Phys Med Rehabil* 87: 351–357, 2006.

Wu CWH, Van Gelderen P, Hanakawa T, Yaseen Z, Cohen LG. Enduring representational plasticity after somatosensory stimulation. *Neuroimage* 27: 872–884, 2005.

Xiang Z, Huguenard JR, Prince D a. Cholinergic switching within neocortical inhibitory networks. *Science (80-)* 281: 985–988, 1998.

Yamawaki N, Borges K, Suter BA, Harris KD, Shepherd GMG. A genuine layer 4 in motor cortex with prototypical synaptic circuit connectivity. *Elife* 3: e05422, 2014.

Yamazaki Y, Sato D, Yamashiro K, Nakano S, Onishi H, Maruyama A. Acute low-intensity aerobic exercise modulates intracortical inhibitory and excitatory circuits in an exercised and a non-exercised muscle in the primary motor cortex. *Front Physiol* 10: 1361, 2019.

Yarnall AJ, Rochester L, Baker MR, David R, Khoo TK, Duncan GW, Galna B, Burn DJ. Short latency afferent inhibition: A biomarker for mild cognitive impairment in Parkinson's disease? *Mov Disord* 28: 1285–1288, 2013.

Yildiz N, Yildiz S, Ertekin C, Aydoğdu I, Uludag B. Changes in the perioral muscle responses to cortical TMS induced by decrease of sensory input and electrical stimulation to lower facial region. *Clin Neurophysiol* 115: 2343–2349, 2004.

Young-Bernier M, Kamil Y, Tremblay F, Davidson PS. Associations between a neurophysiological marker of central cholinergic activity and cognitive functions in young and older adults. *Behav Brain Funct* 8: 17, 2012.

Young-Bernier M, Tanguay AN, Davidson PSR, Tremblay F. Short-latency afferent inhibition is a poor predictor of individual susceptibility to rTMS-induced plasticity in the motor cortex of young and older adults. *Front Aging Neurosci* 6: 1–8, 2014.

Young-Bernier M, Tanguay AN, Tremblay F, Davidson PSR. Age Differences in Reaction Times and a Neurophysiological Marker of Cholinergic Activity. *Can J Aging*

34: 471–480, 2015.

Ziemann U, Corwell B, Cohen LG. Modulation of plasticity in human motor cortex after forearm ischemic nerve block. *J Neurosci* 18: 1115–1123, 1998a.

Ziemann U, Hallett M, Cohen LG. Mechanisms of deafferentation-induced plasticity in human motor cortex. *J Neurosci* 18: 7000–7, 1998b.

Ziemann U, Lönnecker S, Steinhoff BJ, Paulus W. Effects of antiepileptic drugs on motor cortex excitability in humans: A transcranial magnetic stimulation study. *Ann Neurol* 40: 367–378, 1996.

Ziemann U, Reis J, Schwenkreis P, Rosanova M, Strafella A, Badawy R, Müller-Dahlhaus F. TMS and drugs revisited 2014. *Clin. Neurophysiol.* 126: 1847–1868, 2015.

Chapter 10: APPENDIX A
COPYRIGHT PERMISSIONS AND LICENSES

A.1 American Physiological Society Copyright and Permissions (Chapter 3)

A.2 Permissions for Personal Use in a Thesis from The Physiological Society (Chapter 4)

A.3 Permissions for Personal Use in a Thesis from Elsevier (Chapter 5)

A.4 Creative Commons Attribution License 4.0 (Chapter 6)

A.1 American Physiological Society Copyright and Permissions (Chapter 3)

As the first author, please note that I retain the right to include this chapter in my doctoral thesis. Permission is not required, as I have cited ‘Journal of Neurophysiology’ as the original source.

Copyright and Permissions

Reuse by Authors of Their Work Published by APS Reuse by Non-authors of APS Published Content

Reuse in APS Publications of non-APS Published Content

Reuse by Authors of Their Work Published by APS

The APS Journals are copyrighted for the protection of authors and the Society. The Mandatory Submission Form serves as the Society's official copyright transfer form. Author's rights to reuse their APS-published work are described below.

Replication in New Works	Authors may republish parts of their final-published work (e.g., figures, tables), without charge and without requesting permission, provided that full citation of the source is given in the new work.
Meeting Presentations and Conferences	Authors may use their work (in whole or in part) for presentations (e.g., at meetings and conferences). These presentations may be reproduced on any type of media in materials arising from the meeting or conference such as the proceedings of a meeting or conference. A copyright fee will apply if there is a charge to the user or if the materials arising are directly or indirectly commercially supported ¹ . Full citation is required.
Theses and Dissertations	Authors may reproduce whole published articles in dissertations and post to thesis repositories without charge and without requesting permission. Full citation is required.
Open Courseware	Authors may post articles, chapters or parts thereof to a public access courseware website. Permission must be requested from the APS ¹ . A copyright fee will apply to a book chapter and during the first 12 months of a journal article's publication. Full citation is required.
Websites	Authors may not post a PDF of the accepted or final version of their published work to any website including social and research networking platforms; instead, links may be posted to the APS or publisher partner website where the work is published ¹ (see exception to authors' own institution's repository, as note below).
Institutional Repositories (non-theses)	Authors may deposit their accepted, peer-reviewed journal manuscripts into an institutional repository providing: <ul style="list-style-type: none"> the APS retains copyright to the article¹ a 12-month embargo period from the date of final publication of the article is observed by the institutional repository and the author a link to the article published on the APS or publisher-partner website is prominently displayed alongside the article in the institutional repository the article is not used for commercial purposes self-archived articles posted to repositories are without warranty of any kind
	¹ Unless it is published under the APS Open Access (AuthorChoice) option, which allows for immediate public access under a Creative Commons license (CC BY 4.0) (See also the APS Policy on Depositing Articles in PMC.)

[Go to top](#)

Submit with APS Journals Today

<https://journals.physiology.org/author-info.permissions>

A.2 Permissions for Personal Use in a Thesis from The Physiological Society (Chapter 4)



Department of
Kinesiology
Faculty of Science

1280 Main Street
West
Hamilton,
Ontario, Canada
L8S 4K1

Phone 905.525.9140
Fax 905.523.6011
<http://www.science.mcmaster.ca/kinesiology>

February 22, 2021

The Physiological Society
Hodgkin Huxley House,
30 Farringdon Lane,
London, EC1R 3AW

To Whom It May Concern:

I am completing a Ph.D. thesis at McMaster University entitled 'Investigating the Functional Relevance of Afferent Inhibition'. I would like your permission to reprint in full the following journal article in my thesis:

Turco CV, El-Sayes J, Locke MB, Chen R, Baker S, & Nelson AJ (2018). Effects of lorazepam and baclofen on short- and long-latency afferent inhibition. *J Physiol*, 596(21): 5267-5280.

Please note that I am the second author of this work.

I am also requesting that you grant irrevocable, nonexclusive license to McMaster University to reproduce this material as a part of the thesis. Proper acknowledgement of your copyright of the reprinted material will be given in the thesis.

If these arrangements meet with your approval, please sign where indicated below and return this letter to me in the enclosed envelope. Thank you very much.

Sincerely,

A handwritten signature in cursive script that reads "Claudia Turco".

Claudia Turco

PERMISSION GRANTED FOR THE USE REQUESTED ABOVE

The Physiological Society

Authorized by: Sally Howells

Title: Publisher

Date: 23/02/2021

Signature:

A handwritten signature in cursive script that reads "Sally Howells".

A.3 Permissions for Personal Use in a Thesis from Elsevier (Chapter 5)

Gmail - Re: Obtain permission request - Journal (1136796) [210222-017124]

2021-02-23, 8:03 PM



Claudia Turco <turcocv4@gmail.com>

Re: Obtain permission request - Journal (1136796) [210222-017124]

2 messages

Rights and Permissions (ELS) <Permissions@elsevier.com>
Reply-To: "Rights and Permissions (ELS)" <Permissions@elsevier.com>
To: turcocv@mcmaster.ca

Mon, Feb 22, 2021 at 12:08 PM

Dear Claudia Turco,

Thank you for contacting the Permissions Granting Team.

We acknowledge the receipt of your request and we aim to respond within seven business days. Your unique reference number is 210222-017124.

Please avoid changing the subject line of this email when replying to avoid delay with your query.

Regards,
Permission Granting Team

From: Claudia Turco
Date: 22/02/2021 05.08 PM

Submission ID: 1136796
Date: 22 Feb 2021 5:08pm

Name: PhD Candidate Claudia Turco
Institute/company: McMaster University
Address: [8 Gem Court](#)
Post/Zip Code: L9C7S4
City: Hamilton
State/Territory: Ontario
Country: Canada
Telephone: 9055122058
Email: turcocv@mcmaster.ca

Type of Publication: Journal

Title: Brain Research
Auhtors: Turco, C.V. Pesevski, A. McNicholas, P.D. Beaulieu, L.-D. Nelson, A.J.
Year: 2019
From page: 1
To page: 10

ISSN: 18726240

Volume: 1723

Issue: 146394

Article title: Reliability of transcranial magnetic stimulation measures of afferent inhibition

I would like to use: Full article / chapter

I am the author of the Elsevier material: Yes

In what format will you use the material: Print and Electronic

Translation: No

Proposed use: Reuse in a thesis/dissertation

Material can be extracted: No

Additional Comments / Information: I am specifically requesting permission to reproduce this paper within my PhD thesis. I am required to submit a letter stating that I have this permission to my university.

This email is for use by the intended recipient and contains information that may be confidential. If you are not the intended recipient, please notify the sender by return email and delete this email from your inbox. Any unauthorized use or distribution of this email, in whole or in part, is strictly prohibited and may be unlawful. Any price quotes contained in this email are merely indicative and will not result in any legally binding or enforceable obligation. Unless explicitly designated as an intended e-contract, this email does not constitute a contract offer, a contract amendment, or an acceptance of a contract offer.

Elsevier Limited. Registered Office: The Boulevard, Langford Lane, Kidlington, Oxford, OX5 1GB, United Kingdom, Registration No. 1982084, Registered in England and Wales. [Privacy Policy](#)

Rights and Permissions (ELS) <Permissions@elsevier.com>
Reply-To: "Rights and Permissions (ELS)" <Permissions@elsevier.com>
To: turcocv@mcmaster.ca

Tue, Feb 23, 2021 at 6:24 PM

Dear Claudia Turco,

We hereby grant you permission to reprint the material below at no charge in your thesis subject to the following conditions:

1. If any part of the material to be used (for example, figures) has appeared in our publication with credit or acknowledgement to another source, permission must also be sought from that source. If such permission is not obtained then that material may not be included in your publication/copies.
2. Suitable acknowledgment to the source must be made, either as a footnote or in a reference list at the end of your publication, as follows:

"This article was published in Publication title, Vol number, Author(s), Title of article, Page Nos, Copyright Elsevier (or appropriate Society name) (Year)."

3. Your thesis may be submitted to your institution in either print or electronic form.
4. Reproduction of this material is confined to the purpose for which permission is hereby given.
5. This permission is granted for non-exclusive world English rights only. For other languages please reapply separately for each one required. Permission excludes use in an electronic form other than submission. Should you have a specific electronic project in mind please reapply for permission.
6. As long as the article is embedded in your thesis, you can post/share your thesis in the University repository.
7. Should your thesis be published commercially, please reapply for permission.
8. Posting of the full article/ chapter online is not permitted. You may post an abstract with a link to the Elsevier website www.elsevier.com, or to the article on ScienceDirect if it is available on that platform.

Kind Regards
Roopa

Thanks & Regards,
Roopa Lingayath
Sr Copyrights Coordinator – Copyrights Team
ELSEVIER | Health Content Operations
International Tech Park | Crest - 5th Floor | CSIR Road | Taramani | Chennai 600 113 | India
E-mail: r.lingayath@elsevier.com | url: www.elsevier.com Dear Claudia Turco,

We hereby grant you permission to reprint the material below at no charge in your thesis subject to the following conditions:

1. If any part of the material to be used (for example, figures) has appeared in our publication with credit or acknowledgement to another source, permission must also be sought from that source. If such permission is not obtained then that material may not be included in your publication/copies.

2. Suitable acknowledgment to the source must be made, either as a footnote or in a reference list at the end of your publication, as follows:

“This article was published in Publication title, Vol number, Author(s), Title of article, Page Nos, Copyright Elsevier (or appropriate Society name) (Year).”

3. Your thesis may be submitted to your institution in either print or electronic form.
4. Reproduction of this material is confined to the purpose for which permission is hereby given.
5. This permission is granted for non-exclusive world English rights only. For other languages please reapply separately for each one required. Permission excludes use in an electronic form other than submission. Should you have a specific electronic project in mind please reapply for permission.
6. As long as the article is embedded in your thesis, you can post/share your thesis in the University repository.
7. Should your thesis be published commercially, please reapply for permission.

A.4 Creative Commons Attribution License 4.0 (Chapter 6)

All MDPI journals are Open Access and subject to the Creative Commons Attribution License (CC BY). As the first author, please note that I retain the right to include this chapter in my doctoral thesis. Permission is not required, as I have cited ‘Brain Sciences’ as the original source.